



Published in final edited form as:

Adv Drug Deliv Rev. 2008 September ; 60(12): 1347–1370. doi:10.1016/j.addr.2008.04.006.

Bifunctional Coupling Agents for Radiolabeling of Biomolecules and Target-Specific Delivery of Metallic Radionuclides

Shuang Liu

School of Health Sciences, Purdue University, West Lafayette, USA

Abstract

Receptor-based radiopharmaceuticals are of great current interest in early molecular imaging and radiotherapy of cancers, and provide a unique tool for target-specific delivery of radionuclides to the diseased tissues. In general, a target-specific radiopharmaceutical can be divided into four parts: targeting biomolecule (BM), pharmacokinetic modifying (PKM) linker, bifunctional coupling or chelating agent (BFC), and radionuclide. The targeting biomolecule serves as a “carrier” for specific delivery of the radionuclide. PKM linkers are used to modify radiotracer excretion kinetics. BFC is needed for radiolabeling of biomolecules with a metallic radionuclide. Different radiometals have significant difference in their coordination chemistry, and require BFCs with different donor atoms and chelator frameworks. Since the radiometal chelate can have a significant impact on physical and biological properties of the target-specific radiopharmaceutical, its excretion kinetics can be altered by modifying the coordination environment with various chelators or coligand, if needed. This review will focus on the design of BFCs and their coordination chemistry with technetium, copper, gallium, indium, yttrium and lanthanide radiometals.

Keywords

radiopharmaceuticals; radionuclides; target-specific delivery; diagnosis; radiotherapy

1. Introduction

Radiopharmaceuticals are drugs containing a radionuclide, and are used routinely in nuclear medicine for diagnosis or therapy of diseases [1–7]. Almost all radiopharmaceuticals are administered via intravenous injection. They are mostly small organic or inorganic compounds with definite composition. Radiopharmaceuticals can also be macromolecules such as monoclonal antibodies and antibody fragments that are not stoichiometrically labeled with a radionuclide. Depending on their medical applications, radiopharmaceuticals can be divided into two primary classes: diagnostics and therapeutics. They can also be classified according to their biodistribution characteristics: those whose biodistribution is determined exclusively by their chemical and physical properties; and those whose ultimate distribution is determined by their receptor binding capability or other biological interactions. The latter class is often called target-specific radiopharmaceuticals.

Correspondence should be addressed to: Dr. Shuang Liu, School of Health Sciences, Purdue University, Civil Engineering Building Room 1275, 550 Stadium Mall Drive, West Lafayette, IN 47907; Phone: 765-494-0236; Fax 765-496-1377; Email: lius@pharmacy.purdue.edu.

Publisher's Disclaimer: This is a PDF file of an unedited manuscript that has been accepted for publication. As a service to our customers we are providing this early version of the manuscript. The manuscript will undergo copyediting, typesetting, and review of the resulting proof before it is published in its final citable form. Please note that during the production process errors may be discovered which could affect the content, and all legal disclaimers that apply to the journal pertain.

A diagnostic radiopharmaceutical is the molecule labeled with a gamma-emitting isotope for single photon emission computed tomography (SPECT) or a positron-emitting isotope for positron emission tomography (PET) [1–7]. In general, diagnostic radiopharmaceuticals are used in very low concentrations (10^{-6} – 10^{-8} M), and are not intended to have any pharmacological effects. The aim of the diagnostic application is the detailed description of morphologic structure of organs or tissues and above all the testing of their physiological function through accumulation of the radiopharmaceutical. Diagnostic radiopharmaceuticals are predominantly metal complexes with an organic chelator for metal-essential agents or a chelator-biomolecule conjugate for target-specific radiopharmaceuticals. In some cases, they can be organic molecules attached with a non-metallic radionuclide, such as ^{18}F and ^{125}I . Diagnostic radiopharmaceuticals provide a non-invasive method of assessing the disease or disease states by SPECT or PET. They are also useful for monitoring the efficacy of a specific therapeutic treatment [1–7].

Therapeutic radiopharmaceuticals are molecules designed to deliver therapeutic doses of ionizing radiation to the diseased sites. The main obstacles for radiotherapy to assume a wider role in clinical practice are the availability of therapeutic isotopes and techniques for their specific localization in diseased tissues, such as tumors [8]. Therapeutic doses of radiation can be delivered in three different ways: external beam irradiation, implantable “seeds” or systemic administration. Brach therapy involves the use of “seeds”, which are physically placed at the tumor site and will remain there unless they are surgically removed. Brach therapy plays a vital role in the care of prostate cancer patients. It is only useful for treatment of accessible tumors. Systemic administration of radiopharmaceuticals that are designed for target-specific delivery of the therapeutic radionuclide at tumor sites provides opportunities for treatment of the disseminated metastatic tumors [9]. Ideally, therapeutic radiopharmaceuticals should localize in tumor site in sufficient concentration to deliver a cytotoxic radiation dose to tumor cells, and at the same time clear rapidly from blood and non-cancerous organs to minimize radiation damage to normal tissues.

A target-specific radiopharmaceutical is based on the receptor binding of a radiolabeled receptor ligand in the diseased tissue [10–14]. In general, a target-specific radiopharmaceutical can be divided into four parts: targeting biomolecule (BM), pharmacokinetic modifying (PKM) linker, bifunctional coupling or chelating agent (BFC), and radionuclide. The targeting biomolecule serves as a “carrier” for specific delivery of radionuclide to the diseased tissue, which is known to contain a substantial concentration of the targeted receptor. The radiolabeled receptor ligand binds to receptors with high affinity and specificity, which results in selective uptake of the radiopharmaceutical. Many biomolecules, including monoclonal antibodies, small peptides, or non-peptide receptor ligands, have been successfully used for target-specific delivery of radionuclides. Table 1 lists selected commercial target-specific radiopharmaceuticals approved by FDA (Food and Drug Administration) for diagnosis or treatment of diseases, such as thrombosis and cancer. Figure 1 illustrates the structures of two small peptide-based target-specific radiopharmaceuticals. The approval of ^{90}Y -labeled anti-CD20 monoclonal antibody (Zevalin®, IDEC Pharmaceuticals Corp.) represents the most significant milestone in the use of radiolabeled MoAbs for radioimmunotherapy (RAIT) of cancers [15–20]. Many excellent reviews have appeared recently covering a broad range of topics related to target-specific diagnostic and therapeutic radiopharmaceuticals [5–15,21–43].

Radionuclide is the radiation source. Selection of radionuclide is largely dependent on medical application of the radiopharmaceutical. For diagnostic radiopharmaceuticals, $^{99\text{m}}\text{Tc}$, ^{111}In , $^{62/64}\text{Cu}$ and $^{67/68}\text{Ga}$, will be the choice of radionuclides for SPECT or PET imaging. While ^{64}Cu and ^{68}Ga are particularly useful for PET, $^{99\text{m}}\text{Tc}$ is of particular importance for SPECT imaging due to its optimal nuclear properties (6.02 h half-

life with 140 keV gamma photons) and its easy availability at low cost. In contrast, β -emitters (e.g. ^{90}Y , ^{177}Lu and $^{186/188}\text{Re}$) are useful for development of therapeutic radiopharmaceuticals. ^{90}Y is of particular interest since it is a pure β -emitter with a long penetration range (~12 mm), which may yield a more homogeneous dose distribution even when the radiotracer is heterogeneously distributed in the tumor.

An important aspect during the radiopharmaceutical development is to improve target-to-background (T/B) ratios by modifying excretion kinetics of radiolabeled biomolecules with various PKM linkers. Figure 2 shows several types of PKM linkers (cationic, anionic, neutral or metabolically cleavable). The linker can be a simple hydrocarbon chain to increase lipophilicity, a peptide sequence (such as polyaspartic acid) to improve hydrophilicity and renal clearance, or a poly(ethyleneglycol) linker to slow extraction by hepatocytes. It has been reported that linker groups have significant effect on biodistribution of ^{111}In and $^{99\text{m}}\text{Tc}$ -labeled antibodies [44–46]. Metabolizable linkers have been used for ^{111}In -labeled somatostatin analogs [47]. A tetrapeptide linker Gly-Gly-Gly-L-(p-NO₂)-Phe-CONH₂ that is cleaved between Gly and Phe residues has been used to modify pharmacokinetics of ^{90}Y -labeled antibodies [48–51]. A sugar moiety was used to increase tumor/liver ratios of ^{125}I and ^{18}F -labeled cyclic RGD (Arg-Gly-Glu) peptides [52–55]. The di(cysteic acid) linker was used to minimize liver accumulation of the radiolabeled nonpeptide integrin $\alpha_v\beta_3$ antagonists [56–59]. It has been reported that introduction of the polyethylene glycol (PEG) linker can improve not only tumor uptake but also excretion kinetics of the ^{125}I and ^{18}F -labeled cyclic RGD monomer [60], and ^{64}Cu -labeled cyclic RGD dimer [61]. PEG₄ and amino acid linkers have also been used to improve excretion kinetics of ^{111}In and $^{99\text{m}}\text{Tc}$ -labeled E[c(RGDfK)]₂ [62, 63]. The ultimate goal of using PKM linkers is to modify the radiotracer excretion kinetics so that its T/B ratios can be optimized by minimizing its uptake in non-tumor organs while maintaining its high tumor uptake [5,6,12].

BFC is needed for radiolabeling of biomolecules with a metallic radionuclide. BFC is covalently attached to the targeting molecule either directly or through a PKM linker, and strongly coordinates to the radiometal. The choice of BFC is largely determined by the nature and oxidation state of the radiometal. Different radiometals require BFCs with different donor atoms and chelator frameworks. Therefore, it is important to understand the coordination chemistry of BFCs with any given radiometal to be labeled. An ideal BFC is that which is able to form a stable radiometal chelate with high thermodynamic stability and kinetic inertness.

Since many reviews have covered a broad range of topics related to the target-specific radiopharmaceuticals [5,6,21–43,64–68], this critical review will focus on the fundamental coordination chemistry of BFCs with technetium, copper, gallium, indium, yttrium and lanthanide metals. Whenever possible, references from the last 10 years will be used. The author would apologize to those whose work has not been presented in this review, and for the omission of ^{18}F -labeled and iodinated biomolecules as diagnostic and therapeutic radiotracers, details of which can be found in recent review articles [15,16,20,21,69,70].

2. Radiometals for Diagnostic and Therapeutic Radiopharmaceuticals

2.1. Why Metallic Radionuclides?

Receptor-based radiopharmaceuticals provide a unique tool for target-specific delivery of radionuclide. The overwhelming majority of diagnostic radiopharmaceuticals currently available in nuclear medicine are either radiometal complexes or target-specific biomolecules labeled with metallic radionuclides (Table 1), such as $^{99\text{m}}\text{Tc}$ and ^{111}In . It should be noted that the choice of radionuclide depends largely upon its nuclear properties (half-life, type of radiation, energy, and presence or lack of other particulate radiation emissions) and potential for wide clinical applications of the radiotracer. For example, ^{18}F is an excellent PET isotope,

and has been widely used for the development of target-specific PET radiotracers for research purposes. However, the wide clinical applications of the ^{18}F -based target-specific radiotracers will be limited due to its short-half life ($t_{1/2} = 110$ min), difficulties in radiosynthesis and chromatographic purification under GMP (Good Manufacturing Practice) conditions, and high cost to maintain the radionuclide production infrastructure. In this respect, metallic radionuclides, such as ^{68}Ga and ^{64}Cu , become viable alternatives to ^{18}F in part because of their availability, which makes it much more feasible to develop target-specific radiotracers with wider clinical applications. ^{68}Ga is readily available from the ^{68}Ge - ^{68}Ga generator. ^{64}Cu has a much longer half-life ($t_{1/2} = 12.7$ h) and can be produced with very high specific activity. In addition, the use of metallic radionuclides offers many opportunities for the design and development of new target-specific radiotracers. Different radiometals have significant differences in their coordination chemistry. Since the radiometal chelate can have a significant impact on biological properties, the biodistribution of a target-specific radiopharmaceutical can be systematically changed by either modifying the coordination environment around the radiometal with a variety of chelators or by the use of various coligands if the radiometal chelate contains two or more ligands.

2.2. Radiometals for SPECT

The diagnostic radionuclide is often a gamma-emitting isotope for SPECT or positron-emitter for PET. Table 2 lists several metallic radionuclides useful for scintigraphy and SPECT imaging. In general, generator-produced radiometals are ideal since the daughter radionuclide that can be easily separated from the parent isotope by ion-exchange chromatography. For SPECT imaging, $^{99\text{m}}\text{Tc}$ remains the most widely used isotope due to its optimal nuclear property and easy availability at low cost. ^{111}In is also useful for gamma and SPECT imaging, and is often used as the imaging surrogate for ^{90}Y analogs since ^{90}Y is a pure β -emitter.

2.2.1. Technetium-99m— $^{99\text{m}}\text{Tc}$ is produced from ^{99}Mo , a fission product with a half-life of 2.78 days. In a ^{99}Mo - $^{99\text{m}}\text{Tc}$ generator, $^{99}\text{MoO}_4^{2-}$ is adsorbed to an alumina column and $^{99\text{m}}\text{Tc}$ is formed by decay of ^{99}Mo . $^{99\text{m}}\text{TcO}_4^-$ is eluted from the column with saline. The $^{99\text{m}}\text{Tc}$ produced by the generator is never carrier-free because thirteen percent of ^{99}Mo decays directly to the long-lived isotope ^{99}Tc ($t_{1/2} = 2.13 \times 10^5$ y). The specific activity (the amount of radioactivity per unit mass of the radionuclide) of eluted $^{99\text{m}}\text{Tc}$ is dependent upon prior-elution time (the time interval between elutions). The total technetium ($^{99\text{m}}\text{Tc}$ and ^{99}Tc) concentration in the generator eluant is in the range of $10^{-7} - 10^{-6}$ M.

2.2.2. Gallium-67—Among several radionuclides of gallium, ^{67}Ga is the most utilized due to its ability to identify inflammation and soft tissue tumors. ^{67}Ga is a cyclotron-produced radionuclide by the $^{68}\text{Zn}(p, 2n)$ - ^{67}Ga nuclear reaction, and has a half-life of 78 h. ^{67}Ga decays to ^{67}Zn by electron capture with emission of several gamma photons of 93 keV (40%), 184 keV (20%), 300 keV (17%) and 393 keV (5%). ^{67}Ga is separated from the target (^{68}Zn) by solvent extraction with isopropyl ether, and is then back extracted from ether to HCl, which is then evaporated to dryness. Citric acid is often added to prevent hydrolysis of $^{67}\text{Ga}(\text{III})$. The pH is adjusted to near neutral and finally the ^{67}Ga -citrate solution is sterilized for clinical use [64,68].

2.2.3. Indium-111— ^{111}In is a cyclotron-produced isotope by the $^{111}\text{Cd}(p, n)$ - ^{111}In nuclear reaction, and has a half-life of 67.9 h (2.83 days). ^{111}In is separated from the cadmium using solvent extraction, ion exchange, or both even though co-precipitation with ferric hydroxide has also been used. ^{111}In decays by electron capture with two γ -photon emissions at 173 and 247 keV (89% and 95% abundance, respectively), and has been widely used in gamma scintigraphy.

2.3. Radiometals for PET

Table 3 lists metallic radionuclides useful for PET imaging. In general, it is highly desirable that the radionuclide has no radiation decays other than 511-keV gamma photons from positron annihilation. This will minimize impairment of spatial resolution due to high β^+ energy and reduce radiation burden to the patient. A generator-based isotope would be ideal to achieve high specific activity for target-specific radiopharmaceuticals so that their target uptake can be maximized. It is also much easier for dose preparation, quality control, transportation and delivery using a generator produced isotope. The half-life of parent isotope should be long while the half-life of daughter isotope should be short. Radiolabeling should be readily completed, preferably over 10 – 30 min. In addition, the cost for parent isotope production and availability of the enriched source should also be considered.

2.3.1. Copper-62— ^{62}Cu is a generator-produced radionuclide from the decay of ^{62}Zn . It has a half-life of 9.7 min, which allows repeated dosing without imposing a significant radiation burden to the patient [71–73]. The ^{62}Zn - ^{62}Cu generator is made up of Dowex ion exchange column. Carrier free ^{62}Cu is eluted from the column with 2 N HCl. The ^{62}Zn - ^{62}Cu generator only lasts for 1 – 2 days due to the short half-life (9.3 h) of ^{62}Zn . This makes PET imaging with ^{62}Cu -labeled biomolecules very expensive. However, the cost of ^{62}Zn - ^{62}Cu generators may be significantly reduced as their usage increases [71]. A commercially available ^{62}Zn - ^{62}Cu generator has been successfully used in Phase III clinical trials [74]. There is significant interest in the ^{62}Cu radiopharmaceuticals, such as ^{62}Cu -PTSM, for heart and tumor imaging by PET [71–78].

2.3.2. Copper-61 and Copper-64— ^{61}Cu has a relatively high β^+ emission rate (61%) with maximum β^+ energy of 1.22 MeV and a half-life of 3.32 h. It also has two gamma rays with $E_\gamma = 283$ (13%) and 380 keV (3%). Several nuclear reactions can be used for the production of ^{61}Cu . These include nuclear reactions [$^{59}\text{Co}(\alpha, 2n)^{61}\text{Cu}$] (40 MeV), [$^{nat}\text{Ni}(\alpha, p)^{61}\text{Cu}$] (21 MeV), and [$^{61}\text{Ni}(p, n)^{61}\text{Cu}$]. The latter methods are often free from ^{64}Cu radio-impurity. Although the nuclear properties are very attractive for PET imaging, ^{61}Cu has not been used to the same extent as ^{64}Cu , which has a low β^+ emission rate (18%) with maximum β^+ energy of 0.66 MeV and a half-life of 12.7 h. The longer half-life of ^{64}Cu is much more feasible for the radiolabeling of small biomolecules for the development of target-specific radiopharmaceuticals. ^{64}Cu can be produced by proton irradiation of ^{nat}Ni or enriched ^{68}Zn . Both methods suffer from low yield and co-production of ^{61}Cu and ^{67}Cu radioimpurities [71, 72]. The enriched ^{64}Ni target has been used for production of ^{64}Cu with very high specific activity (>10,000 Ci/mmol). Using this method, Ci amounts of ^{64}Cu can be produced on demands. ^{64}Cu has been successfully for radiolabeling of small biomolecules for imaging tumors [61,79–86].

2.3.3. Gallium-68— ^{68}Ga is also a generator-produced isotope with a half-life of 68 min. ^{68}Ga decays by positron emission and hence 511-keV annihilation radiation [64,66]. The photon abundance is 178%. In general, the generator is made up of alumina loaded in a plastic or glass column. Carrier free ^{68}Ge in HCl is neutralized in EDTA solution and adsorbed on the column. ^{68}Ga is eluted from the column with 0.05 M EDTA solution. Alternatively, ^{68}Ge is adsorbed on a stannous dioxide column and ^{68}Ga is eluted with 1 N HCl. This generator can be eluted quite frequently since maximum yield is obtained in a few hours. Due to the long half-life (271 days) of ^{68}Ge , the ^{68}Ge - ^{68}Ga generator can be used for 1 – 2 years, allowing PET imaging at facilities without the on-site cyclotron. The half-life of ^{68}Ga is long enough to permit multiple-step radiotracer syntheses and data requisition over longer periods. Thus, cameras with the highest sensitivity are not prerequisite for obtaining high quality images. With properly designed radiotracers, ^{68}Ga could become the radionuclide as useful for PET imaging as ^{99m}Tc for planar and SPECT imaging. However, there is a lack of efficient production

methods for ^{68}Ge . As a result, ^{68}Ga is often considered the most cost-prohibitive radionuclide for PET imaging [71]. Right now, ^{68}Ge - ^{68}Ga generators are available from several commercial sources in Russia, Europe and the United States.

2.3.4. Technetium-94m— $^{94\text{m}}\text{Tc}$ has a half-life of 52 min and β^+ energy of 2.47 MeV (72%). It can be obtained from a number methods, including $^{94}\text{Mo}(\text{p}, \text{n})/^{94\text{m}}\text{Tc}$ (13.5 – 11 MeV), $^{\text{nat}}\text{Nb}(\text{}^3\text{He}, 2\text{n})/^{94\text{m}}\text{Tc}$ (18 – 10 MeV), $^{92}\text{Mo}(\alpha, \text{pn})/^{94\text{m}}\text{Tc}$ (26 – 18 MeV). To obtain sufficient yield using small cyclotrons, the reaction $^{94}\text{Mo}(\text{p}, \text{n})/^{94\text{m}}\text{Tc}$ is preferred. Access to this isotope makes it possible to use PET to estimate the uptake of $^{99\text{m}}\text{Tc}$ radiotracers. The quantitative superiority of PET permits modeling of radiotracer kinetics and dosimetry measurements. Commercially kits for $^{99\text{m}}\text{Tc}$ radiotracers (e.g. $^{99\text{m}}\text{Tc}$ -Sestamibi and $^{99\text{m}}\text{Tc}$ -Tetrofosmin) might be used to prepare $^{94\text{m}}\text{Tc}$ analogs. The use of dual isotopes $^{99\text{m}}\text{Tc}/^{94\text{m}}\text{Tc}$ (SPECT/PET) may provide much better imaging quality. The integration of PET and SPECT radiotracer would pave the way for better exploitation of current strengths of both imaging modalities. However, the availability of $^{94\text{m}}\text{Tc}$ for clinical applications remains a significant challenge.

2.3.5. Zirconium-89— ^{89}Zr has a half-life of 78.5 h with a β^+ emission (897 keV, 23%) and EC (77%). ^{89}Zr is produced by cyclotron from the nuclear reaction [$^{89}\text{Y}(\text{p}, \text{n})/^{89}\text{Zr}$], but the separation of ^{89}Zr is requires both solvent extraction and ion-exchange chromatography [64, 66]. A simplified production method using the [$^{89}\text{Y}(\text{d}, 2\text{n})/^{89}\text{Zr}$] reaction requires only one-step ion-exchange separation. Due to its long half-life, it is an attractive isotope for ^{89}Zr -labeling of biomolecules. Theoretically, all the BFCs, such as DTPA and DOTA derivatives, for ^{111}In and ^{90}Y -labeling can be used for ^{89}Zr -labeling of biomolecules.

2.4. Radiometals for Therapeutic Radiopharmaceuticals

Table 4 lists some selected isotopes useful for radiotherapy. Identifying an appropriate radionuclide for radiotherapy often requires weighing various factors [5,6,9,12,68], including tumor uptake and tumor retention, blood clearance, rate of radiation delivery, half-life and specific activity of the radionuclide, and the feasibility of large-scale production of the radionuclide in an economical fashion. The main objective for the receptor-based target-specific radiotherapy is to deliver a tumoricidal radiation dose to tumor cells without causing unmanageable side-effects. Other practical considerations in selecting a radionuclide for a given targeting biomolecule in target-specific tumor radiotherapy are availability and quality. The radiochemical purity has to be sufficient and reproducible, as trace amounts of impurities (particularly the radionuclide impurities) can affect the radiolabeling and radiochemical purity of the radiopharmaceutical. The receptor sites in tumors are typically limited in number. This requires that the chosen radionuclide have high specific activity, which depends primarily on the production method. Trace metal contaminants must be minimized as they often compete with the radionuclide for the “cold” BFC-BM conjugate and their metal complexes may compete for receptor binding with the radiolabeled BFC-BM conjugate. Among various radionuclides, ^{90}Y and radiolanthanides are of particular interest. There are several lanthanide isotopes to choose: low energy β -emitter ^{177}Lu , medium energy β -emitters, ^{153}Sm , and high-energy β -emitters, ^{166}Ho and ^{90}Y . Depending on the tumor size and location, the choice of the β -emitter may be different. For example, medium or low energy β -emitters such as ^{177}Lu are better for smaller metastases while high-energy β -emitters such as ^{90}Y are used for larger tumors. Chelation chemistry of ^{90}Y and lanthanide radionuclides is well developed and understood. In addition, β -emitters have relatively long penetration range (2 – 12 mm), which is particularly important for solid tumors with high heterogeneity. The β -particle emitters yield a homogeneous dose distribution due to the “cross-fire effect” even when they are heterogeneously distributed in the tumor.

2.3.1. Yttrium-90— ^{90}Y is a generator-produced radionuclide, resulting from the decay of ^{90}Sr . It decays with the high energy β -particle ($E_{max} = 2.28$ MeV, 100% abundance) to form ^{90}Zr . ^{90}Y has a half-life of 2.7 days, which is short enough to achieve a critical dose rate and at the same time is long enough to allow the radiopharmaceutical to be manufactured, transported and delivered for clinic use. The specific activity for ^{90}Y is very high, and is well suited for development of receptor-based therapeutic radiopharmaceuticals. For quantitative imaging, the corresponding ^{111}In -labeled BFC-BM conjugate is often used as a surrogate to determine the biodistribution characteristics and radiation dosimetry of the ^{90}Y -labeled BFC-BM conjugate.

2.3.2. Samarium-153— ^{153}Sm has three β -emissions (30% 0.64 MeV, 50% 0.71 MeV, and 20% 0.81 MeV) and a γ -emission (28% 103 keV) with a half-life of 1.95 days. It can be produced in large amount with high specific activity by neutron activation of enriched ^{152}Sm [65]. The short half-life of ^{153}Sm allows for the delivery of fractionated dose regimes while the 103-keV gamma ray is useful for biodistribution determination via gamma imaging.

2.3.3. Holmium-166— ^{166}Ho emits a beta particle with maximum energy of 1.85 MeV (maximum penetration range ~9 mm) and a small portion of gamma rays (80.6 keV at 6.6% and 1.38 MeV at 0.9%), which are useful for biodistribution determination of the therapeutic radiopharmaceutical via gamma imaging. It has a half-life of 26.78 h. ^{166}Ho is produced with relatively high specific activity by neutron capture reaction [$^{165}\text{Ho}(n, \gamma)^{166}\text{Ho}$] [65].

2.3.4. Lutetium-177— ^{177}Lu is a reactor-produced radionuclide. It has three β -emissions (12% 0.176 MeV, 9% 0.384 MeV, and 79% 0.497 MeV) and two γ -emissions (6.4% 113 keV and 11% 208 keV) with a half-life of 6.75 days. One method for the production of ^{177}Lu involves irradiation of enriched ^{176}Lu in a reactor. By this method, ^{177}Lu can be prepared in high yield and medium high specific activity at low cost. The specific activity of ^{177}Lu from University of Missouri Research Reactor is routinely more than 20 Ci/mg [65].

2.3.5. Rhenium-186—Rhenium has two isotopes (^{186}Re and ^{188}Re). ^{186}Re has a half-life of 3.68 days with a β -emission ($E_{max} = 1.07$ MeV, 91% abundance) and a gamma-photon ($E = 137$ keV, 9% abundance) which should allow imaging during therapy. ^{186}Re is a reactor-produced radionuclide. There is only one possibility to produce ^{186}Re by the irradiation of ^{185}Re with neutrons ($^{185}\text{Re}(n, \gamma)^{186}\text{Re}$). The yield of ^{186}Re depends on the amount of Re in the target, the energy of the neutrons available, and the neutron reflux. The specific activity is from low to medium, but a carrier-free product is not possible.

2.3.6. Rhenium-188— ^{188}Re has a half-life of 16.98 h with a high-energy β -emission ($E_{max} = 2.12$ MeV, 85% abundance) and 155 keV gamma photons (15% abundance). ^{188}Re can be prepared either from the nuclear reaction ($^{187}\text{Re}(n, \gamma)^{188}\text{Re}$) or from the ^{188}W - ^{188}Re generator. The generator-produced ^{188}Re is carrier-free and has very high specific activity. The major advantage of using ^{188}Re is the inexpensive and readily available ^{188}W - ^{188}Re generator, which has a long useful shelf-life. The 155-keV gamma photons are useful for biodistribution determination and radiation dosimetry calculation of the ^{188}Re -labeled BFC-BM conjugate.

2.3.7. Copper-67—Among several copper isotopes, ^{67}Cu has the longest half-life ($t_{1/2} = 62$ h). ^{67}Cu decays by three β -emissions (45% 0.40 MeV, 3% 0.48 MeV, and 20% 0.58 MeV), and two γ -emissions with energies of 93 (17%), and 185 (48%) keV. The γ -emissions permit imaging of the radionuclide distribution during therapy; but they may become problematic due to extra radiation burden to normal organs if ^{67}Cu is used in therapeutic radiopharmaceuticals. ^{67}Cu is produced by bombarding a natural Zn target with 200 MeV

protons ($^{68}\text{Zn}(p, 2p)$) in an accelerator. It is difficult to obtain very high specific activity using this production method. More recently, the production of ^{67}Cu on low and medium-energy cyclotrons has been reported. Kastleiner et al predicted that up to 400 mCi of ^{67}Cu can be obtained at saturation using a small cyclotron ($E_p = 17 - 18 \text{ MeV}$; 80 μA beam current [72]).

3. BFCs for $^{99\text{m}}\text{Tc}$ and $^{186/188}\text{Re}$ -Labeling of Biomolecules

3.1. Why $^{99\text{m}}\text{Tc}$?

Nearly 80% of radiopharmaceuticals currently available in clinical nuclear medicine are $^{99\text{m}}\text{Tc}$ compounds due to ideal nuclear properties of $^{99\text{m}}\text{Tc}$. The 6 h half-life is long enough to allow a radiopharmacist to carry out radiosynthesis and prepare the dose, and for nuclear medicine practitioners to collect clinically useful images. At the same time, it is short enough to permit administration of millicurie amounts of $^{99\text{m}}\text{Tc}$ radiopharmaceutical without causing a significant radiation dose to the patient. The monochromatic 140 KeV photons are readily collimated to give images of high spatial resolution. Furthermore, $^{99\text{m}}\text{Tc}$ is readily available from the ^{99}Mo - $^{99\text{m}}\text{Tc}$ generators at low cost.

3.2. Diverse Redox Chemistry of Technetium

One of the characteristics of technetium is its diverse redox chemistry. Table 5 summarizes various oxidation states of technetium. Since there is no effective chemistry that can be used to attach $^{99\text{m}}\text{TcO}_4^-$ to biomolecules, the Tc(VII) in $^{99\text{m}}\text{TcO}_4^-$ has to be reduced to a lower oxidation state. When $^{99\text{m}}\text{TcO}_4^-$ is reduced, the oxidation state of Tc depends upon the reducing agent, chelator, and reaction conditions. The rich and diverse redox chemistry makes it difficult to control the oxidation state and solution stability of Tc chelates. At the same time, it also provides opportunities to modify structures and properties of technetium complexes by the choice of chelators with high affinity for a specific oxidation state of Tc. Technetium chemistry has been reviewed recently [10,11,87].

3.3. Isomerism

Another aspect of technetium chemistry is isomerism, including geometric isomers, epimers, enantiomers, and diastereomers [4,8,10,11,88]. Figure 3 shows selected examples of isomerism in technetium chelates. Epimers are often found in square pyramidal or octahedral oxotechnetium complexes containing chelating ligands with substituents on the ligand backbone or a tertiary amine-N donor atom. Formation of epimers is due to the relative orientation (*anti* and *syn*) of substituents to the $[\text{Tc}=\text{O}]^{3+}$ core [10,88]. Enantiomers are often found in Tc(V)-oxo complexes, such as $[\text{TcO}(\text{MAG}_3)]^-$, due to asymmetrical bonding of chelator to the $[\text{Tc}=\text{O}]^{3+}$ core even though the free chelator does not have a chiral center. Enantiomers are also formed when the Tc chelate contains a pro-chiral chelator, such as tricine in ternary ligand Tc complexes (Figure 3). Enantiomers are indistinguishable by NMR methods; but they are separable under chiral chromatographic conditions (chiral solid phase or chiral mobile phase) by HPLC. If a Tc complex contains two or more chiral centers, diastereomers may be formed, and are often separated by reversed phase HPLC methods. Isomers often have different lipophilicity and biodistribution patterns. This is particularly true for small Tc complexes as their biological properties are determined by physical and chemical properties of the Tc chelate. For example, $[\text{TcO}(\text{map})]^-$ (map = 2,3-bis(mercaptoacetamido)propanoate), has two epimers (*anti* and *syn*) due to the disposition of the COOH group on the chelate ring relative to the Tc=O moiety. It was reported that in humans 58% of *syn* isomer was excreted at 30 min as compared to only 19% of *anti* isomer [89]. For receptor-based target-specific radiopharmaceuticals, the target uptake is largely dependent on receptor binding affinity of the radiolabeled receptor ligand, receptor population and the blood clearance, which is determined by physical properties of both the targeting biomolecule and Tc chelate. Formation of isomers for the Tc chelate may have significant impact on biological properties

of a target-specific radiopharmaceutical. Therefore, the choice of BFCs should be those which form technetium complexes with minimal isomerism.

3.4. Challenges for ^{99m}Tc -Labeling of Biomolecules

^{99m}Tc radiopharmaceuticals are used in very low concentrations (10^{-8} to 10^{-6} M). Therefore, the radiolabeling kinetics must be taken into consideration in the development of ^{99m}Tc radiopharmaceuticals. ^{99m}Tc is obtained from the ^{99}Mo - ^{99m}Tc generator as $^{99m}\text{TcO}_4^-$ in saline. This requires that the radiolabeling be performed in aqueous solution. Due to the short half-life ($t_{1/2} = 6.02$ h) of ^{99m}Tc , radiosynthesis must be completed within 30 min. The radiochemical purity (RCP) of the radiopharmaceutical must be greater than 90% since injection of a mixture of different ^{99m}Tc -containing species will decrease organ specificity, and needlessly increases the radiation burden to patient. Since all ^{99m}Tc radiopharmaceuticals are administered by intravenous injection, radiosynthesis has to be conducted under sterile and pyrogen free conditions. This requirement virtually eliminates any chromatographic purification of the desired ^{99m}Tc radiopharmaceutical. Each of these constraints provides a unique challenge for inorganic chemistry. Fortunately, most of these challenges have been successfully met with the development of coordination chemistry of technetium and new ^{99m}Tc -labeling techniques.

3.5. Requirements for Ideal BFCs

An ideal BFC is that which is able to form a stable ^{99m}Tc complex in high yield at very low concentration of the BFC-BM conjugate. To achieve this goal, the BFC must selectively stabilize an intermediate or lower oxidation state of Tc so that the ^{99m}Tc complex is not subject to redox reactions. Oxidation state changes are often accompanied by transchelation of ^{99m}Tc from a ^{99m}Tc -BFC-BM complex to the native chelating ligands in biological systems. The BFC should form a ^{99m}Tc complex which has thermodynamic stability and kinetic inertness with respect to dissociation or release of ^{99m}Tc . The BFC should form the ^{99m}Tc complex with a minimum number of isomers since different isomeric forms of the ^{99m}Tc -chelate may result in significantly different biological and pharmacokinetic characteristics of the ^{99m}Tc -BFC-BM complex. Finally, the conjugation group should be easily attached to the targeting biomolecule.

3.6. Kit Formulation

Due to the 6 h half-life of ^{99m}Tc , a kit formulation is required for ^{99m}Tc radiopharmaceuticals. The kit formulation is particularly important for consistency and reproducibility in the RCP performance during ^{99m}Tc -labeling. In general, the kits are sterile, pyrogen free, and non-radioactive mixtures, which are dried by lyophilization and stored under nitrogen in glass vials. For target-specific ^{99m}Tc radiopharmaceuticals, a kit contains a BFC-BM conjugate and a reducing agent, if necessary. Kit components are often dissolved in a buffer system, which is used for pH control during the manufacturing and radiolabeling processes. Sometimes a bulking agent is needed so that kit components can crystallize on the crystals of the bulking agent. Other components (antioxidants, solubilizing agents, and weak transferring ligands) may be needed to improve the yield and solution stability of the ^{99m}Tc radiopharmaceutical. In many cases, ^{99m}Tc -labeling can be accomplished simply by adding $^{99m}\text{TcO}_4^-$ to the kit. It must be emphasized that all kit components be non-toxic and suitable for intravenous injection. The amount of BFC-BM conjugate in the kit formulation has to be sufficiently high so that high RCP can be achieved for the intended ^{99m}Tc radiopharmaceutical. However, a large amount of the BFC-BM may result in receptor site saturation, blockage of the receptor binding of the ^{99m}Tc radiotracer, as well as unwanted side effects. To avoid these problems, the BFC-BM concentration in each kit has to be very low (e.g. $20 \mu\text{g/mL}$ or $\sim 2 \times 10^{-6}$ M for a BFC-BM conjugate with molecular weight of 1000 Daltons). Otherwise, post-labeling purification is needed to remove excess unlabeled BFC-BM conjugate, which is time consuming and not

amenable for the kit formulation. Compared to the total Tc concentration ($\sim 5 \times 10^{-7}$ M) in 100 mCi of $^{99m}\text{TcO}_4^-$ (eluted with 24 h prior-elution time), 20 μg of the BFC-BM conjugate is not in overwhelming excess. It should be noted that the amount of BFC-BM conjugate also depends largely on receptor population, receptor ligand binding affinity and possible side effect caused from the BFC-BM conjugate. A careful study is recommended to determine the optimum amount of BFC-BM conjugate in the kit formulation.

3.7. Technetium Cores

Figure 4 shows some selected Tc cores, which have been used for ^{99m}Tc -labeling of biomolecules, including antibodies, antibody fragments, small peptides, and nonpeptide receptor ligands. Since Tc chemistry and Tc cores have been reviewed in detail recently [3,4, 8,10,11,87], we will focus on the bifunctional coupling systems and their related coordination chemistry with the $[\text{Tc}=\text{O}]^{3+}$, $[\text{Tc}\equiv\text{N}]^{2+}$, $[\text{Tc}(\text{CO})_3]^+$ and $[\text{Tc}]\text{HYNIC}$ cores.

3.7.1. $[\text{Tc}=\text{O}]^{3+}$ Core—The $[\text{Tc}=\text{O}]^{3+}$ core is very stable in the presence of a good chelator in aqueous solution. It is the most frequently used technetium core for ^{99m}Tc -labeling of biomolecules (Table 4). The $[\text{Tc}=\text{O}]^{3+}$ core forms square pyramidal Tc(V)-oxo complexes with tetradentate chelators, such as N_2S_2 diamidedithiols (Figure 5: DADS), N_3S triamidethiols, N_2S_2 monoamidemonoaminedithiols (Figure 5: MAMA), and N_2S_2 diaminedithiols (Figure 6: DADT). N_2S_2 DADS chelators contain two amide-N and two thiolate-S donors, and form stable anionic oxotechnetium complexes with the $[\text{Tc}=\text{O}]^{3+}$ core [89–91]. Like N_2S_2 DADS, N_3S triamidethiols also form very stable anionic Tc(V)-oxo complexes [91–93]. Fritzberg and coworkers first reported the use of 4,5-bis(thioacetamido) pentanoate (mapt) as the BFC in labeling antibodies and their fragments with ^{99m}Tc by the preformed chelate approach [94–96]. Other N_2S_2 DADS and N_3S triamidethiols have also been used for ^{99m}Tc -labeling of small RGD peptides [97–99]. N_2S_2 DADT chelators (Figure 5) represent another class of BFCs that bind the $[\text{Tc}=\text{O}]^{3+}$ core strongly to form stable Tc(V) complexes. They can be tribasic utilizing two thiolate-S atoms, one deprotonated amine-N and one neutral amine-N to form neutral Tc(V)-oxo complexes, or dibasic using two thiolate-S and two amine-N donor atoms to form cationic Tc(V)-oxo complexes [100–108]. N_2S_2 MAMA chelators (Figure 5) contain an amine-N, an amide-N and two thiolate-S donors, and bind to the $[\text{Tc}=\text{O}]^{3+}$ core to form neutral complexes, $[\text{MAMA}^{99m}\text{TcO}]$ [109]. The N_2S_2 MAMA-type BFCs have been used for ^{99m}Tc -labeling of progesterone receptor ligands [110–112], platelet glycoprotein IIb/IIIa receptor antagonists [97,98], and dopamine transporters [113]. Small peptides, such as Gly-Ala-Gly-Gly and Gly-Ser-Cys (Figure 6) have also been proposed as BFCs for ^{99m}Tc -labeling of biomolecules [114,115]. The attachment of the tripeptide chelating sequences can be easily incorporated into solid-phase peptide synthesis. These tripeptide sequences form stable technetium complexes with the $[\text{Tc}=\text{O}]^{3+}$ core. As a matter of fact, the tripeptide sequence with N_3S donor atoms has been used to bind the $[\text{Tc}=\text{O}]^{3+}$ core in ^{99m}Tc -P280, a FDA-approved thrombosis imaging agent [116–119].

3.7.2. $[\text{Tc}\equiv\text{N}]^{2+}$ Core—The $[\text{Tc}\equiv\text{N}]^{2+}$ core is isoelectronic with $[\text{Tc}=\text{O}]^{3+}$. The nitrido ligand is a powerful π -electron donor and shows a high capacity to stabilize the Tc(V) oxidation state. The $[\text{Tc}\equiv\text{N}]^{2+}$ core forms Tc(V)-nitrido complexes with various chelators [120–126]. The $[\text{MAMA}^{99m}\text{Tc}\equiv\text{N}]^{2+}$ core has been used for ^{99m}Tc -labeling of small peptides and benzodiazepine receptor ligands [127–129]. The PXP bisphosphine ligands (Figure 7) are used as coligands to stabilize the $[\text{MAMA}^{99m}\text{Tc}\equiv\text{N}]^{2+}$ core, and the BFCs containing thiolate-S, amine-N or carboxylate-O donors are attached to the peptide or benzodiazepine receptor ligands. It has been demonstrated that the $[\text{MAMA}^{99m}\text{TcN}(\text{PXP})]^{2+}$ fragment reacts with the cysteine to form asymmetrical ^{99m}Tc -nitrido complexes in very high specific activity [127].

3.7.3. [$^{99m}\text{Tc}(\text{CO})_3$] $^+$ Core—Alberto et al first reported synthesis of Tc(I) and Re(I) complexes $[\text{M}(\text{H}_2\text{O})_3(\text{CO})_3]^+$ ($\text{M} = ^{99m}\text{Tc}$ and ^{188}Re) by direct reduction of [^{99m}Tc] pertechnetate or [^{188}Re]perrhenate with sodium borohydride in aqueous solution [130–132]. The yield of the ^{99m}Tc or ^{188}Re complex was > 95%. In [$^{99m}\text{Tc}(\text{H}_2\text{O})_3(\text{CO})_3$] $^+$, all three water molecules are labile with respect to substitution [133–138]. A variety of BFCs can be used for the ^{99m}Tc -labeling of biomolecules [139–148]. Figure 8 shows examples of bidentate and tridentate chelators containing imidazoles, pyridines, pyrazoles, amides, amines, carboxylic acids or combination thereof. Since it is a natural amino acid, histidine is of particular interest as the BFC for ^{99m}Tc -labeling of monoclonal antibodies and small peptides [144,146]. The diverse coordination chemistry of the [$^{99m}\text{Tc}(\text{CO})_3$] $^+$ core offers a tremendous opportunity for development of new BFCs. However, monodentate and bidentate chelators often form ^{99m}Tc (I)-tricarbonyl complexes with low solution stability, which results in high protein binding and high background activity in the blood stream. In contrast, tridentate chelators form ^{99m}Tc (I)-tricarbonyl complexes with high stability and rapid clearance from blood and other major organs. Alberto and coworkers reviewed organometallic radiopharmaceuticals recently [149, 150].

3.7.4. [Tc]HYNIC Core—Abrams et al first reported the use of 6-hydrazinonicotinamide (Figure 9: HYNIC) for ^{99m}Tc -labeling of polyclonal IgG [151,152]. Since then, HYNIC has been used for ^{99m}Tc -labeling of antibody fragments [153], chemotactic peptides [154–157], somatostatin analogs [158–163], liposomes [164], and antisense oligonucleotides [165,166]. Since HYNIC can only occupy one or two coordination sites, a coligand, such as tricine, is often needed to complete the coordination sphere of technetium. The advantage of using HYNIC as the BFC is its high ^{99m}Tc -labeling efficiency and the choice of coligands such as tricine and glucoheptonate, which allows easy modification of hydrophilicity and pharmacokinetics of the ^{99m}Tc -labeled biomolecules. However, the use of tricine as coligand suffers two major drawbacks: (1) solution instability of [$^{99m}\text{Tc}(\text{HYNIC-BM})(\text{tricine})_2$] (Figure 9), and (2) presence of multiple species in solution due to different bonding modalities of HYNIC and coligands [167,168]. To overcome these problems, Liu et al developed several versatile ternary ligand systems (HYNIC, tricine and water-soluble phosphine or pyridine analogs) that form ternary ligand technetium complexes [$^{99m}\text{Tc}(\text{HYNIC-BM})(\text{tricine})(\text{phosphine})$] (Figure 9) in high yield and high specific activity [168–171]. These ternary ligand ^{99m}Tc complexes have very high solution stability, and often show two peaks in their radio-HPLC chromatograms if the biomolecule contains one or more chiral centers. The presence of two peaks is due to the resolution of two diastereomers resulting from chiral centers on the peptide backbone and the chiral Tc chelate [168–171]. The 1:1:1:1 composition for Tc:HYNIC:L:tricine was determined through a series of mixed ligand experiments [169,170], and has been confirmed by FAB-MS and LC-MS at both ^{99m}Tc and ^{99}Tc levels [171,172]. Many coligands (Figure 9) have been used for ^{99m}Tc -labeling of small biomolecules, such as chemotactic peptides [168] and LTB_4 receptor antagonists [173,174] for imaging infection/inflammation, cyclic RGD peptides for imaging integrin $\alpha_v\beta_3$ -positive tumors [175–179], and a GPIIb/IIIa receptor antagonist for diagnosis of thrombi [169,170,180,181].

3.8. Radiolabeling Approaches

The choice of ^{99m}Tc -labeling approaches depends on biomolecules (antibody versus small biomolecules) and the purpose of study (proof of concept versus product development). In the last three decades, a large number of techniques have been developed for ^{99m}Tc -labeling of biomolecules, including monoclonal antibodies, small peptides and non-peptide receptor ligands. They are often classified into three main categories: direct labeling approach, pre-labeling (or preformed chelate) approach, and post-labeling approach.

3.8.1. Direct Labeling—The direct labeling approach (Chart I) usually uses a reducing agent such as SnCl_2 to convert the disulfide linkages into free thiols, which bind strongly to the Tc. This approach is that it is easy to carry out [182–186]; but it applies only to antibodies or antibody fragments because many small biomolecules do not have any disulfide bonds, or in many cases the disulfide bond is too critical for maintaining their biological properties to be reduced. There are several critical questions to be answered for this approach. These include: oxidation state of technetium, number of $^{99\text{m}}\text{Tc}$ bonded to biomolecule, number of $^{99\text{m}}\text{Tc}$ -species in the radiolabeled kit, and impact of $^{99\text{m}}\text{Tc}$ -labeling on biological activity of the targeting biomolecule? In addition, there is little control over solution stability of the $^{99\text{m}}\text{Tc}$ radiotracer.

3.8.2. Pre-Labeling Approach—The pre-labeling or “pre-formed chelate” approach (Chart II) involves formation of the $^{99\text{m}}\text{Tc}$ -BFC chelate, and conjugation of the $^{99\text{m}}\text{Tc}$ -BFC chelate to a biomolecule in a separate step. This approach has been successfully used in labeling antibodies and their fragments with $^{99\text{m}}\text{Tc}$ [94–96]. In this approach, the chemistry is better defined, and the targeting biomolecule is not exposed to sometimes harsh conditions in the chelation step. For research purposes, this approach is very useful to demonstrate the proof of concept in a short period of time before making extensive efforts in preparing the BFC-BM conjugate. However, the multiple-step radiosynthesis is too complex and time consuming for routine clinical use, and makes it very difficult to develop a kit formulation.

3.8.3. Post-Labeling Approach—In the post-labeling, or indirect labeling, approach (Chart III), a BFC is first attached to the biomolecule to form BFC-BM conjugate. Once the BFC-BM conjugate is prepared, radiolabeling can be accomplished by direct reduction of $^{99\text{m}}\text{TcO}_4^-$ in the presence of a sufficient amount of the BFC-BM conjugate or by ligand exchange with an intermediate $^{99\text{m}}\text{Tc}$ complex, such as [$^{99\text{m}}\text{Tc}$]glucoheptonate. This approach combines the ease of direct labeling with well-defined chemistry of the preformed chelate approach. This is the most practical approach for kit formulation and for development of commercial products.

3.9. $^{99\text{m}}\text{Tc}$ -Labeling Efficiency

$^{99\text{m}}\text{Tc}$ -labeling efficiency is a term used to describe the ability of a BFC to achieve a high radiolabeling yield (> 90%) of its $^{99\text{m}}\text{Tc}$ complex. High radiolabeling efficiency is required for BFC in target-specific radiopharmaceuticals. However, there is little experimental data to compare the $^{99\text{m}}\text{Tc}$ -labeling efficiency of various BFCs. In general, there are several factors influencing $^{99\text{m}}\text{Tc}$ -labeling efficiency of a BFC. These include identity of donor atoms, BFC concentration, reaction temperature and time, and pH value in the mixture [187]. If BFC concentration is fixed, the conditions for $^{99\text{m}}\text{Tc}$ -labeling depend largely upon the nature of donor atoms. For example, high pH and heating at 100 °C for 30 min is required for successful $^{99\text{m}}\text{Tc}$ -labeling of N_3S triamidethiols and N_2S_2 DADS at low concentrations (10^{-5} – 10^{-6} M) while N_2S_2 MAMA chelators are well labeled under milder conditions. For the N_2S_2 DADT chelators, the ligand exchange with [$^{99\text{m}}\text{Tc}$]glucoheptonate can be completed within 60 min at room temperature [187]. In general, HYNIC and N_2S_2 DADT chelators are better BFCs for small biomolecules with high receptor binding affinity mainly due to their high $^{99\text{m}}\text{Tc}$ -labeling efficiency. In some cases, N_3S triamidethiol, N_2S_2 DADS, or N_2S_2 MAMA can also be used as BFCs if the use of a large amount (> 100 $\mu\text{g}/\text{mL}$) of BFC-BM conjugate does not cause unwanted side effects. For example, there is 100 μg of bibapcitide (P280) in each lyophilized AcuTect™ vial. This allows the use of less than 50 mCi of [$^{99\text{m}}\text{Tc}$]pertechnetate for radiolabeling [116–119].

3.10. ^{99m}Tc -Labeling of BFC-BM Conjugates

Once it is decided to use the indirect labeling approach, the next question will be how to synthesize the ^{99m}Tc -BFC-BM radiotracer. In general, there are three different approaches for successful preparation of the ^{99m}Tc -BFC-BM. These include direct reduction, ligand exchange, and reduction-exchange. The choice of synthetic route is largely dependent on both BFC and targeting biomolecule.

3.10.1. Direct Reduction—Using the reduction route, $^{99m}\text{TcO}_4^-$ is reduced in one step in presence of a BFC-BM conjugate [10,11,188]. The conditions employed in these preparations are dictated by short half-life of ^{99m}Tc , low concentration of $^{99m}\text{TcO}_4^-$, and chemical stability of the BFC-BM conjugate. The reaction generally produces a mixture of reduced ^{99m}Tc -species, and in many cases the chemical form and oxidation state in these ^{99m}Tc -containing species are not known. However, the ^{99m}Tc -BFC-BM complex can be prepared as a single predominant product by the choice of reducing agent and BFC under well-controlled conditions. Many reducing agents can be used to reduce $^{99m}\text{TcO}_4^-$ during radiolabeling. These include stannous chloride, borohydride, dithionate, dithionite, hypophosphoric acid, hydroxamine, formamidinium sulfonic acid, and water soluble phosphines. While most of these reductants can be used for synthesis of simple Tc complex radiopharmaceuticals, only a few of them have been used in commercial kits for routine preparation of target specific radiopharmaceuticals.

Sn(II) is the most commonly used reducing agent in commercial kits for the rapid preparation of ^{99m}Tc radiopharmaceuticals due to its fast reduction kinetics. However, the use of Sn(II) often leads to several problems. For example, during the synthesis of a ^{99m}Tc radiopharmaceutical, initial reduction of $^{99m}\text{TcO}_4^-$ leads to rapid formation of the Tc(VI) intermediate $^{99m}\text{TcO}_4^{2-}$, which is unstable with respect to disproportionation. The reduction of $^{99m}\text{TcO}_4^-$ can lead to the formation of Tc(IV), which undergoes rapid hydrolysis in aqueous solution to form $^{99m}\text{TcO}_2$. Sn(IV) also undergoes rapid hydrolysis to form insoluble SnO_2 . The formation of colloids ($^{99m}\text{TcO}_2/\text{SnO}_2$) compromises the radiolabeling yield of the radiotracer. Therefore, a weak chelating agent such as glucoheptonate (GH) is often used to stabilize Sn(II) and Tc in its intermediate oxidation state.

3.10.2. Ligand Exchange—The second route for successful ^{99m}Tc -labeling of a BFC-BM conjugate is the two-step ligand exchange synthesis. This route involves reduction of $^{99m}\text{TcO}_4^-$ by a reducing agent in the presence of a chelating agent such as glucoheptonate to form the $^{99m}\text{TcO}(\text{GH})_2^{n-}$ intermediate, which is then allowed to react with the BFC-BM conjugate under milder conditions to give the ^{99m}Tc -BFC-BM complex. This route is often used for the ^{99m}Tc -labeling of biomolecules that are sensitive to harsh reaction conditions (e.g. high pH and heating at elevated temperatures). $^{99m}\text{TcO}(\text{GH})_2^{n-}$ has been used for ^{99m}Tc -labeling of small peptides [97–99,116–119]. $^{99m}\text{TcO}(\text{L})_2^{n-}$ (L = tricine, mannitol, and glucamine) have also been used for ^{99m}Tc -labeling of HYNIC-conjugated biomolecules, such as small peptides [151–172]. Unlike tetradentate thiol-containing chelators, which replace glucoheptonate ligands in $^{99m}\text{TcO}(\text{GH})_2^{n-}$, HYNIC reacts with the $[\text{Tc}=\text{O}]^{3+}$ core [151–157]. The exchange ligand is the oxo-O atom while Tc(V) is reduced to Tc(III) when HYNIC binds to the Tc [10,11,32,33]. Tricine or glucoheptonate serves two purposes: as a ligand to stabilize the reduced ^{99m}Tc in its Tc(V) oxidation state, and as a coligand to stabilize the ^{99m}Tc HYNIC core.

3.10.3. Reduction-Substitution—The reduction/substitution route involves the use of a reducing chelator, such as bidentate 1,2-bis[bis(2-ethoxyethyl)phosphino]ethane [189,190], or a monodentate ligand, such as triphenylphosphine-3,3'-trisulfonate (TPPTS) [167–169]. The reducing ligand/chelator serve for two purposes: reducing $^{99m}\text{TcO}_4^-$ to a lower oxidation

state and acting as ligand/chelator in bonding to the Tc. Examples of this type of reducing chelator or ligands include 1,2-bis[bis(2-ethoxyethyl)phosphino]ethane in ^{99m}Tc -Tetrofosmin [189,190], and TPPTS in complexes [$^{99m}\text{Tc}(\text{HYNIC-BM})(\text{tricine})(\text{TPPTS})$] [167–169]. If TPPTS is replaced by an imine-N containing heterocycle, SnCl_2 has to be used to reduce $^{99m}\text{TcO}_4^-$ [170]. TPPTS has also been used as a reducing agent for preparation of Tc-nitrido complexes [$^{99m}\text{TcN}(\text{dithiocarbamate})_2$] [121,122].

3.11. BFCs for $^{186/188}\text{Re}$ -Labeling of Biomolecules

Rhenium is the group II congener of technetium. The coordination chemistry of rhenium is very similar (not identical) to that of technetium due to their periodic relationship. As a consequence, the BFCs developed for the ^{99m}Tc -labeling can be used for the $^{186/188}\text{Re}$ -labeling of biomolecules [191–193]. As a matter of fact, many therapeutic rhenium radiopharmaceuticals have been developed on the basis of ^{99m}Tc imaging agents. Despite of their similarities, there are also significant differences in ^{99m}Tc and $^{186/188}\text{Re}$. For example, a stronger reducing agent is needed to reduce Re(VII) in $^{186/187}\text{ReO}_4^-$ to a lower oxidation state due to slow reduction rate. The ternary ligand system (Figure 10: HYNIC-BM, tricine and TPPTS) works well for the ^{99m}Tc -labeling of small biomolecules [167–181]; but it has very limited success for the $^{186/188}\text{Re}$ -labeling of the same biomolecules due to slow redox chemistry of rhenium. To avoid this problem, the preformed chelate approach is often the choice for successful $^{186/188}\text{Re}$ -labeling of antibodies and their fragments [194–196]. A peptide-based BFC has also been successfully used for ^{186}Re -labeling of monoclonal antibodies [197]. The chemistry of rhenium in nuclear medicine has been reviewed by Blower, Griffiths and their coworkers [192,193].

4. BFCs for Radiolabeling of Biomolecules with Gallium and Indium Radionuclides

Current interest in the coordination chemistry of gallium stems, at least in large part, from potential applications of ^{68}Ga -labeled biomolecules as PET imaging agents. ^{111}In is a gamma emitter with the γ -photon energy of 173 (89%) and 247 keV (95%) and is widely used (second only to ^{99m}Tc) in gamma scintigraphy. The coordination chemistry and radiochemistry related to gallium and indium radionuclides have been reviewed recently [6,7,13].

4.1. Gallium and Indium Chemistry

Both gallium and indium are group IIIB metals. The most prevalent oxidation state of gallium and indium in aqueous solution is +3. Due to their high charge density, Ga(III) and In(III) prefer hard donors, such as amine-N and carboxylate-O atoms. Because of the small size, Ga(III) is often six-coordinated [198–203]. Both Ga(III) and In(III) are similar to Fe(III) with respect to their coordination chemistry and biological properties. Since they are highly charged cations, hydrolysis of Ga(III) and In(III) at pH >4 remains a significant challenge during radiolabeling. Another challenge is the ligand exchange with transferrin after ^{68}Ga and ^{111}In radiopharmaceuticals are injected into biological system. It is no surprising that the BFCs for target-specific ^{68}Ga and ^{111}In radiopharmaceuticals are dominated by polydentate chelators (Figure 10) with hard donors, such as amine-N and carboxylate-N atoms. Among these macrocyclic and acyclic BFCs, NODASA (1,4,7-triazacyclononane-N-succinic acid-N',N''-diacetic acid) and NODAGA (1,4,7-triazacyclononane-N-glutamic acid-N',N''-diacetic acid) are particularly useful for chelation of ^{68}Ga due to the perfect fit between the size of Ga(III) and coordination cavity formed by the N_3O_3 donor atoms [201–205]. The coordination cavity of DOTA (1,4,7,10-tetraazacyclododecane-1,4,7,10-tetraacetic acid) is too big for Ga(III), and only six (N_4O_2) out of N_4O_4 donors are used in bonding to Ga(III) [206]. As a result, the thermodynamic stability constant of Ga(NOTA) (log $K = 30.98$; $\text{NOTA} = 1,4,7$ -

triazacyclononane-1,4,7-triacetic acid) is much higher than that of Ga(DOTA) ($\log K = 21.33$) [207].

4.2. Differences between Gallium and Indium

Despite their similarities, Ga(III) and In(III) are different in their size and charge density. This difference is often reflected by their different coordination chemistry with DTPA (diethylenetriaminepentaacetic acid) and DOTA derivatives. For example, Ga(III) has an ionic radius of 0.65 Å [208]. The coordination number of Ga(III) is 6 in its complexes, such as [Ga(Brbad)]ClO₄·DMSO (H₂Brbad = 1,10-bis(2-hydroxy-5-bromobenzyl)-1,4,7,10-tetraazadecane) [209], Ga(DOTA-D-Phe-NH₂) (DOTA-D-PheNH₂ = 1,4,7,10-tetraazacyclododecane-4,7,10-tricarboxymethyl-1-yl-acetyl-D-Phe-NH₂) [206], Ga(NODASA) [204], Ga(HDOTA) [210], and Ga(DO3A-xy-TPP)⁺ (DO3A-xy-TPP = triphenyl(4-((4,7,10-tris(carboxymethyl)-1,4,7,10-tetraazacyclododecan-1-yl)methyl)benzyl)phosphonium) [211]. In(III) has an ionic radius of 0.92 Å [208], and is either seven-coordinated in its complexes, such as In(DO3A-xy-TPP)⁺ [211] and In(DO3A) (DO3A = 1,4,7,10-tetraazacyclododecane-1,4,7-triacetate) [212], or 8-coordinated in In(DTPA)²⁻ [213], In(DOTA-D-Phe-NH₂) [208], In(DOTA-AA) (DOTA-AA = 1,4,7,10-tetraazacyclododecane-1,4,7,10-tetraacetic acid mono(*p*-aminoanilide)) [214], and In(DTPA-BA₂) (BA = benzylamine) [215]. The structural difference has been attributed to the higher tumor uptake of ⁶⁷Ga-DOTATOC than that of ¹¹¹In-DOTATOC, and much lower kidney uptake of ⁶⁷Ga-DOTATOC than that of ¹¹¹In-DOTATOC [206].

4.3. BFCs for ⁶⁸Ga and ¹¹¹In-Labeling of Biomolecules

DTPA, DOTA and NOTA derivatives (Figure 10) are often used for the ⁶⁸Ga and ¹¹¹In-labeling of small biomolecules [204, 205, 216–222]. Among different BFCs, NODASA and NODAGA are particularly useful for ⁶⁸Ga-labeling due to the high hydrophilicity and stability of their ⁶⁸Ga chelates, and their higher ⁶⁸Ga-labeling efficiency than that of the corresponding DOTA analogs [204, 217]. The fast and efficient radiolabeling is especially critical for the ⁶⁸Ga-labeled small biomolecules due to its short half-life ($t_{1/2} = 68$ min). It is important to note that free ⁶⁸Ga and ¹¹¹In tend to localize in liver and lungs due to their strong binding capability to transferrin while ⁹⁰Y and lanthanide isotopes are readily deposited on the bone [223].

5. BFCs for Radiolabeling of Biomolecules with Copper Radionuclides

5.1. Why Copper Radionuclides?

Copper has several radionuclides, such as ⁶⁰Cu, ⁶¹Cu, ⁶²Cu, ⁶⁴Cu and ⁶⁷Cu. The rich coordination chemistry of copper in combination with diverse nuclear properties of its radionuclides offers many opportunities for development of diagnostic (⁶⁰Cu, ⁶¹Cu, ⁶²Cu and ⁶⁴Cu) and therapeutic (⁶⁴Cu and ⁶⁷Cu) radiotracers. The coordination chemistry of Cu(II) with various acyclic and macrocyclic chelators is well understood. In addition, the availability of ⁶²Zn-⁶²Cu generators and ⁶⁴Cu with high specific activity makes it more feasible to develop target-specific radiopharmaceuticals with copper radionuclide. Copper radionuclide production, coordination chemistry, radiochemistry, and nuclear medicine applications have been reviewed exhaustively [6,7,13,72,224–228].

5.2. Copper Chemistry

Copper is a first-row transition metal. Its chemistry in aqueous solution is restricted to two oxidation states: Cu(I) and Cu(II). Cu(I) has the d^{10} configuration. Its complexes remain stable in aqueous solution only when chelators contain soft donors, such as phosphine-P and thioether-S. The coordination geometry for Cu(I) complexes are almost always tetrahedron. Cu(II) has

the d^9 configuration. The coordination number is 4, 5 or 6 depending on denticity of the chelator. The 4-coordinated Cu(II) complexes are normally square-planar while the square-pyramid coordination geometry is often seen in 5-coordinated Cu(II) complexes. In six-coordinated Cu(II) complexes, the two apical donor atoms are weakly bonded to the Cu(II) in a distorted octahedral arrangement, due to John-Teller distortion. Because of the d^9 configuration, Cu(II) complexes are often kinetically labile with respect to ligand dissociation. Therefore, the design of BFCs (Figure 11) for copper radionuclides has been focused on macrocyclic chelators that are able to form Cu(II) complexes with both high thermodynamic stability and kinetic inertness [224–228]. BFCs for radiolabeling of biomolecules with copper radionuclide have been reviewed recently [225].

5.3. BFCs for Copper Radionuclides

Meares and coworkers reported the first use macrocyclic chelators, such as cyclam and cyclen (Figure 11), for ^{67}Cu -labeling of monoclonal antibodies [229]. Since then, many DOTA and TETA (1,4,8,11-tetraazacyclotetradecane-1,4,8,11-tetraacetic acid) derivatives have been successfully used for the $^{64/67}\text{Cu}$ -labeling of biomolecules [79–86, 230–237], including antibodies and small peptides. The $^{64/67}\text{Cu}$ -labeled antibody conjugates often have high liver uptake and long liver retention, which was attributed to the transfer of $^{64/67}\text{Cu}$ from the $^{64/67}\text{Cu}$ -TETA chelate to ceruloplasmin and/or superoxide dismutase in the liver [238]. The cross-bridged cyclam derivatives (Figure 11) are developed to improve the stability of their $^{64/67}\text{Cu}$ chelates. The ^{64}Cu -labeling requires extensive incubation time at $>75^\circ\text{C}$ to complete chelation of ^{64}Cu [239, 240]. For small molecules, heating at elevated temperatures will not be a significant challenge as long as it can improve the radiolabeling efficiency. CB-TE2A (Figure 11: CB-TE2A = 2,2'-(1,4,8,11-tetraazabicyclo[6.6.2]hexadecane-4,11-diyl) diacetic acid) has also been used for ^{64}Cu -labeling of bombesin peptides [241, 242]. It was found that the ^{64}Cu -labeled CB-TE2A-bombesin conjugates have better *in vivo* stability than their DOTA analogs. SarAr (Figure 11: SarAr = N1-(4-aminobenzyl)-3,6,10,13,16,19-hexaazabicyclo[6.6.6]icosane-1,8-diamine) is a relatively new BFC, and has been conjugated to the whole and fragmented B72.3 murine antibody [225, 245]. It was claimed that the resultant immunoconjugate was radiolabeled quantitatively using slight molar excess ($<10\%$) of ^{64}Cu . The ^{64}Cu -labeling was reported to be significantly faster than other macrocyclic BFCs under the same reaction conditions [245]. It must be noted that such a high ^{64}Cu -labeling efficiency is truly remarkable, and is extremely intriguing. However, small biomolecules should be used to demonstrate if ^{64}Cu is indeed attached to the SarAr BFC or simply bonded to amino acid residues (histidine and cysteine) of the whole or fragmented B72.3 murine antibody. Recently, Prasanphanich and coworkers reported the use of ^{64}Cu -labeled NOTA and DOTA-bombesin conjugates for imaging gastrin-releasing peptide receptor-positive tumors [246]. It has been clearly demonstrated that the NOTA chelator has high ^{64}Cu -labeling efficiency, and its ^{64}Cu chelate has very high solution stability. Results from both biodistribution and microPET imaging studies indicate that the ^{64}Cu -labeled NOTA-bombesin conjugates have very little or no *in vivo* dissociation of ^{64}Cu from the radiotracer [246].

6. BFCs for Radiolabeling of Biomolecules of Yttrium and Lanthanide Radionuclides

6.1. Requirements for Therapeutic Radiopharmaceuticals

While diagnostic radiotracers rely on high T/B ratios in a short period of time, the success of tumor radiotherapy depends on high concentration of radionuclide in tumor for a long duration [3–7, 12, 15, 16]. Thus, an ideal therapeutic radiopharmaceutical must have the following characteristics: high tumor uptake, high tumor-to-background ratio, long tumor residence time, and fast clearance. High tumor uptake and fast renal clearance are important to improve the T/B ratio and to reduce radiation burden to normal organs, such as kidneys and bone marrow.

The radiopharmaceutical must have high RCP $\geq 90\%$ and high solution stability. Since the radiopharmaceutical is manufactured in a centralized facility, it must retain its chemical and biological integrity during storage and transportation. This requires that the BFC form a metal chelate with high thermodynamic stability and kinetic inertness. Once again, the coordination chemistry of BFCs plays a significant role in the development of therapeutic radiopharmaceuticals [4,6,12].

6.2. Fundamentals of Yttrium and Lanthanide Chemistry

Yttrium and lanthanide metals favor the +3 oxidation state. Due to their similar charge, ionic radii (Figure 12) and coordination chemistry, yttrium is often treated as a “pseudo-lanthanide” metal. Since the *4f* electrons are inner electrons, shielded from external influences by overlying *5s*², *5p*⁶ and *6s*²- electron shells, and are normally not involved in the bonding, interactions between “hard”-donor atoms, such as amine-N and carboxylate-O, and lanthanide metal ions are predominately ionic. Free Y(III) and Ln(III) ions are coordinated by a number of water molecules in aqueous solution. The metal chelate formation involves replacement of water molecules by a polydentate chelator. Due to their large size, coordination numbers of Y(III) and Ln(III) ions are typically between 7 and 10. While few six coordinate species are known, coordination numbers of 8 and 9 are very common in Y(III) and Ln(III) complexes with polydentate chelators [247, 248].

6.2.1. Hydrolysis and Precipitation—One of the characteristics of Y(III) and Ln(III) cations in aqueous solution is their easy precipitation with commonly occurring anions like hydroxide, phosphate or carbonate. Both phosphate and carbonate are able to compete for Y(III) and Ln(III) with the BFC-BM conjugate. The effect of metal hydroxide formation may not play a significant role in the release of radionuclide from radiometal chelate, mainly due to the presence of more phosphate and carbonate anions in the blood circulation. The high affinity of Y(III) and Ln(III) for phosphate anions may also explain their affinity for the bone.

6.2.2. Thermodynamic Stability—Once the radiopharmaceutical is injected into the blood stream, its concentration may become so low that dissociation of the radiometal from its metal chelate will eventually become favored. Loss of radiometal may result in accumulation of radioactivity in non-target organs. It has been reported that ⁹⁰Y and lanthanide isotopes are readily deposited on the bone [223]. If free ⁹⁰Y is injected in a human subject, about 50% of the injected dose will localize in the bone, 25% of the injected dose will go to liver, 10% of the injected dose is evenly distributed in many other organs while only 15% of the injected dose is excreted via renal system. Thus, the BFC must form a metal chelate with high thermodynamic stability to retain its chemical integrity in competition with natural chelators, such as transferrin. However, high thermodynamic stability is not the sole requirement because it only reflects the direction, not the rate, of the dissociation reaction. As a matter of fact, the solution stability of a radiopharmaceutical in the blood is predominantly determined by the kinetic inertness, not thermodynamic stability, of the metal chelate.

6.2.3. Kinetic Inertness—The term kinetic inertness refers to the rate of dissociation of the radionuclide from a metal chelate. Dissociation kinetics plays a significant role for the *in vivo* stability of radiopharmaceuticals. While fast dissociation kinetics are characteristic of metal complexes of acyclic BFCs [249–259], an accumulated body of literature has shown that metal complexes of macrocyclic chelators are much more kinetically inert [260–267]. This has been demonstrated by the high solution stability of ⁹⁰Y-labeled DOTA-BM conjugates even though the stability constant of Y(DOTA)[−] is comparable to that of Y(DTPA)^{2−} [247,248]. If DOTA is the BFC, acid-catalyzed dissociation of radionuclide from its metal chelate should be minimal in blood circulation. Recently, McMurry and coworkers studied ⁸⁸Y-labeled antibodies with acyclic BFCs, and found that acid-catalyzed dissociation is not the dominant

pathway for in vivo release of ^{88}Y [257]. There are many receptors in the bone marrow or on the bone surface for radiotracers to bind. Some small radiometal chelates of polyaminocarboxylates, such as HEDTA (N-hydroxyethylethylenediamine-N,N,'N'-triacetic acid), often show very high bone uptake [268–271]. Therefore, accumulation of radioactivity in the bone may not be caused by loss of radionuclide from its metal chelate. The overwhelming importance on the acid-catalyzed dissociation of radionuclide found in the literature is, in some way, oversimplified. Biological studies in different animal models remain the most appropriate method for evaluating in vivo stability of the radiopharmaceutical.

It is important to note that the choice of kinetic characteristics for the metal chelate of a BFC is also dependent on pharmacokinetics of radiotracer. Radiolabeled antibodies have long biological half-lives in blood circulation and at the tumor site. Since they are often metabolized in liver, the radiometal chelate must have extremely high thermodynamic stability and kinetic inertness to withstand the competition from metal ions and native chelators, such as transferrin, in the blood circulation, and to tolerate the hepatobiliary metabolism. For the radiolabeled small biomolecules, their biological half-lives in the blood are much shorter than that of the radiolabeled antibodies and antibody fragments. The requirement of kinetic inertness for the BFC radiometal chelate may not be as demanding. The main goal in choosing a successful BFC is to minimize the in vivo dissociation of radionuclide from the radiometal chelate in radiopharmaceuticals.

6.3. BFCs for ^{90}Y and Lanthanide Radionuclides

There are several requirements for an ideal BFC in chelation of ^{90}Y and lanthanide radionuclides [5,12]. The BFC must form a metal chelate with high thermodynamic stability and kinetic inertness in order to keep the metal chelate intact under physiological conditions. Decomposition of the metal chelate produces free metal ion, which may deposit on the bone and cause bone marrow toxicity. The BFC must form a metal chelate with minimum isomerism since the tumor uptake of a radiopharmaceutical depends not only on the receptor binding affinity of targeting biomolecules but also on the physical and chemical properties of both biomolecule and metal chelate. Formation of isomers may have a significant impact on physical and biological properties of the radiopharmaceutical. The BFC should have high hydrophilicity to improve blood clearance and renal excretion of the labeled and unlabeled BFC-BM conjugate. Fast renal clearance of unlabeled BFC-BM will minimize its competition with the radiolabeled BFC-BM bioconjugate for receptors. In addition, the BFC has to be able to withstand radiolysis because a large dose of β -radiation can produce free radicals and result in a significant amount of decomposition of the metal chelate during the manufacturing process and transportation.

6.3.1. Denticity Requirement—The denticity requirement of a BFC is largely dependent on the size and coordination geometry preference of the metal ion. Yttrium and lanthanide metal ions are large and need 8 – 9 donor atoms to complete the coordination sphere [12,247, 248]. It is not surprising that most of BFCs (Figure 13) contain at least eight donor atoms. It should be noted that the denticity requirement for ^{90}Y and lanthanide radiopharmaceuticals is different from that for MRI contrast agents. For MRI contrast agents, the chelator is most likely hepta- or octadentate, leaving at least one site open for water coordination to enhance the proton relaxation rates. For therapeutic radiopharmaceuticals, higher denticity may provide the enhanced thermodynamic stability and the improved kinetic inertness, particularly when extra donors are incorporated into a chelating arm attached to the macrocyclic framework.

6.3.2. Selectivity of BFCs—The high selectivity for Y(III) and Ln(III) ions can be achieved by using macrocyclic BFCs with 8 or more donor atoms. In this respect, DOTA derivatives are particularly useful for ^{90}Y and lanthanide therapeutic radiopharmaceuticals. The

macrocyclic framework is well organized so that they form metal complexes with extremely high thermodynamic stability and kinetic inertness. The low pKa values (2 – 5) of carboxylic groups result in less competition from protons and minimum acid-assisted demetallation. The acetate chelating arms have low molecular weight so that the contribution of BFC to overall molecular weight of the BFC-BM conjugate is minimized. The high hydrophilicity of acetate chelating arms will favor faster clearance from blood, liver and kidneys. Recently, Brechbiel et al reported 2,2'-(2-(4,7-bis(carboxymethyl)-1,4,7-triazonan-1-yl)ethylazanediyl)diacetic acid (Figure 13: BCNOTA) as the BFC for the ^{86}Y -chelation. It was found that BCNOTA has very high radiolabeling efficiency and forms the ^{86}Y complex with high solution stability [272].

6.3.3. Attachment Position of Biomolecules—For illustration purpose, DOTA will be used as an example. Generally, there are three approaches to attach a biomolecule to a BFC. In the first approach, the attachment of the targeting biomolecule is at one of carbon atoms of the macrocycle (Figure 13). In the second approach, the targeting biomolecule is attached to one of four acetate chelating arms (Figure 13). In both cases, conjugation of the biomolecule does not lead to a significant change in thermodynamic stability and kinetic inertness of the metal chelate as compared to those of the DOTA chelate. In the third approach, the targeting biomolecule is conjugated to one of four acetate groups via a CO-NH amide bond (Figure 10 and Figure 13). Compared to the carboxylate-oxygen, the carbonyl-oxygen is a relatively weak donor for Y(III) and Ln(III) ions. This is consistent with the significantly lower thermodynamic stability of the Y(III) complex (e.g. $K_{\text{Y-DOTA-monoamide}} \sim 21.8$; $K_{\text{Y-DOTA}} = 23.5$) [273]. However, the kinetic inertness of the Y(III) complex remains relatively unchanged as evidenced by the high solution stability of ^{90}Y -labeled DOTA-BM conjugates [263–267, 274, 275].

6.3.4. Conjugation Groups—A number of conjugation techniques have been developed for modification of biomolecules. The conjugation groups for attachment of a BFC to the biomolecule include anhydride, bromo- or iodoacetamide, isothiocyanate, N-hydroxysuccinimide (NHS) ester, and maleimide. These conjugation groups are electrophiles, which require a nucleophile functionality in the biomolecule. In some instances, the biomolecule of interest contains only electrophilic functionality (e.g. carboxylic acid), further synthetic elaboration is needed. In these cases, a bis-nucleophilic reagent, such as ethylenediamine or propylenediamine, is often used to convert the electrophilic functionality into a nucleophilic group. These reactive groups, whether they are naturally part of the biomolecule or artificially introduced, can serve as "handles" for conjugation of a BFC. Selection of conjugation group is largely dependent on the "handle" in biomolecules. Very often the "handle" is a primary amine or a thiol group. The functional groups reactive towards primary amines include DTPA dianhydride, NHS-activated esters, and isothiocyanates while maleimide is very reactive to thiols.

6.3.4.1. DTPA Anhydride: DTPA dianhydride is commercially available and reacts readily with primary amines to form the DTPA-biomolecule conjugate [216,217,249]. The reaction can be performed in both aqueous and non-aqueous media. There are two possible products: DTPA-monoamide and DTPA-bisamide (Chart IV). The cross-linking between two macromolecules (antibodies and antibody fragments) is disadvantageous, and may have dramatic impact of the biological and immunogenic properties of the DTPA-biomolecule conjugate. For small biomolecules, however, the cross-linking may prove to be beneficial for the improved receptor binding kinetics because simultaneous binding of two biomolecules on adjacent receptor sites will result in a slow dissociation of the receptor ligand. Asymmetric anhydrides of DTPA and DOTA have also been used to prepare their bioconjugates [249, 273,274]. However, the yield is often very low [273].

6.3.4.2. NHS-Ester: The NHS-esters (Chart IV) have intermediate reactivity toward amines, with high selectivity for aliphatic amines. The optimum pH for reaction in aqueous systems is 8.0 – 9.0. Virtually any molecule that contains a carboxylic group can be converted into its NHS ester, making NHS-activated ester groups among the most powerful and the most commonly used conjugation groups for antibodies and small biomolecules. Water-soluble NHS-activated ester has also been used for conjugation of biomolecules to DOTA [80,275, 276].

6.3.4.3. Isothiocyanates: Like NHS esters, isothiocyanates (Chart IV) are amine-reactive groups with intermediate reactivity, and form thiourea bonds with primary amines from proteins or small biomolecules. They are somewhat more stable in water than the NHS esters and react with amines in aqueous solution at pH 9.0 – 9.5. Isothiocyanates may not be suitable for modifying biomolecules sensitive to alkaline pH conditions. Aromatic isothiocyanates are often used to conjugate biomolecules onto DTPA and DOTA analogs [252–255,260,277–279].

6.3.4.4. Maleimide: Maleimide (Chart IV) is a thiol-reactive group [276,280], and reacts selectively with a thiol to form a thioether bond without any interference from histidine and other reactive groups. The optimum pH for the reaction is near 7.0. At pH higher than 8.0, maleimides may hydrolyze to form non-reactive maleamic acids. Since many biomolecules contain no thiol groups, the use of maleimide as a conjugation group is in some way limited.

6.4. Radiolabeling of DTPA-BM Conjugates

A major advantage of using DTPA analogs as BFCs is their extremely high radiolabeling efficiency under mild conditions, but the kinetic lability of their metal chelates often results in dissociation of radiometal from the metal chelate. Stimmel et al studied the ^{90}Y , ^{153}Sm and ^{177}Lu -chelation properties of DOTA and DTPA analogs [261,262], and found that the ^{90}Y -chelation efficiency of acyclic BFCs (Figure 13: DTPA, nitro-CHX-A-DTPA, and nitro-MX-DTPA) was much higher than that of macrocyclic BFCs, and that trace metal contamination had minimal effect on radiolabeling.

6.5. Radiolabeling of DOTA-BM Conjugates

The advantage of using DOTA analogs as BFCs is the kinetic inertness of their radiometal chelates. However, the radiolabeling kinetics of DOTA-based BFCs is normally very slow, and more dependent on radiolabeling conditions [220,261–267], including DOTA-BM concentration, pH, reaction temperature and heating time, buffering agent and buffer concentration, and presence of other metal ions, such as Zn(II) and Fe(III). At room temperature, the radiolabeling yield of the DOTA-BM conjugate is very low. Therefore, heating at the elevated temperatures ($>50\text{ }^{\circ}\text{C}$) is needed for successful radiolabeling [220, 261–267]. The high temperature radiolabeling may not cause any significant degradation of radiolabeled small biomolecules; but it often causes a significant loss of immunoreactivity of radiolabeled antibodies. In spite of the high solution stability of their radiometal chelates, slow radiolabeling kinetics remains a major obstacle for the wide use of DOTA analogs as BFCs in target-specific radiopharmaceuticals. Hopefully, the successful use of BCNOTA (Figure 13) will help overcome this problem for the ^{90}Y -labeled monoclonal antibodies [272].

6.6. Differences between ^{90}Y and ^{111}In -Labeled Biomolecules

Many acyclic and macrocyclic BFCs have been used for ^{90}Y and ^{111}In -labeling of biologically active molecules. While the ^{90}Y -labeled BFC-BM bioconjugates are used for radiotherapy, the ^{111}In -labeled BFC-BM bioconjugates are often used as surrogates for imaging and dosimetry determination since ^{90}Y has no γ -emission. ^{111}In has a half-life ($t_{1/2} = 2.8$ days)

almost identical to that of ^{90}Y ($t_{1/2} = 2.7$ days). Although In(III) and Y(III) share very similar coordination chemistry, results from recent literature have shown different biodistribution patterns between ^{90}Y and ^{111}In -labeled BFC-BM bioconjugates [282–284]. Before using ^{111}In -labeled BFC-BM bioconjugates as imaging surrogates, several critical questions need to be addressed. Are the ^{90}Y and ^{111}In -labeled BFC-BM bioconjugates biologically equivalent? What are the factors contributing to their differences, if any? How does the radiometal chelate and PKM linkers affect biological properties of the radiolabeled BFC-BM bioconjugates?

6.6.1. Structure Differences—In(III) and Y(III) are trivalent metal cations. The main difference is their size. As a result, In(III) and Y(III) often have different coordination chemistry with DTPA and DOTA derivatives. For example, Y(III) has an ionic radius of 1.02 Å [208], which fits perfectly to the cavity of DOTA. Y(III) complexes with DOTA derivatives are eight-coordinated and maintain their rigid structure in solution [206,214,220]. In(III) has an ionic radius of 0.92 Å [208]. The coordination number of In(III) is 6 or 7 [200,206,209–212]. Only a few eight-coordinated In(III) complexes are known [212–215]. Due to its smaller size, In(III) does not fit to the cavity of DOTA. Although In(III) is shown to be eight-coordinated in solid state of In(DOTA-AA) [214], the carbonyl-oxygen may become dissociated in solution. As a result, In(DOTA-BA) and Y(DOTA-BA) show significant differences in their solution properties as demonstrated by their variable temperature ^1H NMR spectra. Y(DOTA-BA) becomes fluxional only at > 60 °C while In(DOTA-BA) is fluxional at room temperature [220].

6.8.2. Differences in Lipophilicity—Onthinks et al reported the ^{111}In and ^{90}Y complexes of a DOTA-conjugated integrin $\alpha_v\beta_3$ antagonist TA138 [57]. By a reversed phase HPLC method, it was found that the retention time of ^{111}In -TA138 is ~ 4.5 min shorter than that of ^{90}Y -TA138. Since the only difference in ^{111}In -TA138 and ^{90}Y -TA138 is the radiometal, different HPLC retention times strongly suggest that In(III) and Y(III) do not share the same coordination sphere in solution. Similar lipophilicity differences were observed for the ^{111}In and ^{90}Y -labeled DOTA-BA [220], and cyclic RGD peptide DTPA conjugates [216,281]. It is believed that the lipophilicity differences between ^{111}In and ^{90}Y -labeled DOTA-BM and DTPA-BM conjugates are caused by structural differences between In(III) and Y(III) chelates in solution. It must be emphasized that the lipophilicity difference between ^{111}In and ^{90}Y -labeled bioconjugates depends largely on biomolecules. For small biomolecules, this difference is detectable. For ^{111}In and ^{90}Y -labeled antibodies, the radiometal chelate is only a small portion of the radiolabeled bioconjugate; thereby it would be difficult to detect the difference in their lipophilicity.

6.6.3. Biological Equivalence—Onthinks et al reported the bioequivalence between ^{111}In -TA138 and ^{90}Y -TA138 using the c-neu Oncomouse[®] tumor model [57]. Despite their significant differences in lipophilicity [57], biodistribution data showed that ^{111}In -TA138 and ^{90}Y -TA138 are biologically equivalent with respect to their uptake in tumors and other organs, such as liver, spleen, bone and kidneys. Thus, ^{111}In -TA138 is useful as an imaging surrogate for ^{90}Y -TA138, and should be able to accurately predict the biodistribution characteristics and radiation dosimetry of ^{90}Y -TA138, the radiopharmaceutical useful for tumor radiotherapy.

Mäcke and coworkers [206] reported the solution stability, somatostatin receptor binding and biodistribution characteristics of the ^{90}Y and ^{111}In -labeled DOTA-D-Phe¹-Tyr³-Octreotide (DOTATOC). The solution stability of ^{111}In -DOTATOC and ^{90}Y -DOTATOC in the blood serum is very high with half-lives for radiometal exchange being 1850 h and 2100 h, respectively [206]. This suggests that there is no significant release of radionuclide from ^{111}In -DOTATOC and ^{90}Y -DOTATOC. The IC_{50} values for ^{111}In -DOTATOC (2.57 ± 0.2

nM) and ^{90}Y -DOTATOC (2.2 ± 0.3 nM) indicated that there was no difference in the receptor binding affinity of ^{111}In -DOTATOC and ^{90}Y -DOTATOC. Biodistribution data of ^{111}In -DOTATOC and ^{90}Y -DOTATOC in nude mice bearing the AR4-2J tumor xenografts also showed that there was no significant difference in kidney and tumor uptake for ^{111}In -DOTATOC and ^{90}Y -DOTATOC at 4 h and 24 h post-injection. These data clearly demonstrated that ^{111}In -DOTATOC and ^{90}Y -DOTATOC are biologically equivalent even though In(III) and Y(III) do not share the same coordination chemistry in their radiometal chelate [206,220]. It should be noted that the metal chelate is only a part of ^{111}In or ^{90}Y -labeled DOTA-BM conjugate. ^{111}In and ^{90}Y chelates may have different solution structures, which causes a slight difference in lipophilicity between the ^{111}In -DOTA-BM and ^{90}Y -DOTA-BM. Ultimately, it will be the biological equivalence that determines whether the ^{111}In -labeled DOTA-BM conjugate can be used to accurately predict the radiation dosimetry of its ^{90}Y analog.

7. Conclusions

There is a tremendous effort in the development of target-specific radiopharmaceuticals for early detection of diseases and radiotherapy of cancer. This effort relies heavily on the use of radiolabeled receptor ligands. Because of their high specificity and selectivity, the radiolabeled receptor ligands offer advantages over traditional perfusion radiotracers. Identification of targets and receptor ligands is critical for successful development of receptor-based radiotracers. Eventually, the challenge remains to be fundamentals of bioconjugate chemistry for target-specific delivery of radionuclide to the diseased tissues. There is no such an easy task that one can simply attach a radiometal chelate onto the selected biomolecule without significantly changing its receptor binding affinity and biodistribution characteristics.

Coordination chemistry plays a significant role in the design of BFCs, radiolabeling kinetics, solution stability, modification of pharmacokinetics, and formulation development. Because the receptor population in the diseased organ or tissues is often limited in numbers, using a large amount of BFC-BM bioconjugate may block receptor binding of the radiolabeled BFC-BM bioconjugate. Thus, selection of an appropriate BFC and optimization of its radiolabeling efficiency should be a significant part of the radiopharmaceutical development. The choice of BFC depends on the nature and oxidation state of radiometal, and requires a good understanding of its coordination chemistry of the radiometal to be labeled. The main objective is to select an efficient bifunctional coupling or chelating system that forms the radiometal chelate with very high thermodynamic stability and kinetic inertness. The ultimate goal is to develop a new generation of target-specific radiopharmaceuticals that will satisfy the unmet medical need for early detection of diseases or systemic radiotherapy of cancers.

List of Abbreviations for Common Chelators

BCNOTA, 2,2'-(2-(4,7-bis(carboxymethyl)-1,4,7-triazonan-1-yl)ethylazanediyl)diacetic acid
 CB-TE2A, 2,2'-(1,4,8,11-tetraazabicyclo[6.6.2]hexadecane-4,11-diyl)diacetic acid
 DADS, N_2S_2 diamidedithiols
 DO3A, 1,4,7,10-tetraazacyclododecane-1,4,7-triacetate
 DOTA, 1,4,7,10-tetraazacyclododecane-1,4,7,10-tetraacetic acid
 DOTA-AA, 1,4,7,10-tetraazacyclododecane-1,4,7,10-tetraacetic acid mono(*p*-aminoanilide)
 DOTA-D-PheNH₂, 1,4,7,10-tetraazacyclododecane-4,7,10-tricarboxymethyl-1-yl-acetyl-D-Phenylalanine-amide)
 DTPA, diethylenetriaminepentaacetic acid
 HEDTA, N-hydroxyethylethylenediamine-N,N,'N'-triacetic acid
 HYNIC, 6-hydrazinonicotinamide
 MAMA, monoamidemonoaminedithiols

map, 2,3-bis(mercaptoacetamido)propanoate
mapt, 4,5-bis(thioacetamido)pentanoate
NOTA, 1,4,7-triazacyclononane-1,4,7-triacetic acid
NODAGA, 1,4,7-triazacyclononane-N-glutamic acid-N',N''-diacetic acid
NODASA, 1,4,7-triazacyclononane-N-succinic acid-N',N''-diacetic acid
SarAr, N1-(4-aminobenzyl)-3,6,10,13,16,19-hexaazabicyclo[6.6.6]icosane-1,8-diamine
TETA, 1,4,8,11-tetraazacyclotetradecane-1,4,8,11-tetraacetic acid

References

1. Banerjee S, Pillai MRA, Ramamoorthy N. Evolution of Tc-99m in diagnostic radiopharmaceuticals. *Semin. Nucl. Med* 2001;31:260–277. [PubMed: 11710769]
2. Jain D. Technetium-99m labeled myocardial perfusion imaging agents. *Semin. Nucl. Med* 1999;29:221–236. [PubMed: 10433338]
3. Jurisson SS, Lydon JD. Potential technetium small molecule radiopharmaceuticals. *Chem. Rev* 1999;99:2205–2218. [PubMed: 11749479]
4. Liu S. Ether and crown ether-containing cationic ^{99m}Tc complexes useful as radiopharmaceuticals for heart imaging. *Dalton Trans* 2007:1183–1193. [PubMed: 17353949]
5. Liu S, Edwards DS. Fundamentals of receptor-based diagnostic metalloradiopharmaceuticals. *Topics in Current. Chem* 2002;222:259–278.
6. Liu S. The role of coordination chemistry in development of target-specific radiopharmaceuticals. *Chem. Soc. Rev* 2004;33:1–18. [PubMed: 14737504]
7. Reichert DE, Lewis JS, Anderson CJ. Metal complexes as diagnostic tools. *Coord. Chem. Rev* 1999;184:3–66.
8. McEwan AJB. Unsealed source therapy of painful bone metastases: an update. *Semin. Nucl. Med* 1997;27:165–182. [PubMed: 9144858]
9. Volkert WA, Hoffman TJ. Therapeutic radiopharmaceuticals. *Chem. Rev* 1999;99:2269–2292. [PubMed: 11749482]
10. Liu S, Edwards DS, Barrett JA. ^{99m}Tc -labeling of highly potent small peptides. *Bioconj. Chem* 1997;8:621–636.
11. Liu S, Edwards DS. ^{99m}Tc -labeled small peptides as diagnostic radiopharmaceuticals. *Chem. Rev* 1999;99:2235–2268. [PubMed: 11749481]
12. Liu S, Edwards DS. Bifunctional chelators for target specific therapeutic lanthanide radiopharmaceuticals. *Bioconj. Chem* 2001;12
13. Anderson CJ, Welch MJ. Radiometal labeled agents (non-technetium) for diagnostic imaging. *Chem. Rev* 1999;99:2219–2234. [PubMed: 11749480]
14. Heeg MJ, Jurisson SS. The role of inorganic chemistry in the development of radiometal agents for cancer therapy. *Acc. Chem. Res* 1999;32:1053–1060.
15. Illidge TM, Brock S. Radioimmunotherapy of cancer: using monoclonal antibodies to target radiotherapy. *Current Pharmaceutical Design* 2000;6:1399–1418. [PubMed: 10903400]
16. Vriesendorp HM, Quadri SM, Borchardt PE. Tumor therapy with radiolabeled antibodies: optimization of therapy. *BioDrugs* 1998;10:275–293. [PubMed: 18020601]
17. Potamianos S, Varvarigou AD, Archimandritis SC. Radioimmunoscintigraphy and radioimmunotherapy in cancer: Principles and applications. *Anticancer Res* 2000;20:925–948. [PubMed: 10810378]
18. Wun T, Kwon DS, Tuscano JM. Radioimmunotherapy: potential as a therapeutic strategy in non-Hodgkin's lymphoma. *BioDrugs* 2001;15:151–162. [PubMed: 11437681]
19. Witzig TE. The use of ibritumomab tiuxetan radioimmunotherapy for patients with relapsed B-cell non-Hodgkin's lymphoma. *Semin. Oncol* 2000;27:74–78.
20. Culy CR, Lamb HM. ^{131}I Tositumomab. *BioDrugs* 2000;14:195–202. [PubMed: 18034570]
21. Chatal JF, Hoefnagel CA. Radionuclide therapy. *Lancet* 1999;354:931–935. [PubMed: 10489968]
22. Joensuu H, Tenhunen M. Physical and biological targeting of radiotherapy. *Acta Oncologica* 1999;38:75–83. [PubMed: 10612500]

23. Britton KE. Towards the goal of cancer-specific imaging and therapy. *Nucl. Med. Commun* 1997;18:992–1007. [PubMed: 9423199]
24. Reubi JC. Regulatory peptides receptors as molecular targets for cancer diagnosis and therapy. *Q. J. Nucl. Med* 1997;41:63–70. [PubMed: 9203845]
25. Heppeler A, Froidevaux S, Eberle AN, Maecke HR. Receptor targeting for tumor localization and therapy with radiopeptides. *Current Med. Chem* 2000;7:971–994.
26. Lister-James J, Moyer BR, Dean RT. Small peptides radiolabeled with Tc-99m. *Q. J. Nucl. Med* 1996;40:221–233. [PubMed: 8961801]
27. Blok D, Feitsma RIJ, Vermeij P, Pauwel EJK. Peptide radiopharmaceuticals in nuclear medicine. *Eur. J. Nucl. Med* 1999;26:1511–1519. [PubMed: 10552097]
28. Okarvi SM. Recent developments in Tc-99m-labelled peptide-based radiopharmaceuticals: an overview. *Nucl. Med. Commun* 1999;20:1093–1112. [PubMed: 10664991]
29. Kwekkeboom D, Krenning EP, de Jong M. Peptide receptor imaging and therapy. *J. Nucl. Med* 2000;41:1704–1713. [PubMed: 11038002]
30. Boerman OC, Oyen WJG, Corstens FHM. Radiolabeled receptor-binding peptides: A new class of radiopharmaceuticals. *Semi. Nucl. Med* 2000;30:195–208.
31. Ercan MT, Caglar M. Radiopharmaceuticals for the visualization of infectious and inflammatory lesions. *Current Pharmaceutical Design* 2000;6:1159–1177. [PubMed: 10903388]
32. Liu S, Edwards DS. New Radiopharmaceuticals for imaging infection and inflammation. *Drugs of the Future* 2001;26:375–382.
33. Liu S. HYNIC derivatives as bifunctional coupling agents for ^{99m}Tc-labeling of small biomolecules. *Topics in Current Chem* 2005;252:193–216.
34. Liu S, Robinson SP, Edwards DS. Radiolabeled integrin $\alpha_v\beta_3$ antagonists as radiopharmaceuticals for tumor radiotherapy. *Topics in Current Chem* 2005;252:193–216.
35. Signore A, Annovazzi A, Chianelli M, Coretti F, Van de Wiele C, Watherhouse RN, Scopinaro F. Peptide radiopharmaceuticals for diagnosis and therapy. *Eur. J. Nucl. Med* 2001;28:1555–1565. [PubMed: 11685500]
36. Hoffman TJ, Quinn TP, Volkert WA. Radiometallated receptor-avid peptide conjugates for specific in vivo targeting of cancer cells. *Nucl. Med. Biol* 2001;28:527–539. [PubMed: 11516698]
37. Langer M, Beck-Sichinger AG. Peptides as carriers for tumor diagnosis and treatment. *Curr. Med. Chem.–Anti-Cancer Agents* 2001;1:71–93.
38. Weiner RE, Thakur ML. Radiolabeled peptides in the diagnosis and therapy of oncological diseases. *Appl. Radiat. Isot* 57;2002:749–763.
39. de Jong M, Kwekkeboom D, Valkema R, Krenning EP. Radiolabelled Peptides for tumor therapy: current status and future directions. *Eur. J. Nucl. Med* 2003;30:463–469.
40. Fichna J, Janecka A. Synthesis of target-specific radiolabeled peptides for diagnostic imaging. *Bioconj. Chem* 2003;14:3–17.
41. Behr TM, Gotthardt M, Barth A, Béhé M. Imaging tumors with peptide-based radioligands. *Q. J. Nucl. Med* 2001;45:189–200. [PubMed: 11476170]
42. Liu S, Robinson SP, Edwards DS. Integrin $\alpha_v\beta_3$ directed radiopharmaceuticals for tumor imaging. *Drugs of the Future* 2003;28:551–564.
43. Liu S. Radiolabeled multimeric cyclic RGD peptides as integrin $\alpha_v\beta_3$ -targeted radiotracers for tumor imaging. *Molecular Pharmaceuticals* 2006;3:472–487.
44. Quadri SM, Vriesendorp HM. Effects of linker chemistry on pharmacokinetics of radioimmunoconjugates. *Q. J. Nucl. Med* 1998;42:250–261. [PubMed: 9973840]
45. Williams LE, Lewis MR, Bebb GG, Clarcke KG, Odom-Maryon TL, Shively JE, Raubitschek AA. Biodistribution of ¹¹¹In- and ⁹⁰Y-labeled DOTA and maleimidocysteineamido-DOTA conjugated to chimeric anticarcinoembryonic antigen antibody in xenograft-bearing nude mice: comparison of stable and chemically labile linker systems. *Bioconj. Chem* 1998;9:87–93.
46. Arano Y, Matsushima H, Tagawa M, Koizumi M, Endo K, Konish J, Yokoyama A. A novel bifunctional metabolizable linker for the conjugation of antibodies with radionuclides. *Bioconj. Chem* 1991;2:71–76.

47. Smith-Jones PM, Stolz B, Albert R, Knecht H, Bruns C. Synthesis, biodistribution and renal handling of various chelate-somatostatin conjugates with metabolizable linking groups. *Nucl. Med. Biol* 1997;24:761–769. [PubMed: 9428603]
48. Studer M, Meares CF. A convenient and flexible approach for introducing linkers on bifunctional chelating agents. *Bioconj. Chem* 1992;3:420–423.
49. Li M, Meares CF. Synthesis, metal chelate stability studies, and enzyme digestion of a peptide-linked DOTA derivative and its corresponding radiolabeled immunoconjugates. *Bioconj. Chem* 1993;4:275–283.
50. Peterson JJ, Meares CF. Enzymatic cleavage of peptide-linked radiolabels from immunoconjugates. *Bioconj. Chem* 1999;10:553–557.
51. Peterson JJ, Meares CF. Cathepsin substrate as cleavable peptide linkers in bioconjugates, selected from a fluorescence quench combinatorial library. *Bioconj. Chem* 1998;9:618–626.
52. Haubner R, Wester HJ, Senekowitsch-Schmidtke R, Diefenbach B, Kessler H, Stöcklin G, Schwaiger M. RGD-peptides for tumor targeting: biological evaluation of radioiodinated analogs and introduction of a novel glycosylated peptide with improved biokinetics. *J. Labelled Compd. Radiopharm* 1997;40:383–385.
53. Haubner R, Wester HJ, Reuning U, Senekowitsch-Schmidtke R, Diefenbach B, Kessler H, Stöcklin G, Schwaiger M. Radiolabeled $\alpha_v\beta_3$ integrin antagonists: a new class of tracers for tumor imaging. *J. Nucl. Med* 1999;40:1061–1071. [PubMed: 10452325]
54. Haubner R, Wester HJ, Burkhart F, Senekowitsch-Schmidtke R, Weber WA, Goodman SL, Kessler H, Schwaiger M. Glycosylated RGD-containing peptides: tracer for tumor targeting and angiogenesis imaging with improved biokinetics. *J. Nucl. Med* 2001;42:326–336. [PubMed: 11216533]
55. Haubner R, Wester HJ, Weber WA, Mang C, Ziegler SI, Goodman SL, Senekowitsch-Schmidtke R, Kessler H, Schwaiger M. Noninvasive imaging of $\alpha_v\beta_3$ integrin expression using ^{18}F -labeled RGD-containing glycopeptide and positron emission tomography. *Cancer Res* 2001;61:1781–1785. [PubMed: 11280722]
56. Harris TD, Kalogeropoulos S, Nguyen T, Liu S, Bartis J, Ellars CE, Edwards DS, Onthinks D, Silva P, Yalamanchili P, Robinson SP, Lazewatsky J, Barrett JA, Bozarth J. Design, synthesis and evaluation of radiolabeled integrin $\alpha_v\beta_3$ receptor antagonists for tumor imaging and radiotherapy. *Cancer Biotherapy & Radiopharmaceuticals* 2003;18:627–641. [PubMed: 14503959]
57. Onthank DC, Liu S, Silva PJ, Barrett JA, Harris TD, Robinson SP, Edwards DS. ^{90}Y and ^{111}In complexes of a DOTA-conjugated integrin $\alpha_v\beta_3$ receptor antagonist: different but biologically equivalent. *Bioconj. Chem* 2004;15:235–241.
58. Harris TD, Kalogeropoulos S, Nguyen T, Dwyer G, Edwards DS, Liu S, Bartis J, Ellars C, Onthank D, Yalamanchili P, Heminway S, Robinson S, Lazewatsky J, Barrett JA. Structure-activity relationships of ^{111}In - and $^{99\text{m}}\text{Tc}$ -labeled quinolin-4-one peptidomimetics as ligands for the vitronectin receptor: potential tumor imaging agents. *Bioconj. Chem* 2006;17:1294–1313.
59. Harris TD, Cheesman E, Harris AR, Sachleben R, Edwards DS, Liu S, Bartis J, Ellars C, Onthank D, Yalamanchili P, Heminway S, Silva P, Robinson S, Lazewatsky J, Rajopadhye M, Barrett JA. Radiolabeled divalent peptidomimetic vitronectin receptor antagonists as potential tumor radiotherapeutic and imaging Agents. *Bioconj. Chem* 2007;18:1266–1279.
60. Chen X, Park R, Shahinian AH, Bading JR, Conti PS. Pharmacokinetics and tumor retention of ^{125}I -labeled RGD peptide are improved by PEGylation. *Nucl. Med. Biol* 2004;31:11–19. [PubMed: 14741566]
61. Chen X, Sievers E, Hou Y, Park R, Tohme M, Bart R, Bremner R, Bading JR, Conti PS. Integrin $\alpha_v\beta_3$ -targeted imaging of lung cancer. *Neoplasia* 2005;7:271–279. [PubMed: 15799827]
62. Liu S, He Z, Hsieh W, Kim Y, Jiang Y. Impact of PKM linkers on biodistribution characteristics of the $^{99\text{m}}\text{Tc}$ -labeled cyclic RGDfK dimer. *Bioconj. Chem* 2006;17:1499–1507.
63. Dijkgraaf I, Liu S, Kruijtzter JAW, Soede AC, Oyen WJG, Liskamp RMJ, Corstens FHM, Boerman OC. Effects of linker variation on the in vitro and in vivo characteristics of an ^{111}In -labeled RGD Peptide. *Nucl. Med. Biol* 2007;34:29–35. [PubMed: 17210459]
64. Ruth TJ, Pate BD, Robertson R, Porter JK. Radionuclide production for biosciences. *Nucl. Med. Biol* 1989;16:323–336.

65. Ehrhardt GJ, Ketring AR, Ayers LM. Reactor-produced radionuclides at the University of Missouri Research Reactor. *Appl. Radiat. Isot* 1998;49:295–297. [PubMed: 9519439]
66. Karelin YA, Toporov YG. RIAR reactor produced radionuclides. *Appl. Radiat. Isot* 1998;49:299–304.
67. Knapp FF Jr, Mirzadeh S, Beets AL, O'Doherty M, Blower PJ, Verdera ES, Gaudiano JS, Kropp J, Gihlke J, Palmedo H, Biersack HJ. Reactor-produced radioisotopes from ORNL for bone pain palliation. *Appl. Radiat. Isot* 1998;49:309–315. [PubMed: 9519440]
68. Schubiger PA, Alberto R, Smith A. Vehicles, chelators, and radionuclides: choosing the “building blocks” of an effective therapeutic radioimmunoconjugate. *Bioconj. Chem* 1996;7:165–179.
69. Finn, R. Chemistry applied to iodine radionuclides. In: Welch, MJ.; Redvanly, CS., editors. *Handbook of Radiopharmaceuticals: Radiochemistry and Applications*. New York: John Wiley & Sons; 2003. p. 423-440.
70. Snider, SE.; Kilbourn, MR. Chemistry of fluorine-18 radiopharmaceuticals. In: Welch, MJ.; Redvanly, CS., editors. *Handbook of Radiopharmaceuticals: Radiochemistry and Applications*. New York: John Wiley & Sons; 2003. p. 195-227.
71. Welch MJ, McCarthy TJ. The potential role of generator-produced radiopharmaceuticals in clinical PET. *J. Nucl. Med* 2000;41:315–317. [PubMed: 10688117]
72. Anderson, CJ.; Green, MA.; Yashi, YF. Chemistry of copper radionuclides and radiopharmaceutical products. In: Welch, MJ.; Redvanly, CS., editors. *Handbook of Radiopharmaceuticals: Radiochemistry and Applications*. New York: John Wiley & Sons; 2003. p. 402-422.
73. Bormans G, Janssen A, Adriaens P, Crombez D, Witsenboer A, Degoeij J, Mortelmans L, Verbruggen A. $^{62}\text{Zn}/^{62}\text{Cu}$ generator for the routine production of ^{62}Cu -PTSM. *Appl. Radiat. Isot* 1992;43:1437–1441.
74. Haynes NG, Lacy JL, Nayak N, Martin CS, Dai D, Mathias CJ, Green MA. Performance of a $^{62}\text{Zn}/^{62}\text{Cu}$ generator in clinical trials of PET perfusion agent ^{62}Cu -PTSM. *J. Nucl. Med* 2000;41:309–314. [PubMed: 10688116]
75. Lim JK, Mathias CJ, Green MA. Mixed bis(thiosemicarbazone) ligands for the preparation of copper radiopharmaceuticals: synthesis and evaluation of tetradentate ligands containing two dissimilar thiosemicarbazone functions. *J. Med. Chem* 1997;40:132–136. [PubMed: 9016338]
76. Ackerman LJ, West DX, Mathias CJ, MA Green M. Synthesis and evaluation of copper radiopharmaceuticals with mixed bis(thiosemicarbazone) ligands. *Nucl. Med. Biol* 1999;26:551–554. [PubMed: 10473194]
77. Mathias CJ, Green MA, Morrison WB, Knapp DW. Evaluation of Cu-PTSM as a tracer of tumor perfusion: comparison with labeled microsphere in spontaneous canine neoplasms. *Nucl. Med. Biol* 1994;21:83–87. [PubMed: 9234268]
78. Mathias CJ, Bergmann SR, Green MA. Species-dependent binding of copper(II) bis (thiosemicarbazone) Radiopharmaceuticals to serum albumin. *J. Nucl. Med* 1995;36:1451–1455. [PubMed: 7629593]
79. Chen X, Liu S, Hou Y, Tohme M, Park R, Bading JR, Conti PS. MicroPET imaging of breast cancer α_v -integrin expression with ^{64}Cu -labeled dimeric RGD peptides. *Mol. Imag. Biol* 2004;6:350–359.
80. Wu Y, Zhang X, Xiong Z, Cheng Z, Fisher DR, Liu S, Gambhir SS, Chen X. MicroPET imaging of glioma $\alpha_v\beta_3$ integrin expression using ^{64}Cu -labeled tetrameric RGD peptide. *J. Nucl. Med* 2005;46:1707–1718. [PubMed: 16204722]
81. Chen X, Park R, Tohme M, Shahinian AH, Bading JR, Conti PS. MicroPET and autoradiographic imaging of breast cancer α^v -integrin expression using ^{18}F - and ^{64}Cu -labeled RGD peptide. *Bioconj. Chem* 2004;15:41–49.
82. Chen X. Multimodality imaging of tumor integrin $\alpha_v\beta_3$ expression. *Mini-Rev. Med. Chem* 2006;6:227–234. [PubMed: 16472190]
83. Anderson CJ, Pajean TS, Edwards EB, Sherman ELC, Rogers BE, Welch MJ. In vitro and in vivo evaluation of copper-64-octreotide conjugates. *J. Nucl. Med* 1995;36:2315–2325. [PubMed: 8523125]
84. Anderson CJ, Jones LA, Bass LA, Sherman ELC, McCarthy DW, Cutler PD, Lanahan MV, Cristel ME, Lewis JS, Schwarz SW. Radiotherapy, toxicity and dosimetry of In vitro and in vivo evaluation

- of copper-64 TETA-octrotide in tumor bearing rats. *J. Nucl. Med* 1998;39:1944–1951. [PubMed: 9829587]
85. Lewis JS, Srinivasan A, Schmidt MA, Anderson CJ. In vitro and in vivo evaluation of ^{64}Cu -TETA-Tyr³-octreotate. A new somatostatin analog with improved target tissue uptake. *Nucl. Med. Biol* 1999;26:267–273. [PubMed: 10363797]
86. Lewis JS, Lewis MR, Cutler PD, Srinivasan A, Schmidt MA, Schwarz SW, Morris MM, Miller JP, Anderson CJ. Radiotherapy and dosimetry of ^{64}Cu -TETA-Tyr³-octreotate in a somatostatin receptor-positive, tumor-bearing rat model. *Clin. Cancer Res* 1999;5:3608–3616. [PubMed: 10589778]
87. Tisato F, Porchia M, Bolzati C, Refoso F, Vittadini A. The preparation of substitution-inert ^{99}Tc metal-fragments: promising candidates for the design of new $^{99\text{m}}\text{Tc}$ radiopharmaceuticals. *Coord. Chem. Rev* 2006;250:2034–2045.
88. Hansen L, Marzilli LG, Taylor A. The influence of stereoisomerism on the pharmacokinetics of Tc radiopharmaceuticals. *Q. J. Nucl. Med* 1998;42:280–293. [PubMed: 9973843]
89. Klingensmith WC III, Fritzberg AR, Spitzer VM, Johnson DL, Kuni CC, Williamson MR, Washer G, Weil R III. Clinical evaluation of Tc-99m N,N'-bis(mercaptoacetyl)-2,3-diaminopropanoate as a replacement for I-131 hippurate: concise communication. *J. Nucl. Med* 1984;25:42–48. [PubMed: 6427428]
90. Rao TN, Adhikesavalu D, Camerman A, Fritzberg AR. Technetium(V) and rhenium(V) complexes of 2,3-bis(mercaptoacetamido)propanoate. Chelate ring stereochemistry and influence on chemical and biological properties. *J. Am. Chem. Soc* 1990;112:5798–5804.
91. Liu, S.; Edwards, DS. New N₂S₂ diamidedithiol and N₃S triamidethiols as bifunctional chelating agents for labeling small peptides with technetium-99m. In: Nicolini, M.; Banoli, G.; Mazzi, U., editors. *Technetium and Rhenium in Chemistry and Nuclear Medicine*. 4. Padova: SGEEditorali; 1995. p. 383-393.
92. Eshima D, Taylor A Jr, Fritzberg AR, Kasina S, Hansen L, Sorenson JF. Animal evaluation of technetium-99m triamide mercaptide complexes as potential renal imaging agents. *J. Nucl. Med* 1987;28:1180–1186. [PubMed: 2955085]
93. Vanbilloen HP, De Roo MJ, Verbruggen AM. Complexes of technetium-99m with tetrapeptides containing one alanyl and three glycyl moieties. *Eur. J. Nucl. Med* 1996;23:40–48. [PubMed: 8586100]
94. Fritzberg AR, Abrams PG, Beaumier PL, Kasina S, Morgan AC, Rao TN, Reno JM, Sanderson JA, Srinivasan A, Wilbur DS, Vanderheyden JL. Specific and stable labeling of antibodies with technetium-99m with a diamide dithiolate chelating agent. *Proc. Natl. Acad. Sci. USA* 1988;85:4025–4029. [PubMed: 3375252]
95. Eary JF, Schroff RW, Abrams PG, Fritzberg AR, Morgan AC, Kasina S, Reno JM, Srinivasan A, Woodhouse CS, Wilbur DS, Natale RB, Collins C, Stehlin JS, Mitchell M, Nelp WB. Successful imaging of malignant melanoma with technetium-99m-labeled monoclonal antibodies. *J. Nucl. Med* 1989;30:25–32. [PubMed: 2642954]
96. Kasina S, Rao TN, Srinivasan A, Sanderson JA, Fitzner JN, Reno JM, Beaumier PL, Fritzberg AR. Development and biological evaluation of a kit for preformed chelate technetium-99m radiolabeling of an antibody Fab fragment using a diamide dimercaptide chelating agent. *J. Nucl. Med* 1991;32:1445–1451. [PubMed: 2066805]
97. Liu S, Edwards DS, Looby RJ, Harris AR, Poirier MJ, Rajopadhye M, Bourque JP, Carroll TR. Labeling cyclic IIb/IIIa receptor antagonists with $^{99\text{m}}\text{Tc}$ by the preformed chelate approach: effects of chelators on properties of [$^{99\text{m}}\text{Tc}$]chelator-peptide conjugate. *Bioconj. Chem* 1996;7:196–202.
98. Barrett JA, Damphousse DJ, Heminway SJ, Liu S, Edwards DS, Looby RJ, Carroll TR. Biological evaluation of $^{99\text{m}}\text{Tc}$ -labeled cyclic GPIIb/IIIa receptor antagonists in the canine arteriovenous shunt and deep vein thrombosis models: effects of chelators on biological properties of [$^{99\text{m}}\text{Tc}$]chelator-peptide conjugates. *Bioconj. Chem* 1996;7:203–208.
99. Rajopadhye M, Edwards DS, Bourque PJ, Carroll TR. Synthesis and technetium-99m labeling of cyclic GPIIb/IIIa receptor antagonists conjugated to 4,5-bis(mercaptoacetamido)pentanoic acid (mapt). *Bioorg. & Med. Chem. Lett* 1996;6:1737–1740.

100. Lever SZ, Baidoo KE, Mahmood A. Structure proof of *syn/anti* isomerism in N-alkylated diaminedithiol (DADT) complexes of technetium. *Inorg. Chim. Acta* 1990;176:183–184.
101. Walovitch RC, Cheesman EH, Maheu LJ, Hall KM. Studies of the retention mechanism of the brain perfusion imaging agent ^{99m}Tc -Bicisate (^{99m}Tc -ECD). *J. Cerebral Blood Flow and Metabolism* 1994;14:S4–S11.
102. Harris TD, Edwards DS, Platts SH. Synthesis and characteristics of isomers L,L, D,D, and D,L of Tc-99m-ECD in monkeys. *J. Nucl. Med* 1992;33:979–980.
103. Oya S, Kung MP, Frederick D, Kung HF. New bisaminoethanethiol (BAT) ligands which form two interconvertible Tc-99m complexes. *Nucl. Med. Biol* 1995;22:749–757. [PubMed: 8535335]
104. Kung HF, Guo YZ, Yu CC, Billings J, Subramanyam V, Calabrese JC. New brain perfusion imaging agents based on ^{99m}Tc -bis(aminoethanethiol) complexes: stereoisomers and biodistribution. *J. Med. Chem* 1989;32:433–437. [PubMed: 2913304]
105. Francesconi LC, Graczyk G, Wehrli S, Shaikh SN, McClinton D, Liu S, Zubieta J, Kung HF. Synthesis and characterization of neutral M^{VO} (M = Tc, Re) Amine-thiol complexes containing a pendant phenylpiperidine group. *Inorg. Chem* 1993;32:3114–3124.
106. Mach RH, Kung HF, Guo YZ, Yu CC, Subramanyam V, Calabrese JC. Synthesis, characterization and biodistribution of neutral and lipid-soluble ^{99m}Tc -PAT-HM and ^{99m}Tc -TMR for brain imaging. *Nucl. Med. Biol* 1989;16:829–837.
107. Baidoo KE, Lever SZ. Synthesis of a diaminedithiol bifunctional chelating agent for incorporation of technetium-99m into biomolecules. *Bioconj. Chem* 1990;1:132–137.
108. Eisenhut M, Lehmann WD, Becker W, Behr T, Elser H, Strittmatter W, Baum RP, Valerius T, Repp R, Deo Y. Bifunctional NHS-BAT ester for antibody conjugation and stable technetium-99m labeling: conjugation chemistry, immunoreactivity and kit formulation. *J. Nucl. Med* 1996;37:362–370. [PubMed: 8667077]
109. O'Neil JP, Wilson SR, Katzenellenbogen JA. Preparation and structural characterization of monoamine-monoamide bis(thiol) oxo complexes of technetium(V) and rhenium(V). *Inorg. Chem* 1994;33:319–323.
110. DiZio JP, Fiacshi R, Davison A, Jones AG, Katzenellenbogen JA. Progesterone-rhenium complexes: metal labeled steroids with high receptor binding affinity, potential receptor-directed agents for diagnostic imaging or therapy. *Bioconj. Chem* 1991;2:353–366.
111. O'Neil JP, Carlson KE, Anderson CJ, Welch MJ, Katzenellenbogen JA. Progesterone radiopharmaceuticals labeled with technetium and rhenium: synthesis, binding affinity, and in vivo distribution of a new progesterone N_2S_2 -metal conjugate. *Bioconj. Chem* 1994;5:182–193.
112. DiZio JP, Anderson CJ, Davison A, Ehrhardt GJ, Carlson KE, Welch MJ, Katzenellenbogen JA. Technetium- and rhenium-labeled progestins: synthesis, receptor binding and in vivo distribution of an 11β -substituted progesterone labeled with technetium-99 and rhenium-186. *J. Nucl. Med* 1992;33:558–569. [PubMed: 1552341]
113. Meegalla S, Plüssl K, Kung MP, Chumpradit S, Stevenson DA, Frederick D, Kung HF. Tc-99m-labeled tropanes as dopamine transporter imaging agents. *Bioconj. Chem* 1996;7:421–429.
114. Rajagopalan R, Grummon GD, Bugaj J, Hallemann LS, Webb EG, Marmion ME, Vanderheyden JL, Srinivasan A. Preparation, characterization, and biological evaluation of technetium(V) and rhenium(V) complexes of novel heterocyclic tetradentate N_3S ligands. *Bioconj. Chem* 1997;8:407–415.
115. Wong E, Fauconnier T, Bennett S, Valliant J, Nguyen T, Lau F, Lu LFL, Pollak A, Bell RA, Thornback JR. Rhenium(V) and Technetium(V) Oxo Complexes of an $\text{N}_2\text{N}'\text{S}$ Peptidic Chelator: Evidence of Interconversion between the *Syn* and *Anti* Conformations. *Inorg. Chem* 1997;36:5799–5808. [PubMed: 11670202]
116. Lister-James J, Knight LC, Maurer AH, Bush LR, Moyer BR, Dean RT. Thrombus imaging with technetium-99m-labeled, activated platelet receptor binding peptide. *J. Nucl. Med* 1996;37:775–781. [PubMed: 8965144]
117. Muto P, Lastoria S, Varrella P, Vergara E, Salvatore M, Morgano G, Lister-James J, Bernardy JD, Dean RT, Wencker D, Borer JS. Detecting deep venous thrombosis with technetium-99m-labeled synthetic peptide P280. *J. Nucl. Med* 1995;36:1384–1391. [PubMed: 7629582]

118. Pearson DA, Lister-James J, McBride WJ, Wilson DM, Martel LJ, Civitello ER, Dean RT. Thrombus imaging using technetium-99m labeled high potency GPIIb/IIIa receptor antagonists. Chemistry and initial biological studies. *J. Med. Chem* 1996;39:1372–1382. [PubMed: 8691467]
119. Lister-James J, Vallabhajosula S, Moyer BR, Pearson DA, McBride BJ, De Rosch MA, Bush LR, Machac J, Dean RT. Pre-clinical evaluation of technetium-99m platelet receptor-binding peptide. *J. Nucl. Med* 1997;38:105–111. [PubMed: 8998163]
120. Marchi A, Marvelli L, Rossi R, Magon L, Bertolasi V, Ferretti V, Gilli P. Nitrido and oxo-technetium (V) chelate complexes with N_2S_2 ligands: Synthesis and crystal structures. *J. Chem. Soc., Dalton Trans* 1992:1485–1490.
121. Duatti A, Marchi A, Pasqualini R. Formation of the $Tc \equiv N$ multiple bond from the reaction of ammonium pertechnetate with S-methyl dithiocarbamate and its application to the preparation of technetium-99m radiopharmaceuticals. *J. Chem. Soc., Dalton Trans* 1990:3729–3733.
122. Pasqualini R, Duatti A. Synthesis and characterization of the new neutral myocardial imaging agent $[^{99m}TcN(noet)_2]$ (noet = N-ethyl-N-ethoxydithiocarbamate). *J. Chem. Soc., Chem. Commun* 1992:1354–1355.
123. Pasqualini R, Duatti A, Bellande E, Comazzi V, Brucato V, Hoffschir D, Fagret D, Comet M. Bis (dithiocarbamate) nitrido technetium-99m radiopharmaceuticals: a class of neutral myocardial imaging agents. *J. Nucl. Med* 1994;35:334–341. [PubMed: 8295007]
124. Bolzati C, Boschi A, Duatti A, Prakash S, Uccelli L. Geometrically controlled selective formation of nitrido technetium(V) asymmetrical heterocomplexes with bidentate ligands. *J. Am. Chem. Soc* 2000;122:4510–4511.
125. Bolzati C, Boschi A, Uccelli L, Tisato F, Refosco F, Cagnolini A, Duatti A, Prakash S, Bandoli G, Vittadini A. Chemistry of the strong electrophilic metal fragment $[^{99m}Tc(N)(PXP)]^{2+}$ (PXP = diphosphine ligand). A novel tool for the selective labeling of small molecules. *J. Am. Chem. Soc* 2002;124:11468–11479. [PubMed: 12236761]
126. Bolzati C, Refosco F, Cagnolini A, Tisato F, Boschi A, Duatti A, Uccelli L, Dolmella A, Marotta E, Tubaro M. Synthesis, solution-state and solid-state structural characterization of monocationic nitrido heterocomplexes $[M(N)(DTC)(PNP)]^+$ ($M = ^{99}Tc$ and Re; DTC = dithiocarbamate; PNP = heterodiphosphane). *Eur. J. Inorg. Chem* 2004:1902–1913.
127. Boschi A, Bolzati C, Benini E, Malago E, Uccelli L, Duatti A, Piffanelli A, Refosco F, Tisato F. A novel approach to the high specific-activity labeling of small peptides with the technetium-99m fragment $[^{99m}Tc(N)(PNP)]^{2+}$ (PNP = diphosphine ligand). *Bioconj. Chem* 2001;12:1035–1042.
128. Boschi A, Uccelli L, Duatti A, Bolzati C, Refosco F, Tisato F, Malagnoli R, Baradli PG, Borea PA. Asymmetrical nitrido Tc-99m heterocomplexes as potential imaging agents for benzodiazepine receptors. *Bioconj. Chem* 2003;14:1279–1288.
129. Boltzati C, Muhmood A, Malago E, Uccelli L, Boschi A, Jones AG, Refosco F, Duatti A, Tisato F. The $[^{99m}Tc(N)(PNP)]^{2+}$ metal fragment: a technetium-nitrido synthon for use with biologically active molecule. The N-(2-methoxyphenyl)piperazylcysteine analogues as examples. *Bioconj. Chem* 2003;14:1231–1242.
130. Alberto R, Schibli R, Egli A, Schubiger PA, Abram U, Kaden TA. A novel organometallic aqua complex of technetium for the labeling of biomolecules: synthesis of $[^{99m}Tc(H_2O)_3(CO)_3]^+$ from $[^{99m}TcO_4]^-$ in aqueous solution and its reaction with bifunctional ligand. *J. Am. Chem. Soc* 1998;120:7987–7988.
131. Alberto R, Ortner K, Wheatley N, Schibli R, Schubiger PA. Synthesis and properties of boranocarbonate: a convenient in situ CO source for the aqueous preparation of $[^{99m}Tc(H_2O)_3(CO)_3]^+$ *J. Am. Chem. Soc* 2001;123:3135–3136. [PubMed: 11457025]
132. Schibli R, Schwarzbach R, Alberto R, Ortner K, Schmalle H, Dumas C, Egli A, Schubiger PA. Steps toward high specific activity labeling of biomolecules for therapeutic application: preparation of precursor $[^{188}Re(H_2O)_3(CO)_3]^+$ and synthesis of tailor-made bifunctional ligand systems. *Bioconj. Chem* 2002;13:750–756.
133. Alberto R, Schibli R, Abram U, Egli A, Knapp FF, Schubiger PA. Potential of the “ $[M(CO)_3]^+$ ” ($M = Re, Tc$) moiety for the labeling of biomolecules. *Radiochim. Acta* 1977;79:99–103.

134. Häfliger P, Mundwiler S, Ortner K, Spingler B, Alberto R, Andócs G, Balogh L, Bodo K. Structure, stability, and biodistribution of cationic $[M(\text{CO})_3]^+$ ($M = \text{Re}, ^{99}\text{Tc}, ^{99\text{m}}\text{Tc}$) complexes with tridentate amine ligands. *Synth. React. Inorg. Met.-Org. Chem* 2005;35:27–34.
135. Rattat D, Eraets K, Cleynhens B, Knight H, Fonge H, Verbruggen A. Comparison of tridentate ligands in competition experiments for their ability to form a $[^{99\text{m}}\text{Tc}(\text{CO})_3]^+$ complex. *Tetrahedron Lett* 2004;45:2531–2534.
136. Wei LH, Banerjee SR, Levadala MK, Babich JW, Zubieta J. Complexes of the *fac*- $[\text{Re}(\text{CO})_3]^+$ core with tridentate ligands derived from arylpiperazines. *Inorg. Chim. Acta* 2004;357:1499–1516.
137. Pak JK, Benny P, Spingler B, Ortner K, Alberto R. N^ϵ functionalization of metal and organic protected L-Histidine for a highly efficient, direct labeling of biomolecules with $[^{99\text{m}}\text{Tc}(\text{H}_2\text{O})_3(\text{CO})_3]^+$. *Chem. Eur. J* 2003;9:2053–2061.
138. Kim Y, He Z, Hsieh W, Liu S. Synthesis, characterization and X-ray crystal structure of $[\text{Re}(\text{PNP})(\text{CO})_3]\text{Br}\cdot 2\text{CH}_3\text{OH}$: model compound for a new class of cationic $^{99\text{m}}\text{Tc}$ radiotracers. *Inorg. Chim. Acta* 2006;359:2479–2488.
139. Schubiger PA, Grünberg J, Ametamey SM, Honer M, Garcia-Garayoa E, Bläuenstein P, Waibel R, Novak-Hofer I, Schibli R. Radiopharmaceuticals: from molecular imaging to targeted radionuclide therapy. *Chimia* 2004;58:731–735.
140. Stichelberger A, Waibel R, Dumas C, Schubiger PA, Schibli R. Versatile synthetic approach to new bifunctional chelating agents tailor made for labeling with the *fac*- $[\text{M}(\text{CO})_3]^+$ core ($M = \text{Tc}, ^{99\text{m}}\text{Tc}, \text{Re}$): synthesis, in vitro, and in vivo behavior of the model complex $[\text{M}(\text{APPA})(\text{CO})_3]$ (APPA = [(5-amino-pentyl)-pyridin-2-yl-methylamino]-acetic acid). *Nucl. Med. Biol* 2003;30:465–470. [PubMed: 12831983]
141. Alberto R, Schibli R, Schubiger PA, Abram U, Pietzsch HJ, Johannsen B. First application of *fac*- $[^{99\text{m}}\text{Tc}(\text{H}_2\text{O})_3(\text{CO})_3]^+$ in bioorganometallic chemistry: design, structure, and in vitro affinity of 5-HT_{1A} receptor ligand labeled with $^{99\text{m}}\text{Tc}$. *J. Am. Chem. Soc* 1999;121:6076–6077.
142. La Bella R, Garcia-Garayoa E, Langer M, Bläuenstein P, Beck-Sickinger AG, Schubiger PA. In vitro and in vivo evaluation of a $^{99\text{m}}\text{Tc}(\text{I})$ -labeled bombesin analogue for imaging of gastrin releasing peptide receptor-positive tumors. *Nucl. Med. Biol* 2002;29:553–560. [PubMed: 12088725]
143. Schibli R, La Bella R, Alberto R, Garcia-Garayoa E, Ortner K, Abram U, Schubiger PA. Influence of the denticity of ligand systems on the in vitro and in vivo behavior of $^{99\text{m}}\text{Tc}(\text{I})$ -tricarbonyl complexes: a hint for the future functionalization of biomolecules. *Bioconj. Chem* 2000;11:345–351.
144. Waibel R, Alberto R, Willuda J, Finnern R, Schibli R, Stichelberger A, Egli A, Abram U, Mach JP, Pflückthun A, Schubiger PA. Stable one-step technetium-99m labeling of His-tagged recombinant proteins with a novel $\text{Tc}(\text{I})$ -carbonyl complex. *Nat. Biotechnol* 1999;17:897–901. [PubMed: 10471933]
145. Banerjee SR, Maresca KP, Francesconi L, Valliant J, Babich JW, Zubieta J. New directions in the coordination chemistry of $^{99\text{m}}\text{Tc}$: a reflection on technetium core structures and a strategy for new chelate design. *Nucl. Med. Biol* 2005;32:1–20. [PubMed: 15691657]
146. Fani M, Psimadas D, Zikos C, Xanthopoulos S, Loudos GK, Bouziotis P, Varvarigou AD. Comparative evaluation of linear and cyclic $^{99\text{m}}\text{Tc}$ -RGD peptides for targeting of integrins in tumor angiogenesis. *Anticancer Res* 2006;26:431–434. [PubMed: 16475729]
147. Zhang X, Chen X. Preparation and characterization of $^{99\text{m}}\text{Tc}(\text{CO})_3\text{-BPy-RGD}$ complex as $\alpha_v\beta_3$ integrin receptor-targeted imaging agent. *Appl. Radiat. Isot* 2007;65:70–78. [PubMed: 17011200]
148. Alves S, Correia JDG, Gano L, Rold TL, Prasanphanich A, Haubner R, Rupprich M, Alberto R, Decristoforo C, Snaos I, Smith CJ. In vitro and in vivo evaluation of a novel $^{99\text{m}}\text{Tc}(\text{CO})_3$ -pyrazolyl conjugate of *cyclo*-(Arg-Gly-Asp-d-Tyr-Lys). *Bioconj. Chem* 2007;18:530–537.
149. Alberto R, Schibli R, Waibel R, Abram U, Schubiger PA. Basic aqueous chemistry of $[\text{M}(\text{H}_2\text{O})_3(\text{CO})_3]^+$ ($M = \text{Re}, \text{Tc}$) directed towards radiopharmaceutical application. *Coord. Chem. Rev* 1999;190–192:901–919.
150. Schibli R, Schubiger PA. Current use and future potential of organometallic radiopharmaceuticals. *Eur. J. Nucl. Med* 2002;29:1529–1542.

151. Abrams MJ, Juweid M, tenKate CI, Schwartz DA, Hauser MM, Gaul FE, Fuccello AJ, Rubin RH, Strauss HW, Fischman AJ. Technetium-99m-human polyclonal IgG radiolabeled via the hydrazino nicotinamide derivative for imaging focal sites of infection in rats. *J. Nucl. Med* 1990;31:2022–2028. [PubMed: 2266401]
152. Schwartz DA, Abrams MJ, Hauser MM, Gaul FE, Larsen SK, Rauh D, Zubieta J. Preparation of hydrazino-modified proteins and their use for the synthesis of ^{99m}Tc -protein conjugates. *Bioconj. Chem* 1991;2:333–336.
153. Ultee ME, Bridger GJ, Abrams MJ, Longley CB, Burton CA, Larsen S, Henson GW, Padmanabhan S, Gaul FE, Schwartz DA. Tumor imaging with technetium-99m-labeled hydrazinonicotinamide-Fab' conjugates. *J. Nucl. Med* 1997;38:133–138. [PubMed: 8998167]
154. Babich JW, Solomon H, Pike MC, Kroon D, Graham W, Abrams MJ, Tompkins RG, Rubin RH, Fischman AJ. Technetium-99m labeled hydrazine nicotinamide derivatized chemotactic peptide analogs for imaging focal sites of bacterial infection. *J. Nucl. Med* 1993;34:1967–1974.
155. Babich JW, Fischman AJ. Effect of "co-ligand" on the biodistribution of ^{99m}Tc -labeled hydrazino nicotinic acid derivatized chemotactic peptides. *Nucl. Med. Biol* 1995;22:25–30. [PubMed: 7735166]
156. Babich JW, Graham W, Barrow SA, Fischman AJ. Comparison of the infection imaging properties of a ^{99m}Tc labeled chemotactic peptide with ^{111}In IgG. *Nucl. Med. Biol* 1995;22:643–648. [PubMed: 7581175]
157. Babich JW, Coco WG, Barrow SA, Fischman AJ, Femia FJ, Zubieta J. ^{99m}Tc -labeled chemotactic peptides: influence of coligands on distribution of molecular species and infection imaging properties. Synthesis and structural characterization of model complexes with the $\{\text{Re}(\eta^2\text{-HNNC}_5\text{H}_4\text{N})(\eta^1\text{-HNNC}_5\text{H}_4\text{N})\}$ core. *Inorg. Chim. Acta* 2000;309:123–136.
158. Decristoforo C, Mather SJ. Preparation, ^{99m}Tc -labeling, and in vitro characterization of HYNIC and N₃S modified RC-160 and [Tyr³]Octreotide. *Bioconj. Chem* 1999;10:431–438.
159. Decristoforo C, Melendez L, Sosabowski JK, Mather SJ. ^{99m}Tc -HYNIC-[Tyr³]-octreotide for imaging somatostatin-receptor-positive tumors: preclinical evaluation and comparison with ^{111}In -Octreotide. *J. Nucl. Med* 2000;41:1114–1119. [PubMed: 10855644]
160. Decristoforo C, Mather SJ. ^{99m}Tc -labeled peptide-HYNIC conjugates: effect of lipophilicity and stability on biodistribution. *Nucl. Med. Biol* 1999;26:389–396. [PubMed: 10382842]
161. Decristoforo C, Mather SJ. Technetium-99m somatostatin analogues: effect of labeling methods and peptide sequence. *Eur. J. Nucl. Med* 1999;26:869–876. [PubMed: 10436200]
162. Bangard M, Béhé M, Guhlke S, Otte R, Bender H, Maecke HR, Birsack HJ. Detection of somatostatin receptor-positive tumours using the new ^{99m}Tc -tricine-HYNIC-D-Phe¹-Tyr³-octreotide: first results in patients and comparison with ^{111}In -DTPA-D-Phe¹-Tyr³-octreotide. *Eur. J. Nucl. Med* 2000;27:628–637. [PubMed: 10901448]
163. Decristoforo C, Mather SJ, Cholewinski W, Donnemiller E, Riccabona G, Moncayo R. ^{99m}Tc -EDDA/HYNIC-TOC: a new ^{99m}Tc -labeled radiopharmaceutical for imaging somatostatin receptor-positive tumors: first clinical results and inpatient comparison with ^{111}In -labeled octreotide derivatives. *Eur. J. Nucl. Med* 2000;27:1318–1325. [PubMed: 11007513]
164. Laverman P, Dams ETM, Oyen WJG, Storm G, Koenders EB, Prevost R, van der Meer JWM, Corstens FHM, Boerman OC. A novel method to label liposomes with ^{99m}Tc by the hydrazinonicotinyl derivative. *J. Nucl. Med* 1999;40:192–197. [PubMed: 9935076]
165. Zhang Y, Liu N, Zhu ZH, Rusckowski M, Hnatowich DJ. Influence of different chelators (HYNIC, MAG₃ and DTPA) on tumor cell accumulation and mouse biodistribution of technetium-99m labeled antisense DNA. *Eur. J. Nucl. Med* 2000;27:1700–1707. [PubMed: 11105827]
166. Hnatowich DJ, Winnard P Jr, Virzi F, Fogarasi M, Santo T, Smith CL, Cantor CR, M Rusckowski M. Technetium-99m labeling of DNA oligonucleotides. *J. Nucl. Med* 1995;36:2306–2314. [PubMed: 8523124]
167. Liu S, Edwards DS, Looby RJ, Harris AR, Poirier MJ, Barrett JA, Heminway SJ, Carroll TR. Labeling a hydrazinonicotinamide-modified cyclic IIB/IIIA receptor antagonist with ^{99m}Tc using aminocarboxylates as co-ligands. *Bioconj. Chem* 1996;7:63–71.

168. Edwards DS, Liu S, Ziegler MC, Harris AR, Crocker AC, Heminway SJ, Barrett JA, Bridger GJ, Abrams MJ, Higgins JD. RP463: A stabilized technetium-99m complex of a hydrazino nicotinamide conjugated chemotactic peptide for infection imaging. *Bioconj. Chem* 1999;10:884–891.
169. Edwards DS, Liu S, Barrett JA, Harris AR, Looby RJ, Ziegler MC, Heminway SJ, Carroll TR. A new and versatile ternary ligand system for technetium radiopharmaceuticals: water soluble phosphines and tricine as coligands in labeling a hydrazino nicotinamide-modified cyclic glycoprotein IIb/IIIa receptor antagonist with ^{99m}Tc . *Bioconj. Chem* 1997;8:146–154.
170. Liu S, Edwards DS, Harris AR. A novel ternary ligand system for technetium radiopharmaceuticals: imine-N containing heterocycles as coligands in labeling a hydrazinonicotinamide-modified cyclic platelet glycoprotein IIb/IIIa receptor antagonist with ^{99m}Tc . *Bioconj. Chem* 1998;9:583–595.
171. Liu S, Edwards DS, Harris AR, Heminway SJ, Barrett JA. Technetium complexes of a hydrazinonicotinamide-conjugated cyclic peptide and 2-hydrazinopyridine: Synthesis and characterization. *Inorg. Chem* 1999;38:1326–1335. [PubMed: 11670921]
172. Liu S, Ziegler MC, Edwards DS. Radio-LC-MS for the characterization of ^{99m}Tc -labeled bioconjugates. *Bioconj. Chem* 2000;11:113–117.
173. Brouwers AH, Laverman P, Boerman OC, Oyen WJG, Barrett JA, Harris TD, Edwards DS, Corstens FHM. A ^{99m}Tc -labeled leukotriene B4 receptor antagonist for scintigraphic detection of infection in rabbits. *Nucl. Med. Commun* 2000;21:1043–1051. [PubMed: 11192710]
174. Liu S, Harris AR, Ziegler MC, Edwards DS, Williams NE. ^{99m}Tc -labeling of a hydrazinonicotinamide-conjugated LTB₄ receptor antagonist useful for imaging infection and inflammation. *Bioconj. Chem* 2002;13:881–886.
175. Liu S, Edwards DS, Ziegler MC, Harris AR, Heminway SJ, Barrett BA. ^{99m}Tc -Labeling of a hydrazinonicotinamide-conjugated vitronectin receptor antagonist. *Bioconj. Chem* 2001;12:624–629.
176. Liu S, Hsieh W, Kim YS, SI Mohammed SI. S. I. Effect of coligands on biodistribution characteristics of ternary ligand ^{99m}Tc complexes of a HYNIC-conjugated cyclic RGDfK dimer. *Bioconj. Chem* 2005;16:1580–1588.
177. Liu S, Hsieh W, Jiang Y, Kim Y, Sreerama SG, Chen X, Jia B, Wang F. Evaluation of a ^{99m}Tc -labeled cyclic RGD tetramer for non-invasive imaging integrin $\alpha_v\beta_3$ -positive breast cancer. *Bioconj. Chem* 2007;18:438–446.
178. Liu S, He Z, Hsieh W, Kim YS, Jiang Y. Impact of PKM linkers on biodistribution characteristics of the ^{99m}Tc -labeled cyclic RGDfK dimer. *Bioconj. Chem* 2006;17:1499–1507.
179. Jia B, Shi J, Yang Z, Xu B, Liu Z, Zhao H, Liu S, Wang F. ^{99m}Tc -labeled cyclic RGDfK dimer: initial evaluation for SPECT imaging of glioma integrin $\alpha_v\beta_3$ expression. *Bioconj. Chem* 2006;17:1069–1076.
180. Liu S, Edwards DS, Harris AR, Ziegler MC, Poirier MJ, Ewels BA, DiLuzio WR, Hui P. Towards developing a non-SnCl₂ formulation for RP444: a new radiopharmaceutical for thrombus imaging. *J. Pharm. Sci* 2001;90:114–123. [PubMed: 11169528]
181. Edwards DS, Liu S, Harris AR, Ewels BA. ^{99m}Tc -labeling hydrazones of a hydrazinonicotinamide conjugated cyclic peptide. *Bioconj. Chem* 1999;10:803–807.
182. Delmon-moingeon LI, Mahmood A, Davison A, Jones AG. Strategies for labeling monoclonal antibodies and antibody-like molecules with technetium-99m. *J. Nucl. Biol. Med* 1991;35:47–59. [PubMed: 1932176]
183. Rhodes BA. Direct labeling of proteins with ^{99m}Tc . *Nucl. Med. Biol* 1991;18:667–676.
184. Eckelman WC, Steigman J. Direct labeling with ^{99m}Tc . *Nucl. Med. Biol* 1991;18:3–7.
185. Griffiths GL, Goldenberg DM, Jones AL, Hansen HJ. Radiolabeling of monoclonal antibodies and fragments with technetium and rhenium. *Bioconj. Chem* 1992;3:91–99.
186. Zamora PO, Rhodes BA. Imidazoles as well as thiolates in proteins bind technetium-99m. *Bioconj. Chem* 1992;3:493–498.
187. Liu S, Edwards DS, Harris AR, Singh PR. ^{99m}Tc -labeling kinetics of four thiol-containing chelators and 2-hydrazinopyridine: factors influencing their radiolabeling efficiency. *Appl. Radiat. Isot* 1997;48:1103–1111.
188. Schwochau K. Technetium radiopharmaceuticals-fundamentals, synthesis, structure, and development. *Angew. Chem. Int. Ed. Eng* 1994;33:2258–2267.

189. Kelly JD, Forster AM, Archer CM, Booker FS, Canning LR, Chiu KW, Edwards B, Gill HK, McPartlin M, Nagle KR, Latham IA, Pickett RD, Storey AE, Webbon PM. Technetium-99m-tetrofosmin as a new radiopharmaceutical for myocardial perfusion imaging. *J. Nucl. Med* 1993;34:222–227. [PubMed: 8429340]
190. Higley B, Smith FW, Smith T, Gemmell HG, Gupta PD, Gvozdanovic DV, Graham D, Hinge D, Davidson J, Lahiri A. Technetium-99m 1,2-bis[bis(2-ethoxyethyl)phosphino]ethane: human biodistribution, dosimetry and safety of a new myocardial perfusion imaging agent. *J. Nucl. Med* 1993;34:30–38. [PubMed: 8418268]
191. Najafi A, Alauddin MM, Sosa A, Ma GQ, Chen DCP, Epstein AL, Siegel ME. The evaluation of ¹⁸⁶Re-labeled antibodies using N₂S₄ chelate in vitro and in vivo using tumor-bearing nude mice. *Nucl. Med. Biol* 1992;19:205–212.
192. Blower PJ, Prakash S. The chemistry of rhenium in nuclear medicine. *Perspectives Bioinorg. Chem* 1999;4:91–143.
193. Visser GWM, Gerretsen M, Herscheid JDM, Snow GB, van Dongen G. Labeling of monoclonal antibodies with rhenium-186 using the MAG3 chelate for radioimmunotherapy of cancer: a technical protocol. *J. Nucl. Med* 1993;34:1953–1963. [PubMed: 8229241]
194. van Gog FB, Visser GWM, Klok R, van der Schors R, Snow GB, van Dongen G. Monoclonal antibodies labeled with rhenium-186 using the MAG3 chelate: relationship between the number of chelated groups and biodistribution characteristics. *J. Nucl. Med* 1996;37:352–362. [PubMed: 8667076]
195. Chen JQ, Strand SE, Tennvall J, Lindgren L, Hindorf C, Sjögren HO. Extracorporeal immunoadsorption compared to avidin chase: enhancement of tumor-to-normal tissue ratio for biotinylated rhenium-188-chimeric BR96. *J. Nucl. Med* 1997;38:1934–1939. [PubMed: 9430473]
196. Beaumier PL, Venkatesan P, Vanderheyden JL, Burgua WD, Kunz LL, Fritzberg AR, Abrams PJ, Morgan AC Jr. Rhenium-186 radioimmunotherapy of small-cell lung carcinoma xenografts in nude mice. *Cancer Res* 1991;51:676–681. [PubMed: 1845957]
197. Ram S, Buchsham DJ. A peptide-based bifunctional chelating agent for ^{99m}Tc and ¹⁸⁶Re labeling of monoclonal antibodies. *Cancer* 1994;73:769–773. [PubMed: 8306258]
198. Liu S, Wong E, Rettig SJ, Orvig C. Hexadentate N₃O₃ amine phenol ligands for group 13 Metal Ions: Evidence for intrastrand and interstrand hydrogen bonds in polydentate tripodal amine phenols. *Inorg. Chem* 1993;32:4268–4276.
199. Liu S, Wong E, Karunaratne V, Rettig SJ, Orvig C. Highly flexible chelating ligands for group 13 metals. Design, synthesis and characterization of hexadentate (N₃O₃) tripodal amine phenol ligand complexes of aluminum, gallium and indium. *Inorg. Chem* 1993;32:1756–1765.
200. Liu S, Rettig SJ, Orvig C. Polydentate ligand chemistry of group 13 metals: Effects of the size and donor-selectivity of metal ions on structures and properties of aluminum, gallium and indium complexes with potentially heptadentate (N₄O₃) amine phenol ligands. *Inorg. Chem* 1992;31:5400–5407.
201. Wong E, Caravan P, Liu S, Rettig SJ, Orvig C. Selectivity of potentially hexadentate amine phenols for Ga³⁺ and In³⁺ in aqueous solution. *Inorg. Chem* 1996;35:715–724.
202. Cox JL, Craig AS, Helps IM, Jankowski KJ, Parker D, Eaton MAW, Millican AT, Millar K, Beeley NRA, Boyce BA. Synthesis of C- and N-functionalized derivatives of 1,4,7-triazacyclononane-1,4,7-triacetic acid (NOTA), 1,4,7,10-tetraazacyclododecane-1,4,7,10-tetraacetic acid (DOTA), and diethylenetriaminepenta-acetic acid (DTPA): bifunctional complexing agents for the derivatization of antibodies. *J. Chem. Soc., Perkin Trans* 1990:2567–2576.
203. Broan CJ, Cox JL, Craig AS, Katakly R, Parker D, Harrison A, Randall AM, Ferguson G. Structure and solution stability of indium and gallium complexes of 1,4,7-triazacyclononane-1,4,7-triacetate and yttrium complexes of 1,4,7,10-tetraazacyclododecane-1,4,7,10-tetraacetic acid and related ligands: kinetically stable complexes for use in imaging and radioimmunotherapy. X-Ray molecular structure of the indium and gallium complexes of 1,4,7-triazacyclononane-1,4,7-triacetic acid. *J. Chem. Soc., Perkin Trans* 1991:87–99.
204. André J, Maecke H, Zehnder M, Macko L, Akyel K. 1,4,7-triazanonane-1-succinic acid-4,7-diacetic acid (NODASA): a new bifunctional chelator for radio gallium-labeling of biomolecules. *Chem. Commun* 1998;12:1301–1302.

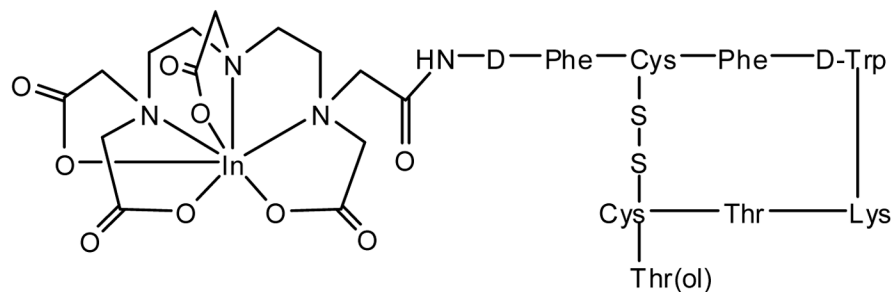
205. Eisenwiener KP, Prata MI, Buschmann I, Zhang HW, Santos AC, Wenger S, Reubi JC, Maecke HR. NODAGATOC, a new chelator-coupled somatostatin analogue labeled with [$^{67}\text{Ga}/^{68}\text{Ga}$] and [^{111}In] for SPECT, PET, and targeted therapeutic applications of somatostatin receptor (hsst2) expressing tumors. *Bioconj. Chem* 2002;13:530–541.
206. Heppeler A, Froidevaux S, Mäcke HR, Jermann E, Béhé M, Powell P, Hennig M. Radiometal-labelled macrocyclic chelator-derivatised somatostatin analogue with superb tumor-targeting properties and potential for receptor-mediated internal radiotherapy. *Chem. Eur. J* 1999;5:1974–1981.
207. Delgado R, Frausto da Siliva JJR. Metal complexes of cyclic tetra azatetraacetic acids. *Talanta* 1982;29:815–822.
208. Shannon RD. Revised effective ionic radii and systematic studies of interatomic distances in halides and chalcogenides. *Acta Cryst* 1976;A32:751–767.
209. Wong E, Liu S, Lügger T, Hahn FE, Orvig C. Hexadentate N_4O_2 amine phenol complexes of gallium and indium. *Inorg. Chem* 1995;34:93–101.
210. Viola NA, Rarig RS Jr, Ouellette W, Doyle RP. Synthesis, structure and thermal analysis of the gallium complex of 1,4,7,10-tetraazacyclododecane- $\text{N},\text{N}',\text{N}'',\text{N}'''$ -tetraacetic acid (DOTA). *Polyhedron* 2006;25:3457–3462.
211. Yang CT, Li YX, Liu S. Synthesis and structural characterization of complexes of a DO3A-conjugated triphenylphosphonium cation with diagnostically important metal ions. *Inorg. Chem. ASAP*.
212. Riesen A, Kaden TA, Ritter W, Mäcke HR. Synthesis and X-ray structural characterization of seven coordinate macrocyclic In^{3+} complexes with relevance to radiopharmaceutical applications. *J. Chem. Soc., Chem. Commun* 1989:460–462.
213. Maecke HR, Riesen A, Ritter W. The molecular structure of indium-DTPA. *J. Nucl. Med* 1989;30:1235–1239. [PubMed: 2738704]
214. Liu S, He Z, Hsieh W, Fanwick PE. Synthesis, characterization, and crystal structure of $\text{In}(\text{DOTA-AA})$ (AA = p-aminoanilide): a model compounds for ^{111}In -labeled DOTA-biomolecule conjugates. *Inorg. Chem* 2003;42:8831–8837. [PubMed: 14686864]
215. Hsieh W, Liu S. Synthesis, characterization, and structures of indium and yttrium complexes $\text{In}(\text{DTPA-BA}_2)$ and $\text{Y}(\text{DTPA-BA}_2)(\text{CH}_3\text{OH})$ (BA= benzylamine): models for ^{111}In - and ^{90}Y -labeled DTPA-biomolecule conjugates. *Inorg. Chem* 2004;43:6006–6014. [PubMed: 15360250]
216. Liu S, Edwards DS. Synthesis and characterization of two ^{111}In labeled DTPA-peptide conjugates. *Bioconj. Chem* 2001;12:630–634.
217. Eisenwiener KP, Powell P, Maecke HR. A convenient synthesis of novel bifunctional pro-chelators for coupling to bioactive peptides for radiometal labeling. *Bioorg. Med. Chem. Lett* 2000;10:2133–2135. [PubMed: 10999487]
218. Janssen M, Oyen WJG, Massuger LFAG, Frielink C, Dijkgraaf I, Edwards DS, Rajopadyhe M, Corsten FHM, OC Boerman OC. Comparison of a monomeric and dimeric radiolabeled RGD-peptide for tumor targeting. *Cancer Biotherapy & Radiopharmaceuticals* 2002;17:641–646. [PubMed: 12537667]
219. Jia B, Liu Z, Liu ZF, Yu ZL, Yang Z, Zhao HY, He Z, Liu S, Wang F. Linker effects on biological properties of ^{111}In -labeled DTPA conjugates of a cyclic RGDfK dimer. *Bioconj. Chem*. Submitted
220. Liu S, Pietryka J, Ellars CE, Edwards DS. Comparison of yttrium and indium complexes of DOTA-BA and DOTA-MBA: models for ^{90}Y - and ^{111}In -labeled DOTA-biomolecule conjugates. *Bioconj. Chem* 2002;13:902–913.
221. Cremonesi M, Ferrari M, Zoboli S, Chinol M, Stabin MG, Orsi F, Maecke HR, Jermann E, Robertson C, Fiorenza M, Tosi G, Paganelli G. Biokinetics and dosimetry in patients administered with ^{111}In -DOTA 0 -D-Phe 1 , Tyr 3]octreotide: implications for internal radiotherapy with ^{90}Y -DOTATOC. *Eur. J. Nucl. Med* 1999;26:877–886. [PubMed: 10436201]
222. De Jong M, Bakker WH, Krenning EP, Breeman WAP, van der Pluijm ME, Bernard B, Visser TJ, Jermann E, Béhé M, Powell P, Mäcke H. Yttrium-90 and indium-111 labeling, receptor binding and biodistribution of [DOTA 0 -D-Phe 1 , Tyr 3]octreotide, a promising somatostatin analogue for radionuclide therapy. *Eur. J. Nucl. Med* 1997;24:368–371. [PubMed: 9096086]

223. Ando A, Ando I, Hiraki T, Hisda K. Relation between the location of elements in the periodic table and various organ-uptake rates. *Nucl. Med. Biol* 1989;16:57–80.
224. Blower PJ, Lewis JS, Zweit J. Copper radionuclides and radiopharmaceuticals in nuclear medicine. *Nucl. Med. Biol* 1996;23:957–980. [PubMed: 9004284]
225. Smith SV. Molecular imaging with copper-64. *J. Inorg. Biochem* 2004;98:1874–1901. [PubMed: 15522415]
226. Morphy JR, Parker D, Alexander R, Bains A, Carne AF, Eaton MAW, Harrison A, Millican A, Phipps A, Rhind SK, Titmas R, Weatherby D. Antibody labeling with functionalized cyclam macrocycles. *J. Chem. Soc., Chem. Commun* 1988:156–158.
227. Parker D, Morphy R, Jankowski K, Cox J. Implementation of macrocycle conjugated antibodies for tumor targeting. *Pure & Appl. Chem* 1989;61:1637–1641.
228. Li WP, Meyer LA, Anderson CJ. Radiopharmaceuticals for positron emission tomography imaging of somatostatin receptor positive tumors. *Topics Curr. Chem* 2005;252:179–192.
229. Meares CF. Chelating agents for the binding of metal ions to antibodies. *Nucl. Med. Biol* 1986;13:311–318.
230. Moi MK, Meares CF, McCall MJ, Cole WC, DeNardo SJ. Copper chelates as probes of biological systems: stable copper complexes with macrocyclic bifunctional chelating agent. *Anal. Chem* 1985;148:249–253.
231. Li WP, Lewis JS, Kim J, Bugaj JE, Johnson MA, Erion JL, Anderson CJ. DOTA-d-Tyr¹-Octreotate: a somatostatin analogue for labeling with metal and halogen radionuclides for cancer imaging and therapy. *Bioconj. Chem* 2002;13:721–728.
232. McQuade P, Miao Y, Yoo J, Quinn TP, Welch MJ, Lewis JS. Imaging of melanoma using ⁶⁴Cu- and ⁸⁶Y-DOTA-ReCCMSH(Arg¹¹), a cyclized peptide analogue of α -MSH. *J. Med. Chem* 2005;48:2985–2992. [PubMed: 15828837]
233. Biddlecombe GB, Rogers BE, de Visser M, Parry JJ, de Jong M, Erion JL, Lewis JS. Molecular imaging of gastrin-releasing peptide receptor-positive tumors in mice using ⁶⁴Cu- and ⁸⁶Y-DOTA-(Pro¹, Tyr⁴)-Bombesin(1–14). *Bioconj. Chem* 2007;18:724–730.
234. Parry JJ, Andrews R, Rogers BE. MicroPET imaging of breast cancer using radiolabeled bombesin analogs targeting the gastrin-releasing peptide receptor. *Breast Cancer Res. Treat* 2007;101:175–183. [PubMed: 16838112]
235. Parry JJ, Kelly TS, Andrews R, Rogers BE. *in vitro* and *in vivo* evaluation of ⁶⁴Cu-labeled DOTA-Linker-Bobesin(7–14) analogues containing different amino acid linker moiety. *Bioconj. Chem* 2007;18:1110–1117.
236. Sprague JE, Kitaura H, Zou W, Ye Y, Achilefu S, Weilbaecher KN, Taitebaum SL, Anderson CJ. Noninvasive imaging of osteoclasts in pyruvate-induced osteolysis using a ⁶⁴Cu-labeled RGD peptide. *J. Nucl. Med* 2007;48:311–318. [PubMed: 17268030]
237. Anderson CJ. Metabolism of radiometal labeled proteins and peptides: what are the real radiopharmaceuticals *in vivo*? *Cancer Biotherapy and Radiopharm* 2001;16:451–455.
238. Deshpande SV, DeNardo SJ, Meares CF, McCall MJ, Adams GP, Moi MK, DeNardo GL. Copper-67-labeled monoclonal antibody Lym-1, a potential radiopharmaceutical for cancer therapy: Labeling and biodistribution in RAJI tumored mice. *J. Nucl. Med* 1988;29:217–225. [PubMed: 3258025]
239. Cole WC, DeNardo SJ, Meares CF, McCall MJ, DeNardo GL, Esptein AL, O'Brien HA, Moi MK. Comparative serum stability of radiochelates for antibody radiopharmaceuticals. *J. Nucl. Med* 1987;28:83–90. [PubMed: 3794813]
240. Bartnikas TB, Gitlin JD. Mechanisms of biosynthesis of mammalian copper/zinc superoxide dismutase. *J. Biol. Chem* 2003;278:33602–33608. [PubMed: 12815046]
241. Boswell CA, Sun X, Niu W, Weisman GR, Wong EH, Rheingold AL, Anderson CJ. Comparative *in vivo* stability of copper-64-labeled cross-bridged and conventional tetraazamacrocyclic complexes. *J. Med. Chem* 2004;47:1465–1474. [PubMed: 14998334]
242. Boswell CA, McQuade P, Weisman GR, Wong EH, Anderson CJ. Optimization of labeling and metabolite analysis of copper-64-labeled azamacrocyclic chelators by radio-LC-MS. *Nucl. Med. Biol* 2005;32:29–38. [PubMed: 15691659]

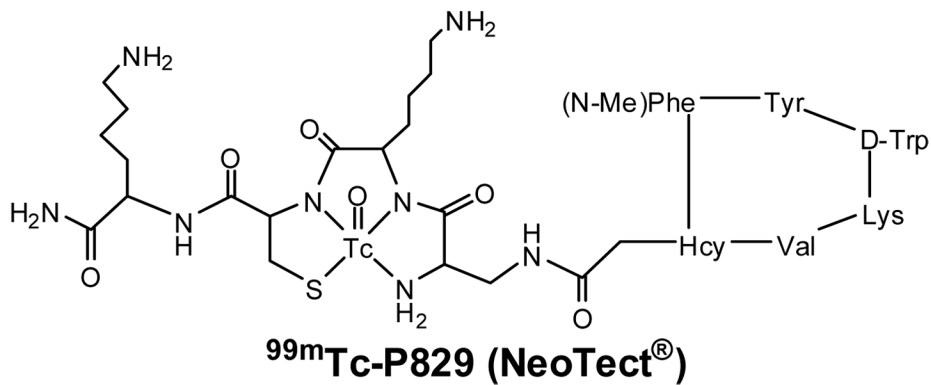
243. Sprague JE, Peng Y, Fiamengo AL, Wooden KS, Southwick EA, Wiseman GR, Wong EH, Golden JA, Rhengold AL, Anderson CJ. Synthesis, characterization and in vivo studies of Cu(II)-64-labeled cross-bridges tetraazamacrocyclic-amide complexes as models of peptide conjugate imaging agents. *J. Med. Chem* 2007;50:311–318.
244. Garrison JC, Rold TL, Sieckman GL, Figueroa SD, Volkert WA, Jurisson SS, Hoffman TJ. In vivo evaluation and small-animal PET/CT of a prostate cancer mouse model using ⁶⁴Cu Bombesin analogs: side-by-side comparison of the CB-TE2A and DOTA chelation systems. *J. Nucl. Med* 2007;48
245. Di Bartolo N, Sargeson AM, Smith SV. New ⁶⁴Cu PET imaging agents for personalised medicine and drug development using the hexa-aza cage. *SarAr. Org. Biomol. Chem* 2006;4:3350–3357.
246. Prasanphanich AF, Nanda PK, Rold TL, Ma L, Lewis MJ, Garrison JC, Hoffman TJ, Sieckman GL, Figueroa SD, Smith CJ. [⁶⁴Cu-NOTA-8-Aoc-BBN(7-14)NH₂] targeting vector for positron-emission tomography imaging of gastrin-releasing peptide receptor-expressing tissues. *PNAS* 2007;104:12462–12467. [PubMed: 17626788]
247. Lauffer RB. Paramagnetic metal complexes as water proton relaxation agents for NMR imaging: theory and Design. *Chem. Rev* 1987;87:901–927.
248. Caravan P, Ellison JJ, McMurry TJ, Lauffer RB. Gadolinium(III) chelates as MRI contrast agents: structure, dynamics, and applications. *Chem. Rev* 1999;99:2293–2352. [PubMed: 11749483]
249. Pippin CG, Parker TA, McMurry TJ, Brechbiel MW. Spectrophotometric method for the determination of a bifunctional DTPA ligand in DTPA-monoconal antibody conjugates. *Bioconj. Chem* 1992;3:342–345.
250. Brechbiel MW, Gansow OA. Backbone-substituted DTPA ligands for ⁹⁰Y radioimmunotherapy. *Bioconj. Chem* 1991;2:187–194.
251. Pulukkody KP, Norman TJ, Parker D, Royle L, Broan CJ. Synthesis of charged and uncharged complexes of gadolinium and yttrium with cyclic polyazaphosphinic acid ligands for in vivo applications. *J. Chem. Soc., Perkin Trans* 1993:605–620.
252. Wu C, Kobayashi H, Sun B, Yoo TM, Paik CH, Gansow OA, Carrasquillo JA, Pastan I, Brechbiel MW. Stereochemical influence on the stability of radio-metal complexes in vivo. Synthesis and evaluation of the four stereoisomers of 2-(p-nitrobenzyl)-trans-CyDTPA. *Bioorg. & Med. Chem* 1997;5:1925–1934. [PubMed: 9370037]
253. Camera L, Kinuya S, Garmestani K, Wu C, Brechbiel MW, Pai LH, McMurry TJ, Gansow OA, Pastan I, Paik CH, Carrasquillo JA. Evaluation of the serum stability and in vivo biodistribution of CHX-DTPA and other ligands for yttrium labeling of monoclonal antibodies. *J. Nucl. Med* 1994;35:882–889. [PubMed: 8176477]
254. Cummins CH, Rutter EW Jr, Fordyce WA. A convenient synthesis of bifunctional chelating agents based on diethylenetriaminepentaacetic acid and their coordination chemistry with yttrium(III). *Bioconj. Chem* 1991;2:180–186.
255. Williams MA, Rapoport H. Synthesis of enantiometrically pure diethylenetriaminepentaacetic acid analogues. L-Phenylalanine as the educt for substitution at the central acetic acid. *J. Org. Chem* 1993;58:1151–1158.
256. Jackson GE, Wynchank S, Woundenberg M. Gadolinium(III) complex equilibria: the implications for Gd(III) MRI contrast agents. *Magnetic Resonance Med* 1990;16:57–66.
257. McMurry TJ, Pippin CG, Wu C, Deal KA, Brechbiel MW, Mirzadeh S, Gansow OA. Physical parameters and biological stability of yttrium(III) diethylenetriaminepentaacetic acid derivative conjugates. *J. Med. Chem* 1998;41:3546–3549. [PubMed: 9719608]
258. Sherry AD, Cacheris WP, Kuan KT. Stability constants for Gd³⁺ binding to model DTPA-conjugates and DTPA-proteins: implications for their use as magnetic resonance contrast agents. *Magnetic Resonance Med* 1988;8:180–190.
259. Wu C, Brechbiel MW, Gansow OA, Kobayashi H, Carrasquillo J, Pastan I. Stability of the four 2-(p-nitrobenzyl)-trans-CyDTPA ⁸⁸Y complexes. *Radiochim. Acta* 1997;79:123–126.
260. Moi MK, Meares CF, DeNardo SJ. The peptide way to macrocyclic bifunctional chelating agents: synthesis of 2-(p-nitrobenzyl)-1,4,7,10-tetraazacyclododecane-N,N',N'',N'''-tetraacetic acid and study of its yttrium(III) complex. *J. Am. Chem* 1988;110:6266–6267.

261. Stimmel JB, Stockstill ME, Kull FC Jr. Yttrium-90 chelation properties of tetraazatetraacetic acid macrocycles, diethylenetriaminepentaacetic acid analogues, and a novel terpyridine acyclic chelator. *Bioconj. Chem* 1995;6:219–225.
262. Stimmel JB, Kull FC Jr. Samarium-153 and lutetium-177 chelation properties of selected macrocyclic and acyclic ligands. *Nucl. Med. Biol* 1998;25:117–125. [PubMed: 9468026]
263. Liu S, Ellars CE, Edwards DS. Ascorbic acid: useful as a buffer agent and radiolytic stabilizer for metalloradiopharmaceuticals. *Bioconj. Chem* 2003;14:1052–1056.
264. Liu S, Edwards DS. Stabilization of ⁹⁰Y-labeled DOTA-biomolecule conjugates using gentisic and ascorbic acid. *Bioconj. Chem* 2001;12:554–558.
265. Liu S, Cheung E, Rajopadyhe M, Ziegler MC, Edwards DS. ⁹⁰Y- and ¹⁷⁷Lu-labeling of a DOTA-conjugated vitronectin receptor antagonist for therapy. *Bioconj. Chem* 2001;12:559–568.
266. Kukis DL, DeNardo SJ, DeNardo GL, O'Donnell RT, Meares CF. Optimized conditions for chelation of yttrium-90-DOTA immunoconjugates. *J. Nucl. Med* 1998;39:2105–2110. [PubMed: 9867151]
267. Jang YH, Blanco M, Dasgupta S, Keire DA, Shively JE, Goddard WA III. Mechanism and energetics for complexation of ⁹⁰Y with 1,4,7,10-tetraazacyclododecane-1,4,7,10-tetraacetic acid (DOTA), a model for cancer radioimmunotherapy. *J. Am. Chem. Soc* 1999;121:6142–6151.
268. Goeckeler WF, Edwards B, Volkert WA, Holmes RA, Simon J, Wilson D. Skeletal localization of samarium-153 chelates: potential therapeutic bone agents. *J. Nucl. Med* 1987;28:495–504. [PubMed: 3572535]
269. Goeckeler WF, Troutner DE, Volkert WA, Edwards B, Simon J, Wilson D. ¹⁵³Sm radiotherapeutic bone agents. *Nucl. Med. Biol* 1986;13:479–482.
270. Kim WD, Kiefer GE, Maton F, McMillan K, Muller RN, Sherry AD. Relaxometry, luminescence measurements, electronphorisis, and animal biodistribution of lanthanide(III) complexes of some polyaza macrocyclic acetates containing pyridine. *Inorg. Chem* 1995;34:2233–2243.
271. Atkins HL, Mausner LF, Srivastava SC, Meinken GE, Straub RF, Cabahug CJ, Weber DA, Wong CT, Sacker DF, Madajewicz S, Park TL, Meek AG. Biodistribution of ^{117m}Sn⁴⁺ DTPA for palliative therapy of painful osseous metastases. *Radiology* 1993;186:279–283. [PubMed: 7677974]
272. Chong HS, Garmestani K, Ma DS, Milenic DE, Overstreet T, Brechbiel MW. Synthesis and biological evaluation of novel macrocyclic ligands with pendent donor groups as potential yttrium chelators for radioimmunotherapy with improved complex formation kinetics. *J. Med. Chem* 2002;45:3458–3464. [PubMed: 12139456]
273. Sherry AD, Brown RD III, Gerades CFG, Koenig SH, Kuan KT, Spiller M. Synthesis and characterization of the gadolinium(3+) complex of DOTA-propylamide: a model DOTA-protein conjugate. *Inorg. Chem* 1989;28:620–622.
274. Sieving PF, Watson A, Rocklage SM. Preparation and characterization of paramagnetic polychelates and their protein conjugates. *Bioconj. Chem* 1990;1:65–71.
275. Lewis MR, Raubitschek A, Shively JE. A facile, water soluble method for modification of proteins with DOTA. Use of elevated temperature and optimized pH to achieve high specific activity and high chelate stability in radiolabeled immunoconjugates. *Bioconj. Chem* 1994;5:565–576.
276. Lewis MR, Shively JE. Maleimidocysteineamido-DOTA derivatives: New reagents for radiometal chelate conjugation to antibody sulfhydryl groups undergo pH-dependent cleavage reactions. *Bioconj. Chem* 1998;9:72–86.
277. Corson DT, Meares CF. Efficient multigram synthesis of the bifunctional chelating agent (S)-1-p-isothiocyanatobenzyl-diethylene-tetraaminepentaacetic acid. *Bioconj. Chem* 2000;11:292–299.
278. DeNardo SJ, Zhong GR, Salako Q, Li M, DeNardo GL, Meares CF. Pharmacokinetics of chimeric L6 conjugated to indium-111- and yttrium-90-DOTA-peptide in tumor bearing mice. *J. Nucl. Med* 1995;36:829–836. [PubMed: 7738660]
279. Brechbiel MW, Gansow OA, Atcher RW, Schlom J, Simpson DE, Esteban J, Colcher D. Synthesis of 1-(p-isothiocyanatobenzyl) derivatives of DTPA and EDTA. Antibody labeling and tumor-imaging studies. *Inorg. Chem* 1986;25:2772–2781.
280. McCall MJ, Diril H, Meares CF. Simplified method for conjugating macrocyclic bifunctional chelating agents to antibodies via 2-iminothiolane. *Bioconj. Chem* 1990;1:222–226.

281. Liu S, Cheung E, Rajopadyhe M, Williams NE, Overoye KL, Edwards DS. Isomerism and solution dynamics of ^{90}Y -labeled DTPA-biomolecule conjugates. *Bioconj.Chem* 2001;12:84–91.
282. Carrasquillo JA, White JD, Paik CH, Raubitschek A, Le N, Rotman M, Brechbiel MW, Gansow OA, Top LE, Perentesis P, Reynolds JC, Nelson DL, Waldmann TA. Similarities and differences in ^{111}In - and ^{90}Y -labeled 1B4M-DTPA antiTac monoclonal antibody distribution. *J. Nucl. Med* 1999;40:268–276. [PubMed: 10025834]
283. Camera L, Kinuya S, Garmestani K, Brechbiel MW, Wu C, Pai LH, McMurry TJ, Gansow OA, Pastan I, Paik CH, JA Carrasquillo JA. Comparative biodistribution of indium- and yttrium-labeled B3 monoclonal antibody conjugated to either 2-(p-SCN-Bz)-6-methyl-DTPA (1B4M-DTPA) or 2-(p-SCN-Bz)-1,4,7,10-tetraazacyclododecane tetraacetic acid (2B-DOTA). *Eur. J. Nucl. Med* 1994;21:640–646. [PubMed: 7957350]
284. Rösch F, Herzog H, Stolz B, Brockmann J, Köhle M, Mühlensiepen H, Marbach P, Müller-Gärtner HW. Uptake kinetics of the somatostatin receptor ligand [^{86}Y]DOTA-d-Phe¹-Tyr³-octreotide ([^{86}Y]SMT487) using positron emission tomography in non-human primates and calculation of radiation doses of the ^{90}Y -labeled analogue. *Eur. J. Nucl. Med* 1999;26:358–366. [PubMed: 10199941]



^{111}In -DTPA-Octreotide (OctreoScan[®])



$^{99\text{m}}\text{Tc}$ -P829 (NeoTect[®])

Figure 1. Structures of two selected target-specific radiopharmaceuticals. The name in the bracket indicates the commercial kit preparation of the corresponding radiopharmaceutical.

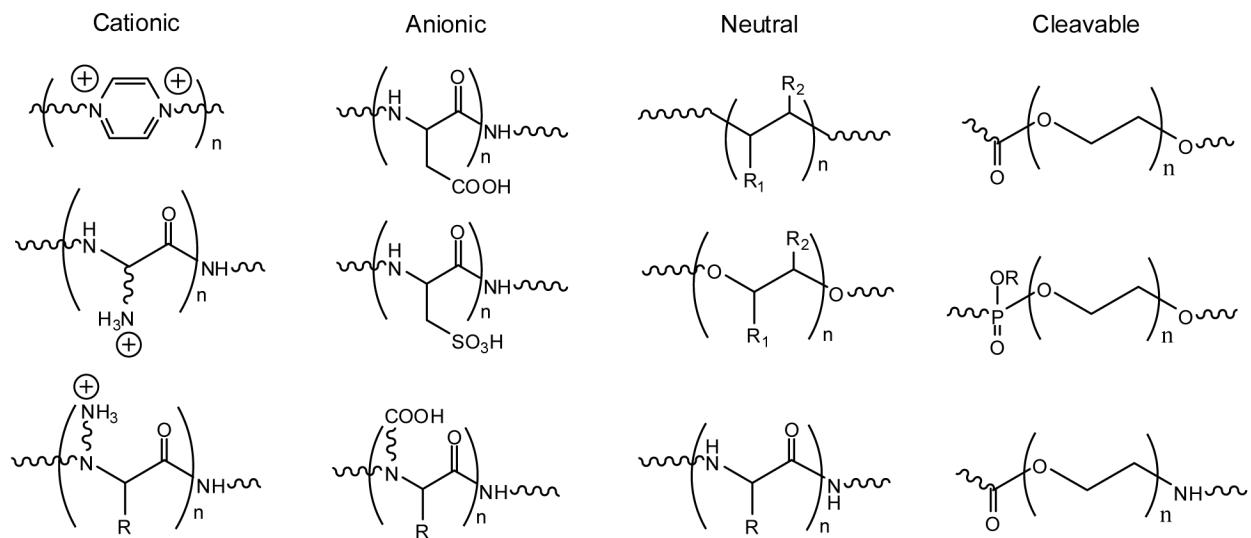


Figure 2. PKM linkers useful for modification of pharmacokinetics of radiopharmaceuticals.

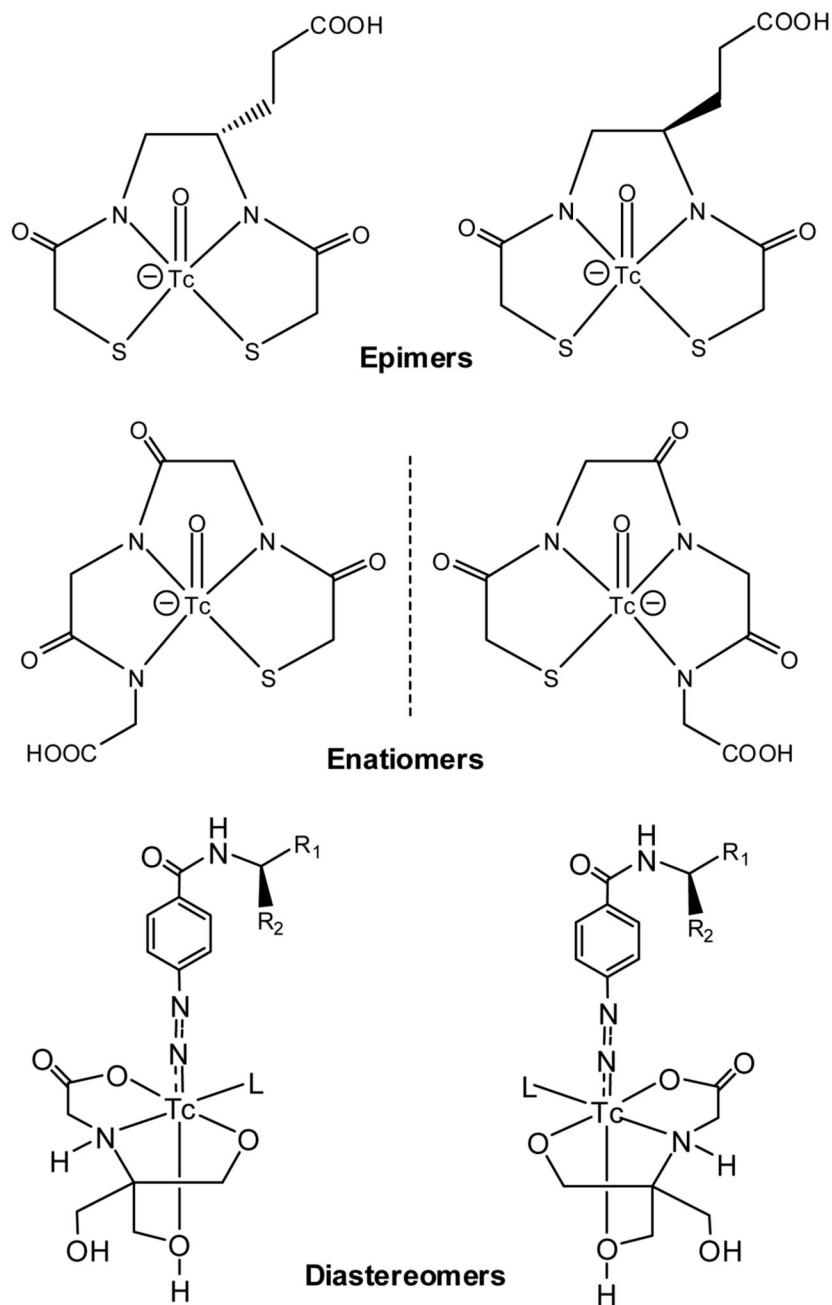


Figure 3.
Examples of isomerism in technetium complexes.

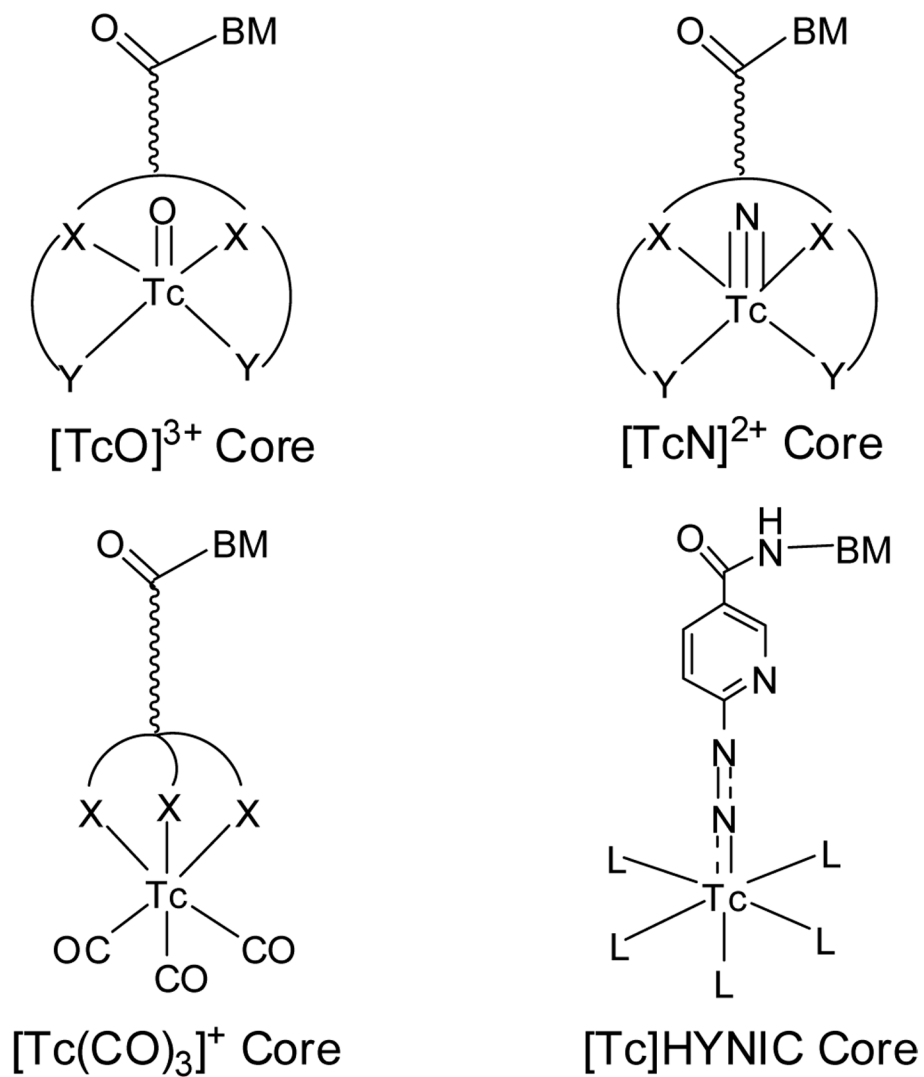
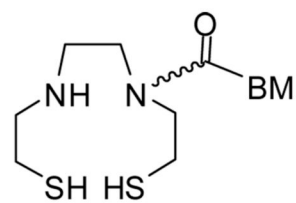
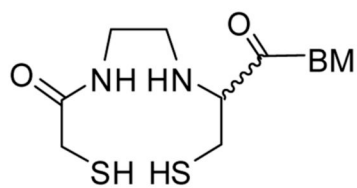
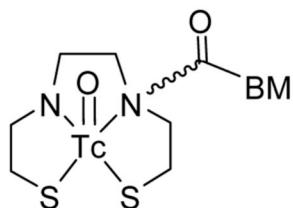
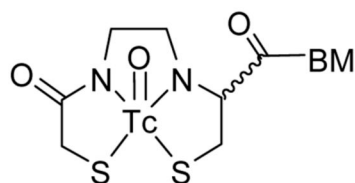


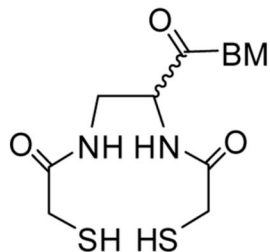
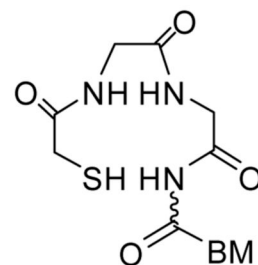
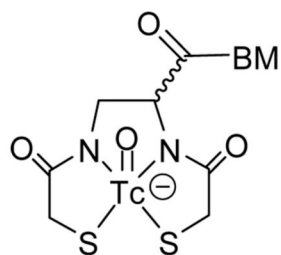
Figure 4. Technetium cores useful for the ^{99m}Tc -labeling of biomolecules.

N₂S₂ DADTN₂S₂ MAMA

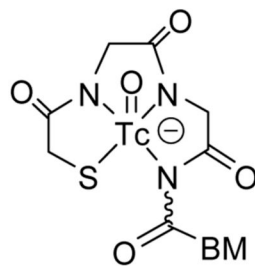
[TcO(DADT)]



[TcO(MAMA)]

N₂S₂ DADSN₃S Triamidethiol

[TcO(DADS)]



[TcO(Triamidethiol)]

Figure 5.
Thiol-containing BFCs and their technetium complexes.

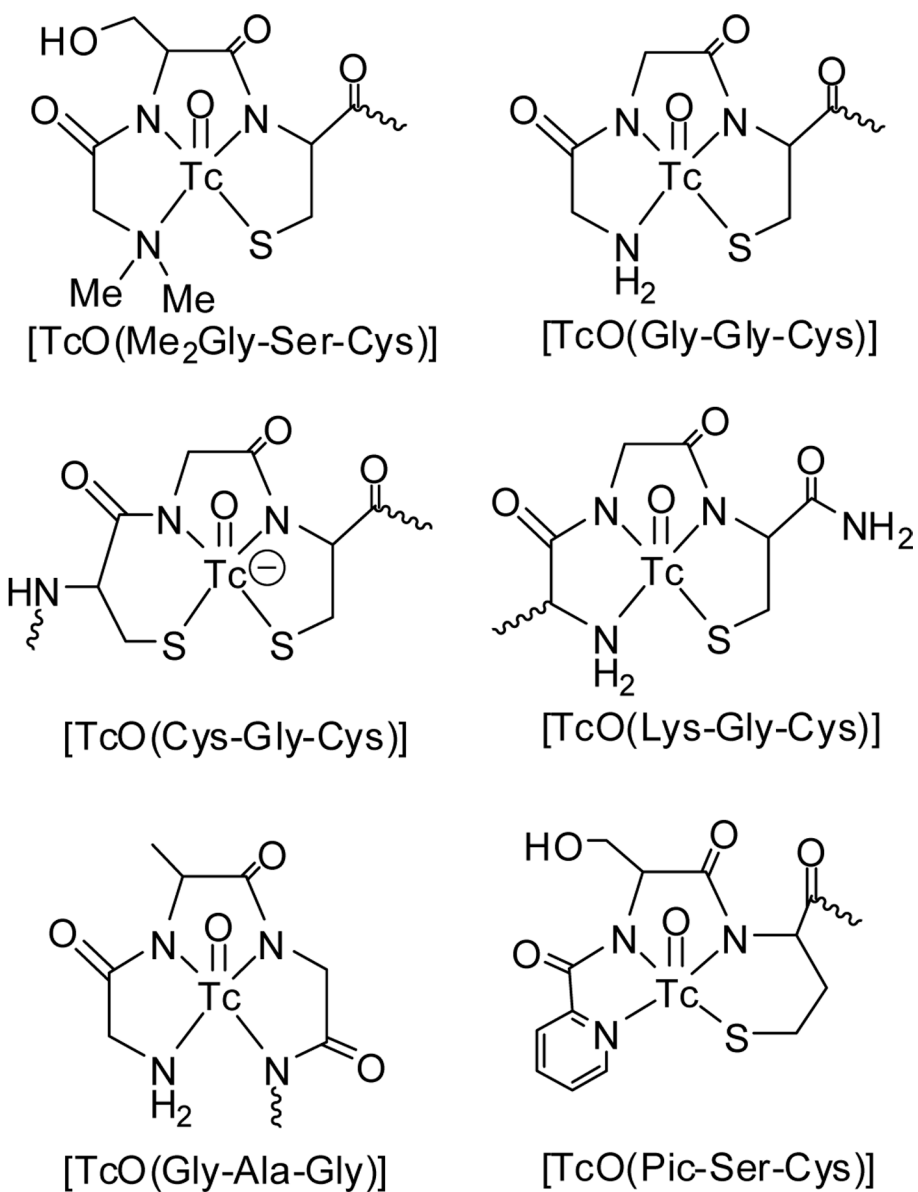


Figure 6.
Tripeptide sequences as BFCs.

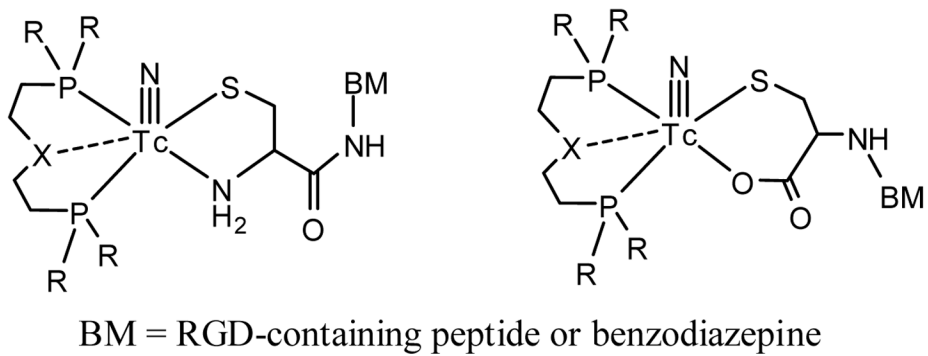


Figure 7.
Examples of the ^{99m}Tc -nitrido core for the labeling of biomolecules.

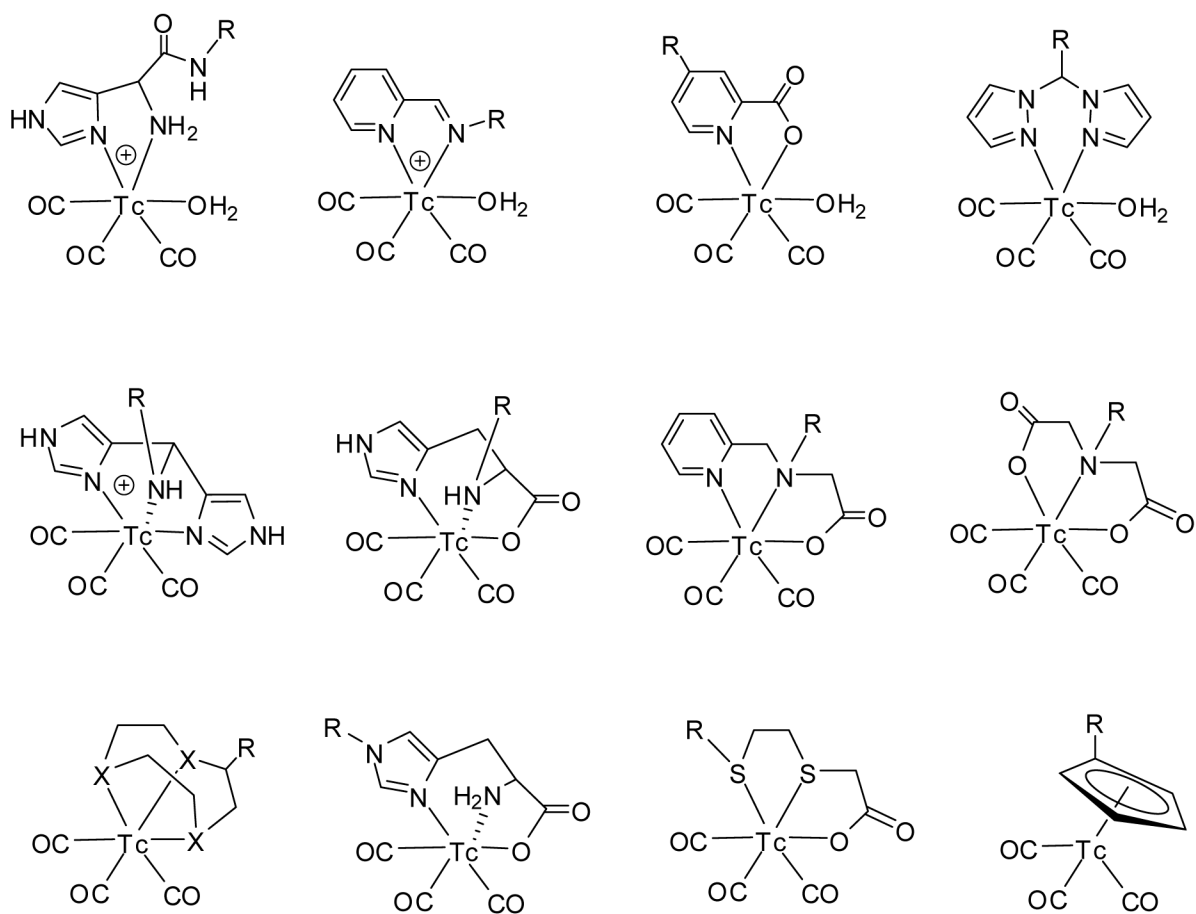


Figure 8. Examples of bidentate and tridentate BFCs for ^{99m}Tc - and $^{186/188}\text{Re}$ -labeling of biomolecules. The R group may be a biomolecule or a linker attached to the biomolecule.

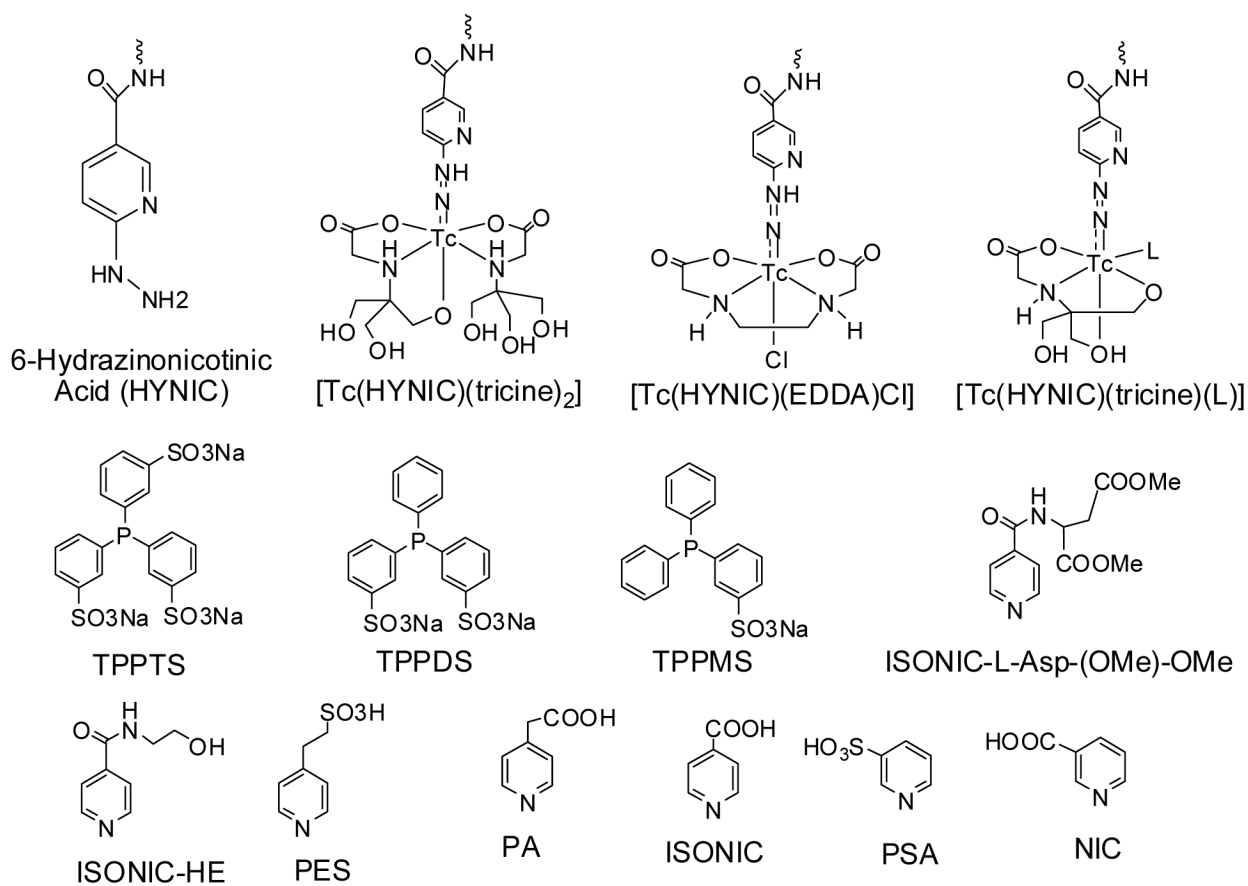


Figure 9. HYNIC, coligands and their binary and ternary ligand ^{99m}Tc complexes.

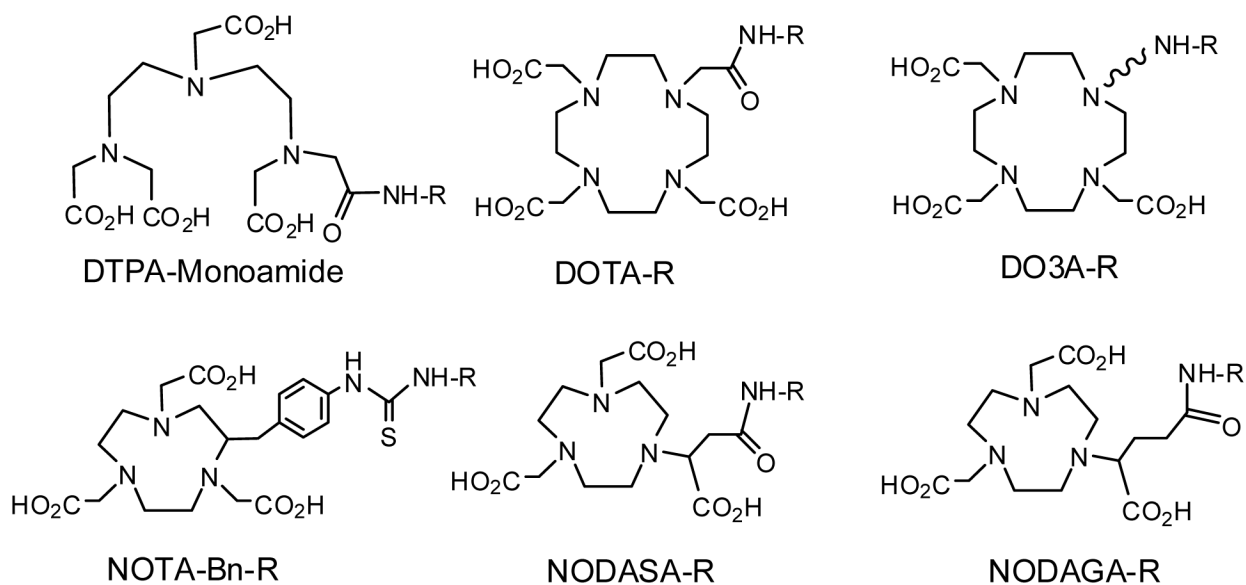
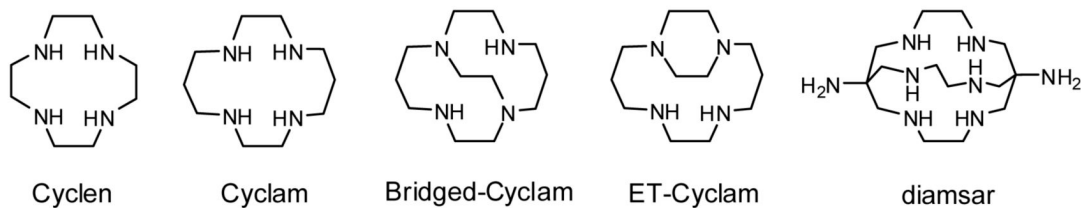
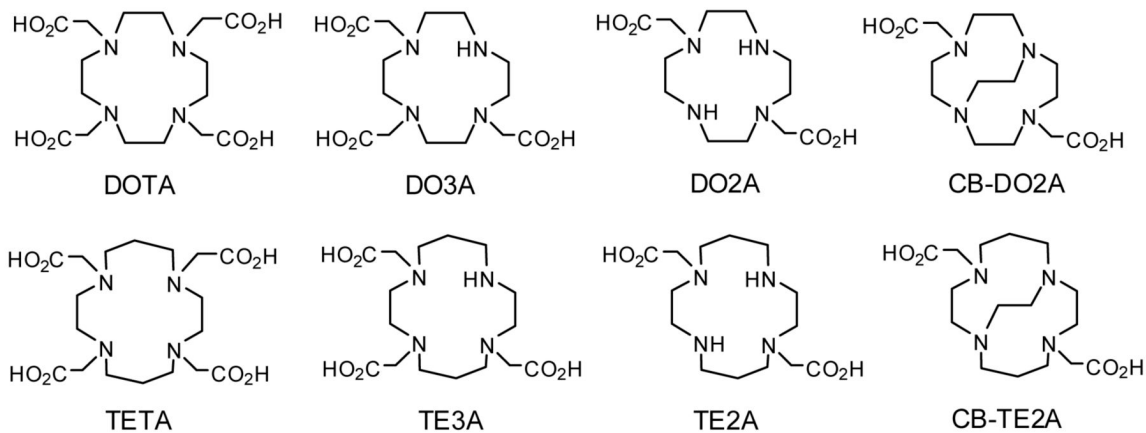


Figure 10. BFCs for $^{67/68}\text{Ga}$ and ^{111}In -labeling of biomolecules. The R group may be a biomolecule or a linker attached to the biomolecule.

Polyaza Macrocycles



Polyaminocarboxylic Macrocycles



Macrocyclic BFCs

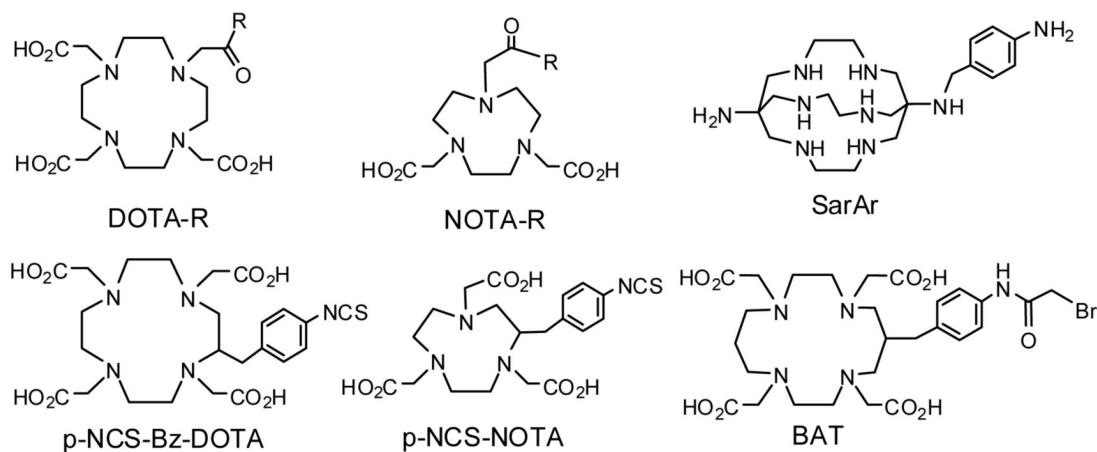


Figure 11.

BFCs for labeling of biomolecules with copper radionuclides. The R group may be a biomolecule or a linker attached to the biomolecule.

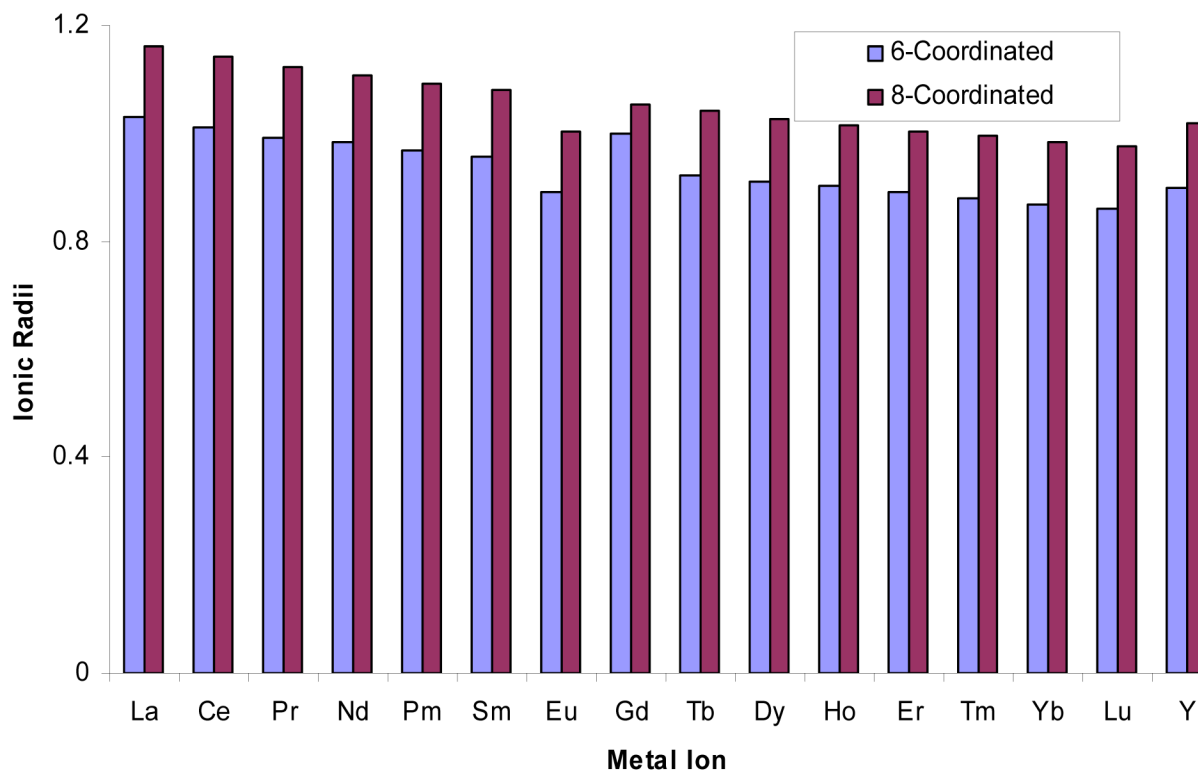


Figure 12. Ionic radii (Å) for trivalent yttrium and lanthanide ions (data from ref. 208).

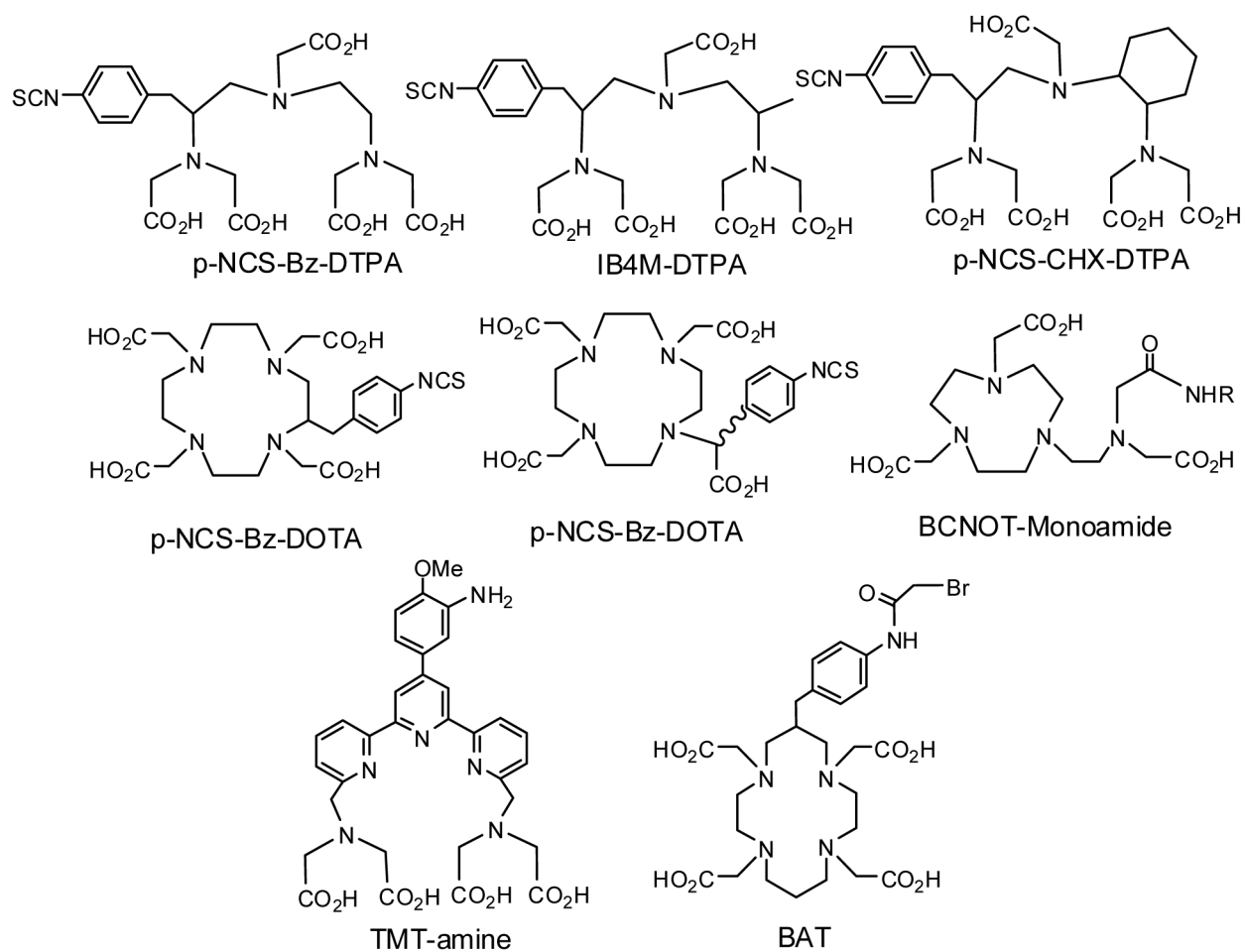


Figure 13. Selected acyclic and macrocyclic BFCs for the radiolabeling of biomolecules with yttrium and lanthanide radionuclides.

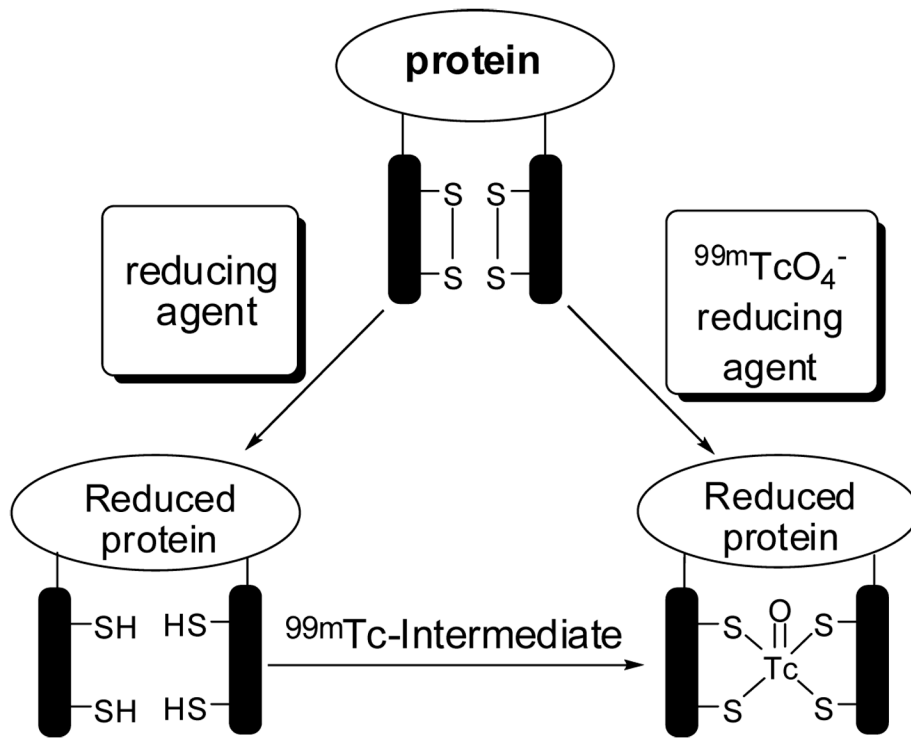


Chart I.
Direct Labeling Approach

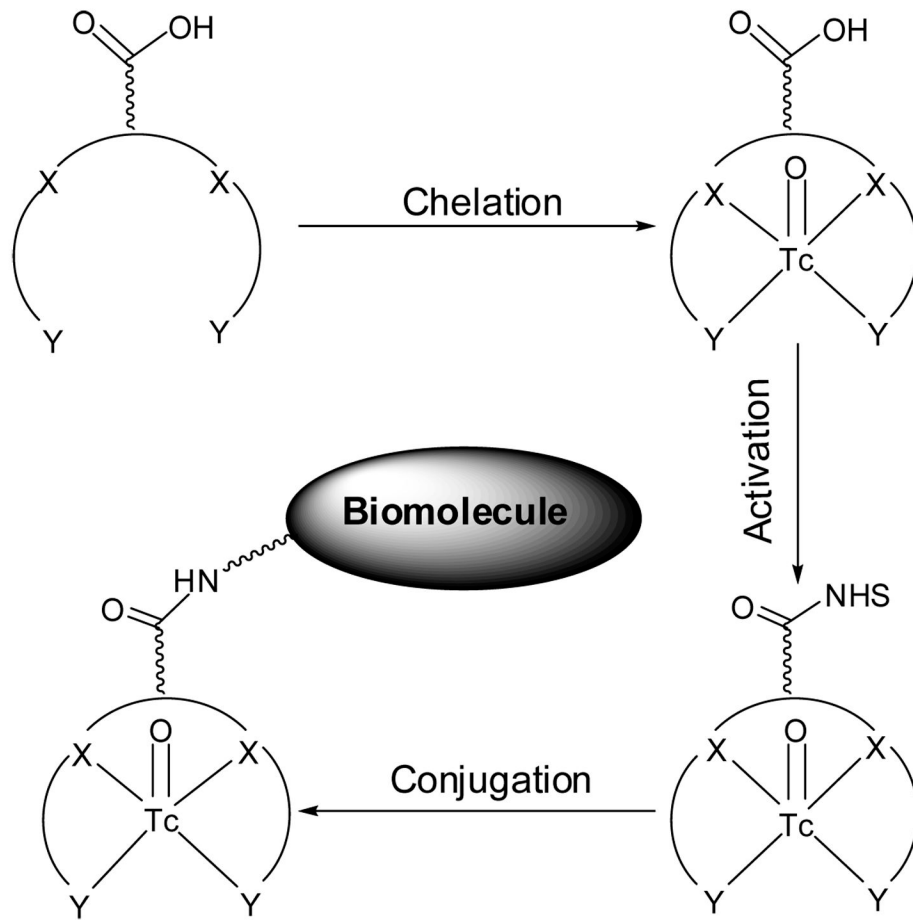


Chart II.
The Pre-Labeling Approach

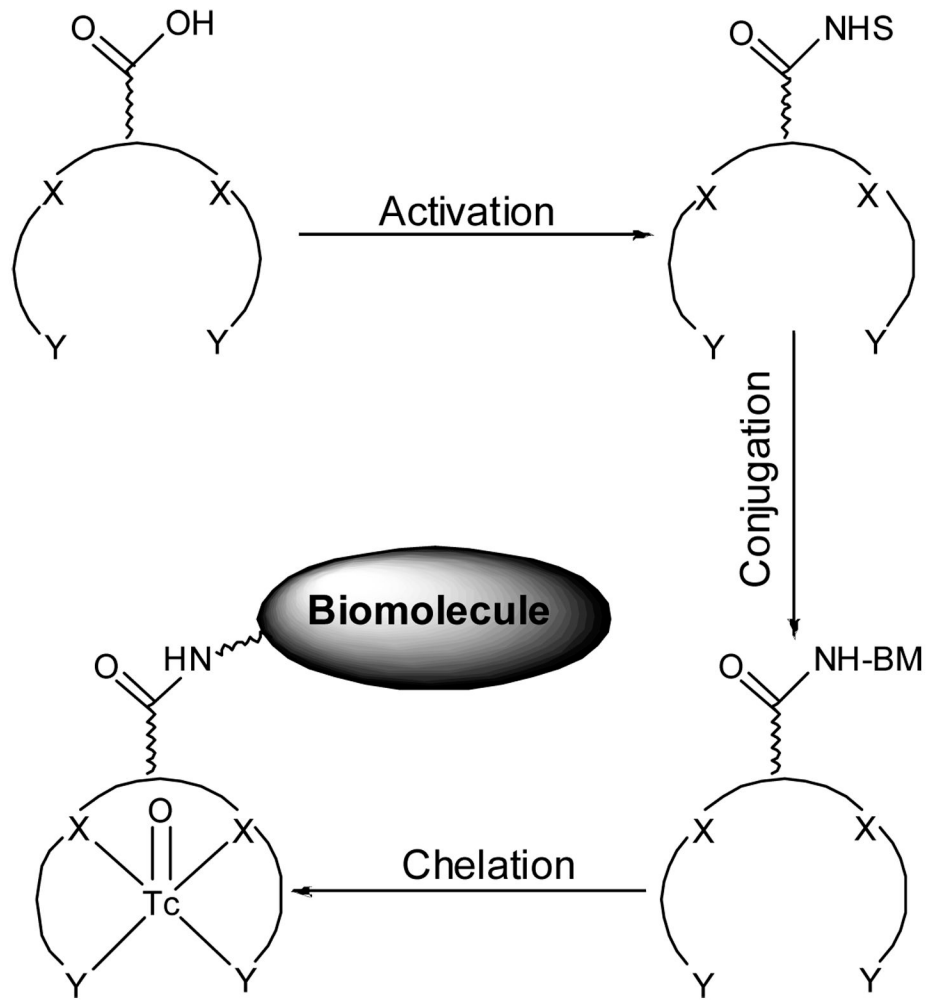


Chart III.
The Post-Labeling Approach

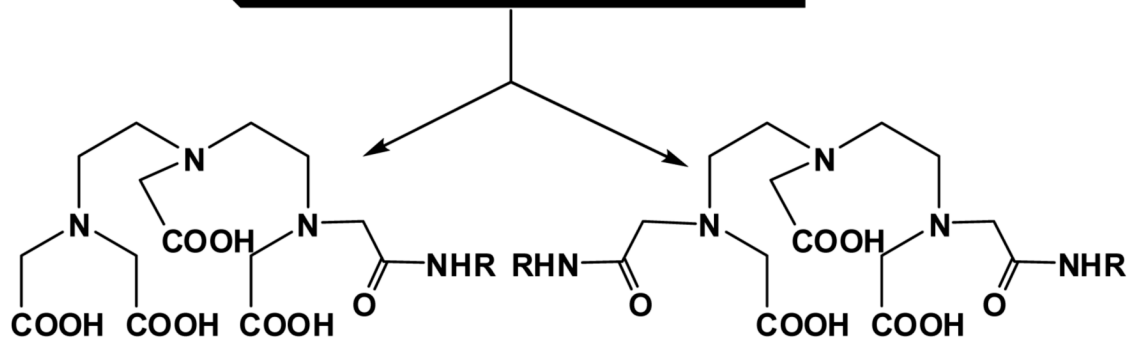
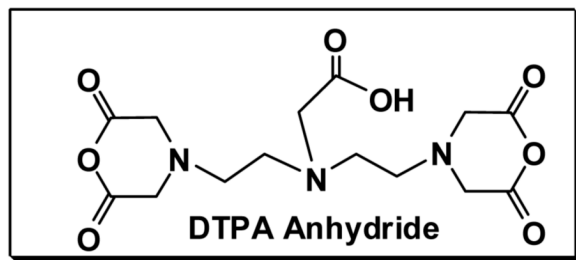
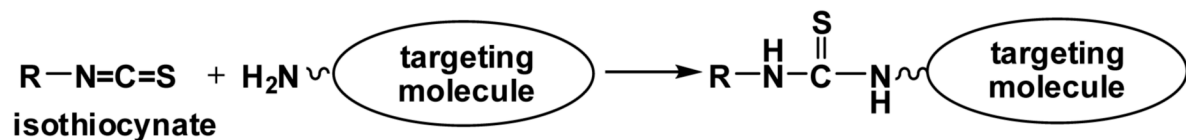
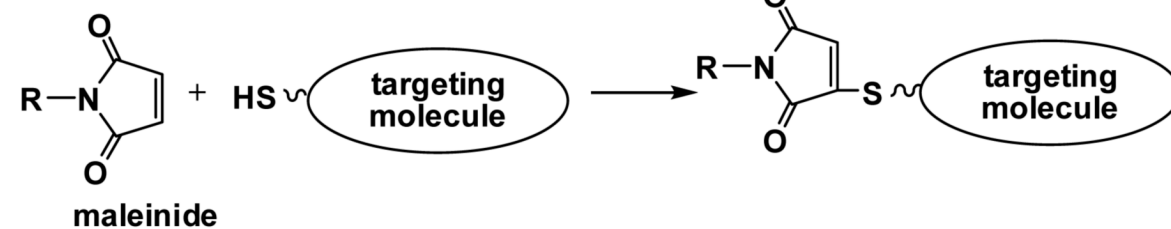
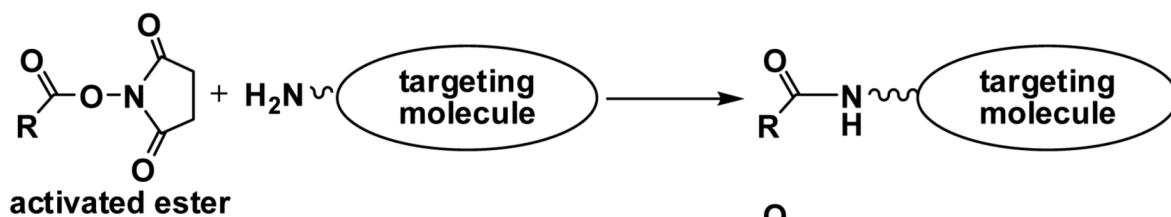
**DTPA-Monoamide****DTPA-Bisamide**

Chart IV.
Conjugation Groups for Acyclic and Macrocyclic BFCs.

Table 1

Selected target-specific diagnostic and therapeutic radiopharmaceuticals.

| Radiopharmaceutical | Trade Name | Primary Uses |
|--------------------------------|-------------------|---|
| Indium-111 Capromab pendetide | ProstaScint® | imaging of prostate cancer |
| Indium-111 pentetretotide | Octreoscan® | imaging of neuroendocrine tumors |
| Indium-111 satumomab pendetide | OncoScint® | imaging of metastatic disease associated with colorectal and ovarian cancer |
| Tc-99m Apcitide | AcuTect® | synthetic peptide for imaging deep vein thrombosis |
| Tc-99m Arcitumomab | CEA-Scan® | monoclonal antibody for imaging colorectal cancer |
| Tc-99m Depreotide | Neotect® | for imaging somatostatin receptor-positive tumors |
| Y-90 Ibitumomab Tiuxetan | Zevalin® | for treatment of Non-Hodgkin's Lymphoma |
| I-131 Tositumomab | Bexxar® | for Treatment of Non-Hodgkin's Lymphoma |

Table 2

Metallic radionuclides useful for scintigraphic imaging.

| Radiouclide | Half-life | γ -Energy (keV) | Decay Mode | Source |
|-------------------|-----------|----------------------------------|------------|-----------|
| ⁶⁷ Ga | 78.3 h | 93 (10%), 185 (24%) 296 (22%) | EC | Generator |
| ^{99m} Tc | 6.02 h | 141 (89%) | IT | Generator |
| ¹¹¹ In | 2.83 d | 171 (88%), 247 (94%) | EC | Cyclotron |

Table 3

Selected metallic radionuclides useful for PET imaging.

| Isotope | Half-life (h) | Decay Mode | E β^+ (keV) | Production Method |
|-------------------|---------------|--|------------------------|---|
| ⁶¹ Cu | 3.3 | β^+ (62%) EC (38%) | 1220, 1150 940, 560 | cyclotron, ⁶¹ Ni(p, n) ⁶¹ Cu |
| ⁶² Cu | 0.16 | β^+ (98%) EC (2%) | 2910 | ⁶² Zn/ ⁶² Cu generator |
| ⁶⁴ Cu | 12.7 | β^+ (19%) EC (41%) | 656 | cyclotron, ⁶⁴ Ni(p, n) ⁶⁴ Cu |
| ⁶⁸ Ga | 1.1 | β^- (40%) β^+ (90%) EC (10%) | 1880, 770 | ⁶⁸ Ge/ ⁶⁸ Ga generator |
| ⁸⁹ Zr | 78.5 | β^+ (23%) EC (77%) | 897 | cyclotron, ⁸⁹ Y(p, n) ⁸⁹ Zr |
| ^{94m} Tc | 0.9 | β^+ (72%) | 2.47 | cyclotron, ⁶³ Cu(α , n γ) ⁶⁶ Ga |

Table 4

Selected radionuclides useful for radiotherapy.

| Nuclide | Half-life (days) | Energy (MeV) | Maximum Range (mm) | Gamma (keV) | Source | Specific Activity* |
|-------------------|------------------|--------------|--------------------|-------------|------------------------|--------------------|
| ^{67}Cu | 2.58 | 0.575 | 1.8 | 185 (40%) | accelerator | low |
| ^{90}Y | 2.66 | 2.27 | 12.0 | --- | generator | high |
| ^{153}Sm | 1.95 | 0.80 | 3.0 | 103 (28%) | reactor | low/medium |
| ^{166}Ho | 1.1 | 1.6 | 8.0 | 81 (6.3%) | reactor or generator | high |
| ^{177}Lu | 6.7 | 0.497 | 1.5 | 208 (28%) | reactor | medium/high |
| ^{186}Re | 3.7 | 1.02 | 5.0 | 137 (9%) | accelerator or reactor | low/medium |
| ^{188}Re | 0.71 | 2.12 | 11.0 | 155 (15%) | reactor generator | high |

* The specific activity of a radionuclide depends on the source and method of production, as well as the technique of separation. In general, generator-produced radionuclides, such as ^{90}Y and ^{188}Re , have a higher specific activity than those accelerator- or reactor-produced radioisotopes. High specific activity can also be achieved by chemical purification of the desired radionuclide from the parent element after direct (n, γ)-activation of the target.

Table 5

Various oxidation states and stereochemistry of technetium.

| Oxidation State | Example | Coordination Geometry | Coordination Number | Magnetic Moment (μB) |
|-----------------|---|-----------------------|---------------------|-----------------------------------|
| +7 (d^0) | $[\text{TcH}_9]^{2-}$ | Trigonal prism | 9 | diamagnetic |
| | TcO_4^- | Tetrahedron | 4 | diamagnetic |
| +6 (d^1) | TcO_4^{2-} | Tetrahedron | 4 | 1.60 |
| +5 (d^2) | $[\text{Tc}(\text{NCS})_6]^-$ | Octahedron | 6 | diamagnetic |
| | $[\text{Tc}(\text{Diars})_2\text{Cl}_4]^{2-}$ | dodecahedron | 8 | 0.9 |
| | TcOCl_4^- | Square pyramid | 5 | diamagnetic |
| | $[\text{TcO}(l, l\text{-ECD})]$ | Square pyramid | 5 | diamagnetic |
| | $[\text{TcO}(d, l\text{-HM-PAO})]$ | Square pyramid | 5 | diamagnetic |
| | $[\text{TcO}_2(\text{tetrofosmin})]^+$ | Octahedron | 6 | diamagnetic |
| | $[\text{TcCl}_6]^{2-}$ | Octahedron | 6 | 4.05 |
| +4 (d^3) | $[\text{Tc}(\text{Diars})_2\text{Cl}_2]^+$ | Octahedron | 6 | diamagnetic |
| +3 (d^4) | $[\text{TcCl}_3(\text{PhP}(\text{OEt})_2)_4]$ | Octahedron | 6 | 1.4 |
| +2 (d^5) | $[\text{Tc}(\text{CNC}(\text{CH}_3)_3)_6]^+$ | Octahedron | 6 | diamagnetic |
| +1 (d^6) | $[\text{Tc}(\text{CO})_5([\text{9}]\text{aneN}_3)]^+$ | Octahedron | 6 | diamagnetic |
| 0 (d^7) | $[\text{Tc}_2(\text{CO})_{10}]$ | Octahedron | 6 | diamagnetic |
| -1 (d^8) | $[\text{Tc}(\text{CO})_5]^-$ | Trigonal bipyramid | 5 | diamagnetic |